

Formation and Crystallization based Separation of Diastereomeric Salts

Der Fakultät für Verfahrens- und Systemtechnik
der Otto-von-Guericke-Universität Magdeburg
zur Erlangung des akademischen Grades

Doktoringenieur
(Dr.-Ing.)

am: 03.05.2012. vorgelegte Dissertation
(Einreichungsdatum)

von: M.Sc. Venkata Subbarayudu Sistla

Schriftliche Erklärung

Ich erkläre hiermit, dass ich die vorliegende Arbeit ohne unzulässige Hilfe Dritter und ohne Benutzung anderer als der angegebenen Hilfsmittel angefertigt habe. Die aus fremden Quellen direkt oder indirekt übernommenen Gedanken sind als solche kenntlich gemacht.

Insbesondere habe ich nicht die Hilfe einer Kommerziellen Promotionsberatung in Anspruch genommen. Dritte haben von mir weder unmittelbar noch mittelbar geldwerte Leistungen für Arbeiten erhalten, die im Zusammenhang mit dem Inhalt der vorgelegten Dissertation stehen.

Die Arbeit wurde bisher weder im Inland noch im Ausland in gleicher oder ähnlicher Form als Dissertation eingereicht und ist als Ganzes auch noch nicht veröffentlicht.

(Magdeburg, 03.05.2012)

(M.Sc. Venkata Subbarayudu, Sistla)

It's an immense pleasure for me to dedicate this work to my Uncle M.K. Ramatarakam garu and to my parents Sistla. Lakshmi Savitri Annapurna Devi and Sistla.Venkateswarlu.

Acknowledgement

First of all, I bow in front of the lord Sita-Rama, Who is there along with me all along in my life and made me to follow the path of truth in all the situations when my mind was not stable. I would like to convey my profound gratitude to Professor Andreas Seidel-Morgenstern and apl. Professor Heike Lorenz as they gave me this great opportunity to explore myself and in the area of Crystallization. I am proud to be in the group PCG under the guidance of Prof. A. Seidel-Morgenstern. I have to say that the immense support and cooperation that apl. Prof. Heike Lorenz gave me was incomparable. They gave me freedom to think; they gave me the path to unleash and allowed me to explore all the new areas which I was not aware of.

I am deeply thankful to my colleagues Dr. Samuel Tulashie and Dr. Jan von Langermann for their fruitful and deep discussions throughout my PhD period. I would also like to say my hearty thanks to all my colleagues of PCG group for their help during my work in the laboratory and outside laboratory. I would like to convey my special thanks to JaqlineKaufann, LuiseBrochert and Dr. Hilfert for their moral and practical support during my research tenure. I am also thankful to all my students who helped me during my Ph.D tenure.

I would love to say that without my wife`s support I cannot reach to this stage. She was there in all my mental developments with her actions.

I am glad to thank my sister and brother for their support to elevate myself to the next level of my life. Without their being I cannot reach here and think about my work peacefully. They are my bowl of energy, concentration and so...on.

Last but not least I would like to thank all my friends in Magdeburg who also played a crucial role in my personal life and made me feel that I was not alone.

Thank u verymuchhhh everyone.

Abstract

The objective of the present thesis is to approach the separation of R- and S-enantiomers of pharmaceutical substances via Classical Resolution systematically. In Classical Resolution a racemate is treated with an optically active resolving agent to form diastereomeric salts that can be separated via crystallization. Unlike enantiomers, diastereomeric salts possess different physical and chemical properties. The difference in properties of diastereomeric salts endorsed the use of less expensive separation technique crystallization and finally pure enantiomers are achieved back. Often in industry, Classical Resolution is performed with limited data on (thermodynamic) phase behavior data and (kinetic) metastable zone widths for diastereomeric salts. In the corresponding binary (melting) and ternary (solubility) phase diagrams diastereomeric salts might show either a simple eutectic, double salts or mixed crystals. This behavior affects the feasibility and performance of separation by crystallization. The separation process can be planned effectively and yields can be improved, provided the above data are available. In addition, in order to achieve complete conversion of reactant, an excess of the resolving agent can be used in the reaction step. However this excess resolving agent could act as an impurity and affect the crystallization thermodynamics and kinetics of one or both of the salts. This influence could either enhance or reduce the resolution of the salt pair.

The present work aims at a systematic experimental study of production and separation of two model compounds via Classical Resolution. In total six suitable resolving agents were selected and pure diastereomeric salts were synthesized and characterized. These pure salt pairs were used to generate binary melting point, ternary solubility phase diagrams and metastable zone width data in selected solvents. The feasibility for separation was decided based on the thermodynamic data. Optimum separation of the less soluble salts from the diastereomeric salt pairs with maximum yield was designed and executed. The yield was further increased by crystallizing the highly soluble salt preferentially. The kinetics of the separation process was controlled effectively by the data obtained from the metastable zone with measurements. The influence of excess resolving agent on solubility of individual diastereomeric salts is also studied in detail. Based on the outcome, the amount of excess resolving agent necessary to improve the resolution process was calculated and the observed influence on the resolution is discussed.

The present work provides generalize conclusions and further suggestions on how to proceed systematically to achieve high yields of diastereomeric salts via Classical Resolution.

Zusammenfassung

Ziel dieser Arbeit ist, systematisch die Trennung von R- und S-Enantiomeren pharmazeutischer Substanzen mittels klassischer Rekristallisation zu untersuchen. Hierbei wird das gelöste Racemat mit einem ebenso chiralen Additiv umgesetzt, sodass ein diastereomeres Salzpaar entsteht, welches anschließend über eine Lösungskristallisation getrennt werden kann. Im Gegensatz zu Enantiomeren, besitzen Diastereomere unterschiedliche physikalische und chemische Eigenschaften. Genau diese erlauben es günstigere Trennprozesse wie zum Beispiel die Kristallisation zur Gewinnung der reinen Enantiomere anzuwenden.

Häufig wird die klassische Rekristallisation in industrieller Umgebung mit geringer Kenntnis von thermodynamischen und kinetischen Prozessdaten durchgeführt. Hierbei ist allerdings zu erwähnen, dass in den entsprechenden binären (Schmelz-) und ternären (Löslichkeits-) Phasendiagrammen verschiedene fest-flüssig Gleichgewichte vorliegen können. Das Auftreten eines (eutektisches System) oder zweier (Doppelsalzsystem) eutektischer Punkte oder die Mischbarkeit in der festen Phase (Mischkristallbildendes System) beeinflusst die Durchführbarkeit und Effektivität der Trennung durch die Kristallisation. Sollten also die erwähnten thermodynamischen und kinetischen Informationen verfügbar sein, kann durch deren Verwendung der Trennprozess optimiert und so Ausbeute als auch Produktivität erhöht werden. Falls zusätzlich die gesamte Umsetzung der Reaktanden erzielt werden soll, wird ein Überschuss an Additiv zur Salzbildung im Reaktionsschritt zugesetzt. Dieser Überschuss kann als Verunreinigung die Thermodynamik und die Kinetik der Kristallisation von einem oder beiden gebildeten Salzen beeinflussen.

In dieser Arbeit soll daher die systematische experimentelle Studie zur Produktion und Trennung von zwei Modellsubstanzen mittels klassischer Rekristallisation beschrieben werden. Insgesamt wurden 6 Additive ausgewählt und die Synthese der korrespondierenden diastereomeren Salze durchgeführt, welche anschließend charakterisiert wurden. Die so gewonnen Salzpaare wurden dann verwendet, um die benötigten binären Schmelzpunkte, ternären Phasendiagramme und Metastabilitätsdaten für ausgewählte Lösemittel zu bestimmen. Die Möglichkeiten der Trennung wurden dann anhand der thermodynamischen Daten bewertet, die optimalen Prozesse für die schlechter löslichen Salze der Salzpaare anschließend ausgelegt und durchgeführt. Weiterhin konnten diese Prozesse hinsichtlich der

Ausbeute durch bevorzugte Kristallisation des höher löslichen Salzes verbessert werden. Hierbei war es möglich die Kristallisation anhand der Messdaten und der gewonnenen kinetischen Informationen effektiv zu steuern. Der Einfluss des Überschusses an Additiv auf die Löslichkeit wurde ebenso detailliert untersucht. Basierend darauf wurde die für die Verbesserung der Rekristallisation benötigte Menge des Salzbildners kalkuliert und entsprechende experimentelle Studien durchgeführt.

Abschließend wird in der vorgelegten Arbeit eine generelle Zusammenfassung und weitere Anregungen für zukünftige systematische Untersuchungen gegeben, um Ausbeutensteigerungen bei der Herstellung von diastereomeren Salzen durch klassische Rekristallisation zu erzielen.

Table of Contents

Abstract.....	v
Zusammenfassung	vi
Table of contents	viii
List of figures	xi
List of tables.....	xv
List of schemes.....	xv
List of symbols.....	xvi
List of abbreviations	xvii
1. Introduction	1
1.1. Introduction.....	2
2. Enantiomers, racemates and separation techniques.....	5
2.1. Enantiomers	6
2.2. Racemates	7
2.2.1. Conglomerates	7
2.2.2. Racemic compounds.....	8
2.2.3. Solid solutions (Pseudo racemates).....	9
2.3. Different production ways of enantiomers	9
2.3.1. Chiral pool	9
2.3.2. Asymmetric synthesis.....	10
2.3.3. Racemate resolution	10
3. Classical Resolution of racemates via diastereomeric salt formation	14
3.1. Principle of Classical Resolution and formation of diastereomeric salts.....	15
3.2. Selection of resolving agent.....	18
3.3. Basic aspects in diastereomeric salt separation via crystallization	19
3.3.1. Different types of diastereomeric salt (mixtures) solid phase behaviour	20
3.3.2. Effect of solvent	22
3.3.3. Measurement of binary melting phase diagram.....	23
3.3.4. Solubility phase diagram	24
3.3.5. Metastable zone width and different types of nucleation possibilities.....	26
3.3.6. Effect of excess resolving agent.....	28
3.3.7. Recovery of enantiomers and resolving agent.....	28
3.4. Dutch resolutions	29
3.5. State of the art	29

4. Substances selected and synthesis of diastereomeric salts	32
4.1. Racemates to be separated	33
4.1.1. Serine	33
4.1.2. Phenyl glycine	34
4.1.3. Selected resolving agents	35
4.2. Synthesis of diastereomeric salts	36
4.2.1. Synthesis of serine diastereomeric salts	36
4.2.2. Synthesis of phenyl glycine diastereomeric salts (Pair 6)	41
4.3. Summary	41
5. Experimental techniques and analytical methods used	42
5.1. Experimental techniques	43
5.1.1. Melting phase diagram measurement	43
5.1.2. Solubility measurements	43
5.1.3. Metastable zone width measurements	46
5.1.4. Resolution experiments	47
5.2. Analytical methods used	53
5.2.1. Differential scanning calorimetry (D.S.C)	53
5.2.2. Nuclear magnetic resonance (NMR)	54
5.2.3. X-ray powder diffraction (XRPD)	55
5.2.4. High Performance Liquid Chromatography (HPLC)	56
5.2.5. Refractometer	58
5.3. Summary	59
6. Results and discussion	60
6.1. Results of L-D, D-D salts (pair 1)	62
6.1.1. Characterization of L-D, D-D salts	62
6.1.2. Binary melting behavior	63
6.1.3. Ternary solubility phase diagram	64
6.1.4. Metastable zone width for primary nucleation	71
6.1.5. Resolution experiments for (L-D, D-D) salt pair 1	72
6.2. Results for L-L and D-L salts (pair 2)	83
6.2.1. Characterization of D-L and L-L salts	83
6.2.2. Thermodynamic data	84
6.2.3. Kinetic data	89
6.2.4. Resolution experiments for D-L, L-L salt mixture	90

6.3.	Results for D-LM and L-LM salts (pair 3)	93
6.3.1.	Characterization of D-LM and L-LM salts	93
6.3.2.	Binary mixtures behavior analysis of D-LM, L-LM salt	93
6.3.3.	Ternary solubility phase diagram	95
6.4.	Results for D-LT and L-LT salts (pair 4)	97
6.4.1.	Characterization of D-LT and L-LT salts	97
6.4.2.	Binary mixtures behavior analysis of D-LT and L-LT salts	97
6.4.3.	Ternary solubility phase diagram	98
6.5.	Results of L-D-Toluyl, D-D-Toluyl salts (pair 5).....	100
6.6.	Results of LPG-CS, DPG-CS salts (pair 6)	102
6.6.1.	Characterization of LPG-CS and DPG-CS	102
6.6.2.	Ternary solubility phase diagram	103
6.6.3.	Resolution experiments for (DPG-CS, LPG-CS) salt pair 6.....	105
6.7.	Summary.....	109
7.	Conclusions and outlook.....	110
7.1.	Conclusions.....	111
7.2.	Outlook	115
	Appendices.....	117
	Bibliographie.....	122

List of Figures

Fig 1: Pair of enantiomers for lactic acid

Fig 2: Model phase diagrams of conglomerates: (1) binary melting phase diagram, (2) ternary solubility phase diagram; D, L-two phase regions, DL-three phase region (dashed line is just to indicate the racemic composition)

Fig 3: Model phase diagrams of racemic-compounds: (1) binary melting phase diagram, (2) ternary solubility phase diagram; D, L, DL-two phase regions; D-DL, L-DL-three phase regions

Fig 4: Model phase diagrams of solid solutions: (1) binary melting phase diagram (2) ternary solubility phase diagram (a,b,c –Roozeboom isotherms)

Fig 5: Schematic explanation of the principle of Classical Resolution

Fig 6: Model phase diagrams of simple eutectic system: (1) binary melting phase diagram, (2) ternary solubility phase diagram

Fig 7: Model phase diagrams of double salts: (1) binary melting phase diagram, (2) ternary solubility phase diagram

Fig 8: Model phase diagrams of mixed crystals: (1) binary melting phase diagram, (2) ternary solubility phase diagram

Fig 9: DSC melting behavior of 1:1 diastereomeric salt mixture

Fig 10: For diastereomeric p-, n-salts (a) Schematic explanation of simple eutectic phase behaviour with single solubility isotherm (b) general approach for separation of pure p-salt via crystallization

Fig 11: Solubility and different nucleation possibilities for a pure diastereomeric salt in a selected solvent

Fig 12: Chemical structure of both L-/D-serine enantiomers

Fig 13: Ternary solubility phase diagram for serine in water

Fig 14: Chemical structure of D-/L-phenylglycine

Fig 15: XRPD patterns for D-/L- and DL-phenyl glycine

Fig 16: Chemical structures of commonly used acidic resolving agents

Fig 17: Determination of the time necessary to reach equilibrium at particular temperature for solubility measurements: (a) Successive solute addition method, (b) Isothermal excess method

Fig 18: Conventional isothermal solubility measurement equipment

Fig 19: Crystal 16 (from Avantium technologies)

Fig 20: Schematic diagram for equipment used for the resolution experiments

Fig 21: Block diagram representing a typical differential scanning calorimeter

Fig 22: DSC thermogram representing different phase transitions

Fig 23: A typical block diagram of Nuclear Magnetic Resonance Spectrometer

Fig 24: The geometry of an XRPD unit

Fig 25: HPLC setup

Fig 26: (a) The total angle of reflection, critical angle and reflection of light from water to air
(b) Setup of the measurement system RE40

Fig 27: (a) ^1H NMR and (b) XRPD patterns for both L-D and D-D salts (main peaks characterizing the individual salts are indicated by arrows)

Fig 28: Melting curves for L-D, D-D-salts and a 70:30 mixture of both salts (sample masses: 8-10 mg)

Fig 29: XRPD pattern comparison of different mixtures of L-D and D-D-salts with the pure single salts

Fig 30: Ternary solubility phase diagram of both L-D- and D-D-salts in methanol (1): Upper 50% of the solubility phase diagram (2): Full ternary phase diagram

Fig 31: Ternary solubility phase diagram for L-D, D-D salts in water (upper 10%)

Fig 32: Solubility change for L-D and D-D salts according to the change in anti-solvent content in methanol

Fig 33: Effect of excess of resolving agent (R.A) (2,3dibenzoyl-D-tartaric acid) on the solubility of L-D salt (blue color), D-D salt (pink color) and 50:50 mixture of L-D: D-D salts (red color) in methanol

Fig 34: Metastable zone with for primary nucleation for a) L-D, b) D-D salt in methanol (Maximum possible subcooling(ΔT_{\max}) from extrapolation to zero K/min cooling rate)

Fig 35: Evaporative crystallization based resolution experiment design for L-D, D-D salts

Fig 36: XRPD analysis for solid phase crystallized during Evaporative crystallization based resolution experiment for L-D, D-D salts

Fig 37: ^1H NMR analysis for solid phase crystallized during Evaporative crystallization based resolution experiment for L-D, D-D salts

Fig 38: Resolution by cooling and anti-solvent crystallization for L-D, D-D salts

Fig 39: Liquid phase (HPLC) analysis of resolution experiments for L-D, D-D salts

Fig 40: XRPD solid phase analysis for both resolution experiments for L-D, D-D salts

Fig 41: Liquid phase composition change during preferential crystallization experiments (1) L-D salt (2) D-D salt

Fig 42: XRPD solid phase analysis for preferential crystallization experiment-1 (for L-D salt) and 2 (for D-D salt)

Fig 43: (a) ^1H NMR and (b) XRPD patterns for both D-L- and L-L-salts

Fig 44: Binary melting point phase diagram for both D-L- and L-L-salts (the eutectic composition was derived from the DSC-experiments)

Fig 45: XRPD patterns of reference D-L and L-L salts and mixtures of different composition

Fig 46: Ternary solubility phase diagram for D-L and L-L salts in methanol (1): Full ternary phase diagram (D-L, L-L, D-L+L-L: existence regions of the respective salts in the phase diagram) (2): Upper 50% of the solubility phase diagram

Fig 47: Ternary solubility phase diagram for D-L, L-L salts in water

Fig 48: Solubility change for D-L, L-L salts according to the change in anti-solvent composition

Fig 49: Metastable zone with for primary nucleation in methanol for (1) D-L salt (2) L-L salts

Fig 50: Liquid phase (HPLC) analysis of resolution experiments for D-L, L-L salts

Fig 51: XRPD solid phase analysis for both resolution experiments for D-L, L-L salts

Fig 52: (1)¹H NMR and (2) XRPD patterns for both D-LM- and L-LM-salts

Fig 53: XRPD patterns for pure D-LM and L-LM salts and mixtures of both (arrows indicate the similar peaks present in both salts and the box represent the extra peaks for mixtures)

Fig 54: DSC melting curves for pure D-LM and L-LM salts and two mixtures

Fig 55: Ternary solubility phase diagram for D-LM and L-LM salts in acetone

Fig 56: (1)¹H NMR and (2) XRPD patterns for both D-LT- and L-LT-salts

Fig 57: XRPD patterns for both D-LT and L-LT salts and their mixtures

Fig 58: Solubility phase diagram for D-LT and L-LT salts in water for 25°C (just the upper 20% of the phase diagram is shown) incl. illustration of the phase conditions

Fig 59: ¹H NMR spectrum for (1) L-D-Toluyl salt (2) D-D-Toluyl salt

Fig 60: XRPD patterns of pure L-D-Toluyl and D-D-Toluyl salts (main peaks characterized with arrows)

Fig 61: Characterization results of DPG-CS, LPG-CS (1)¹H NMR spectrum (2) XRPD analysis

Fig 62: Ternary solubility phase diagram in methanol for DPG-CS, LPG-CS

Fig 63: Ternary solubility phase diagram for DPG-CS, LPG-CS in (1) Water (2) Ethanol (upper 50% of phase diagram)

Fig 64: Cooling and anti-solvent crystallization for resolution of DPG-CS, LPG-CS salts

Fig 65: XRPD solid phase analysis for resolution of DPG-CS, LPG-CS salts

List of Tables

Table 1: Overview of experimental conditions for separation of serine salts

Table 2: The solution preparation and experimental conditions for LPG-CS, DPG-CS separation

Table 3: List of salt pairs

Table 4: Solubilities of pure D-D and L-D-salts in selected solvents at 25°C

Table 5: Purity and Yield analysis of resolution experiments for L-D, D-D salts

Table 6: Mass balances for resolution experiments for L-D, D-D salts

Table 7: Purity and Yield analysis of resolution experiments for D-L, L-L salts

Table 8: Solubility of LPG-CS, DPG-CS in different solvents at 5°C

Table 9: Resolution results for DPG-CS and LPG-CS

List of schemes

Scheme 1: Explanation of Marckwald principle

Scheme 2: Esterification of D-/L-serine

Scheme 3: Formation of D-/L-serine benzyl ester (III)

Scheme 4: Formation of L-L, D-L, L-D and D-D salts (Nomenclature and structures)

Scheme 5: Formation of L-LM, D-LM salts

Scheme 6: Formation of L-LT, D-LT salts

Scheme 7: Formation of L-D-Toluyll, D-D-Toluyll salts

Scheme 8: Formation of LPG-CS, DPG-CS salts

Scheme 9: Schematic representation of preferential crystallization experiments planned for L-D, D-D salts (F: feed to the concerned unit operation, w_F : weight fraction of solute in solution, E1, E2: evaporators; PC1, PC2: preferential crystallizers)

Scheme 10: Overview for formation and resolution of L-D, D-D salts; R-reactor; C-selective crystallizer; E-evaporator; PC-crystallizer for preferential crystallization; F-feed to the concerned unit operation; w_f -weight fraction of solute

List of symbols

S - efficiency of the resolution or resolvability

x - weight fraction

T_E - eutectic melting temperature

T_L - liquidous temperature

ΔH - heat of fusion

X_E - eutectic composition

wt - amount of substance (g)

ΔT - the difference between saturation temperature and the nucleation temperature

ΔT_{Max} - the maximum achievable subcooling for a constant concentration in solution

ΔC_{max} - maximum supersaturation at a constant temperature

F - feed to the concerned unit operation,

w_f - weight fraction of solute in solution

T_g - glass transition temperature

T_c - crystallization temperature

T_m - melting temperature

λ - wavelength of incident wave

λ_r - stoichiometric feed ratio

v - stoichiometric coefficient

$n_A^{\text{Feed}}, n_B^{\text{Feed}}$ - number of moles of reactant A, B in the feed

2θ - theta: diffraction angle

d - Lattice distance

α - incident angle,

β - largest possible angle of refraction,

n_1, n_2 - refractive index of medium 1, 2

List of abbreviations

L-D salt -- L-serine benzyl ester-D-dibenzoyl tartrate salt

D-D salt -- D-serine benzyl ester-D-dibenzoyl tartrate salt

D-L salt -- D-serinebenzylester-L-dibenzoyltartratesalt

L-L salt -- L-serinebenzylester-L-dibenzoyltartratesalt

L-LM salt -- L-serinebenzylester-L-mandelatesalt

D-LM salt -- D-serinebenzylester-L-mandelatesalt

L-LT salt -- L-serinebenzylester-L-tartrate salt

D-LT salt -- D-serinebenzylester-L-tartrate salt

L-D-Toluyll salt -- L-serinebenzylester-D-ditoluoyltartrate salt

D-D-Toluyll salt -- D-serinebenzylester-D-ditoluoyltartrate salt

LPG-CS -- L-phenyl glycine-(+)-camphor sulphonate

DPG-CS -- D-phenyl glycine-(+)-camphor sulphonate

e.e. -- Enantiomeric excess

d.e. -- Diastereomeric excess

NMR -- Nuclear magnetic resonance

XRPD -- X-ray powder diffraction

HPLC -- High performance liquid chromatography

DSC -- Differential scanning calorimetry

FTIR -- Fourier Transform Infrared ray spectroscopy

R.A -- Resolving agent

R -- Reactor

C, C1, C2 -- Selective crystallizers

E1, E2, E -- Evaporators

PC, PC1, PC2 -- Crystallizers for Preferential Crystallization

MW -- Molecular weight

DL-SBE -- DL- serine benzyl ester

DBT -- Dibenzoyl tartaric acid

1. Introduction

Chapter 1

Introduction

1.1. Introduction

In the nature, most influential organic substances are selectively synthesized. It is evident in the case of chiral molecules like enantiomers, which are non-super imposable mirror images to each other [2]. In general these enantiomers possess same physical and chemical properties. The only difference is upon reflection in a plane polarized light, they show same magnitude with different signs [3]. Usually these enantiomers are discriminated with the notation (+, -), (D-, L-) or (R, S) [3-5]. In human body, the essential amino acids that are necessary to produce proteins, enzymes and many antibiotics are also selective in their orientation [6]. In order to support human body therapeutically; mostly one of the enantiomer is active. The other enantiomer might be neutral or sometimes it might also become harmful poison to the functioning of the body [7, 8]. The harmful effects were observed end of 1950s, beginning of 1960s, when thalidomide drug (used for morning sickness) with both enantiomers was given to pregnant women, which caused many disorders in many babies [9]. To mitigate this kind of problems, FDA ascertained that chiral pharmaceutical drugs and agrochemicals, which are to be consumed, must be known the activity of both of its enantiomers and the desired one must be used [10, 11].

These enantiomers can be produced in different ways. Each enantiomer can be synthesized selectively by asymmetric synthesis but this process is not suitable for many substances. Mostly enantiomers are synthesized in the form of a racemate, a 1:1 mixture of both enantiomers and are separated into their pure enantiomers by different separation techniques [12]. Among all of them, Classical Resolution is the most suitable and industrially viable method for resolution of racemates. In applying this technique, a racemate is reacted with an optically active chiral resolving agent to produce equal amounts of two diastereomeric salts [2]. As these diastereomeric salts possess different physical and chemical properties, they can be separated with different types of downstream processes. Out of all separation processes, crystallization is the most economical separation process for Classical Resolution. The best resolving agent is selected depending upon the separation factor in the crystallization process [13]. Many separation processes are performed without systematic study of basic thermodynamic data of newly formed diastereomeric salts like binary melting (both salts) and ternary solubility (two salts and a solvent) phase diagrams and kinetic data (e.g. metastable zone width) to separate via crystallization. This basic information is required in the design of a suitable separation process and improving the final yield by optimizing the process conditions.

Usually, thermodynamic data is helpful for identifying thermal stability of the substances and their behavior at high temperatures, polymorph and solvate formation. It is also useful for knowing the behavior in the binary and ternary mixtures to figure out the number of crystallization steps that can be selected for achieving the maximum yield without any defects in the required product. Kinetic data is helpful in determining the starting and end point of crystallization experiment propagation with respect to nucleation, growth and crystal size distribution and purity of necessary substance [14]. Further, if the reaction in Classical Resolution is non-stoichiometric then there would be some unreacted reactants in the solution. These excess reactants also act as impurities and affect the thermodynamic and kinetic properties of products formed and ultimately influence the outcome via crystallization based separation [15].

According to the literature available, most of the separation experiments were executed without the presence of above mentioned basic information. They were executed on trial and error basis and approached to an empirical maximum based on the product attained. Mostly one of the pure diastereomeric salts was separated and the rest was drained as waste. If both enantiomers of a racemate have different applications then performing Classical Resolution without basic information leads to considerable loss in the yield [2, 13].

Aim and arrangement of thesis structure

The present research work concentrates on investing all basic steps occurring in the Classical Resolution. Steps considered systematically are the selection of a suitable resolving agent, evaluation of the impact of stoichiometry of reactants (racemate and resolving agent), selection of solvent for reaction, analysis of stability of diastereomeric salts formed (polymorphism, solvate formation), effect of different process conditions like temperature, concentration etc, measurement of thermodynamic (melting and solubility phase behavior) and kinetic (metastable zone width) properties of both diastereomeric salts formed, evaluating the effect of excess resolving agent on the above basic properties of both diastereomeric salts. Based on practically determined data optimized separation processes via crystallization are designed and checked regarding their separation efficiency.

In chapter 2, the basic concepts of chirality like enantiomers, racemate properties are presented. Different types of behavior of racemates are explained schematically. Here different ways to approach optically pure enantiomers are also explained.

In chapter 3, enantioseparation via diastereomeric salt formation (Classical Resolution) is explained systematically. All the basic steps that influence the final separation are considered as an individual aspect and discussed in detail.

The properties of the model substances and selected suitable resolving agents for Classical Resolution are introduced in chapter 4. Synthesis procedure of diastereomeric salts for chosen racemic substances with suitable resolving agents are explained in chapter 4 as well.

The purity analysis of the diastereomeric salts was done with different analytical techniques. Various types of experimental setups were also used for measuring required data and executing effective separation via Classical Resolution in this research work. All the practical methods and analytical techniques that were used to obtain data for the final results are explained in chapter 5.

The final application oriented part is devoted to basic experimental results obtained and the approach to design an effective separation process for diastereomeric salt pairs of model chemicals are shown in the chapter 6. Here the results of optimum yield that was obtained during the separation experiments are also discussed in detail.

Finally, the whole work is summarized. Suggestions are given for possible improvements in Classical Resolution processes.

2. Enantiomers, racemates and separation techniques

Chapter 2

Enantiomers, racemates and separation techniques

2.1. Enantiomers

Enantiomers are one of the subset of stereoisomers. Generally they possess one or more asymmetric carbon atoms (a chiral center) and a chemical structure which is a non-super imposable mirror image to each other. A general example is shown in Figure 1. This property of enantiomers is generally called as enantiomerism[16]. Usual nomenclature for these enantiomers are (+,-) or (D-, L-) or (R-, S-).

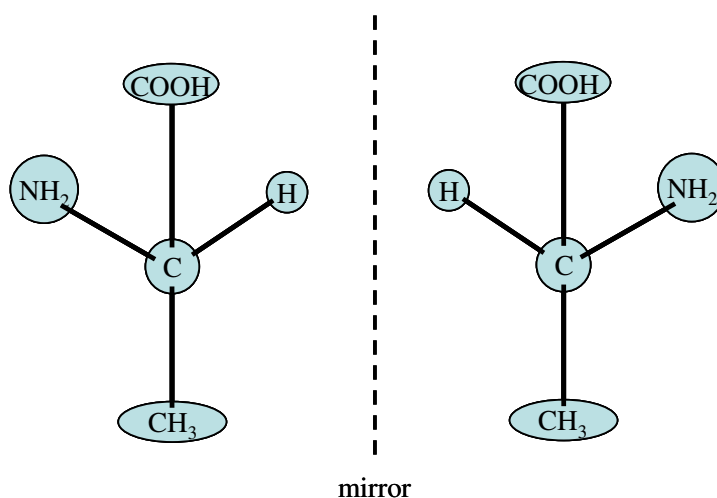


Fig 1: Pair of enantiomers for lactic acid

When these enantiomers are placed in a symmetric medium (in the absence of external chiral influence), they show equality in all corresponding physical and chemical properties like melting point, solubility, chromatographic retention time (in an achiral column), infrared spectra (IR), nuclear magnetic resonance (NMR), XRPD etc. But passage of plane polarized light through these substances yields a rotation angle with same magnitude but opposite signs (+/-). The chemical activity of these enantiomers on the chiral environment is also selective. Usually in pharmaceutical drugs only one enantiomer gives the suitable response for the appropriate physiological effect while the other one is inactive in that specific function or it might show different significance in its effect on the body which might lead to side effects [17]. This is clearly found for many pharmaceuticals and agrochemicals. Due to these possible adverse effects only the active enantiomer should be used for the desired purpose for all enantiomeric applications. By using the pure enantiomers in drugs, the pharmaceutical efficacy can be improved and the adverse effect can also be eliminated.

2.2. Racemates

Racemates constitute 50:50 mixture of both ((+) - and (-)) or (D- and L-) or (R- and S)-enantiomers. In general these racemates are referred as (+-), (DL-) or (RS). When a racemate is dissolved in a non-chiral solvent, then the optical rotation (α) of the solution is 0° . Thus, the plane polarized light shows no deviation in its rotation. At this status the chiral substance can be referred as optically inactive [18]. Usually, a normal synthesis of chiral substances leads to the production of a racemate. Generally racemates are divided into three types based on their solid phase behavior: (1) conglomerate, (2) racemic-compound and (3) solid solutions [19].

2.2.1. Conglomerates

Conglomerates are a kind of racemates that are just mechanical mixtures of both (+)- and (-)-optically active enantiomers together. In conglomerates, the affinity for like enantiomer is greater compared to the affinity for the opposite enantiomer. These constitute only 5-10% of all racemates so far discovered [13, 20-22]. Conglomerates can be distinguished from the other types via melting point and solubility phase diagrams. The general phase diagrams are shown in Figure 2.

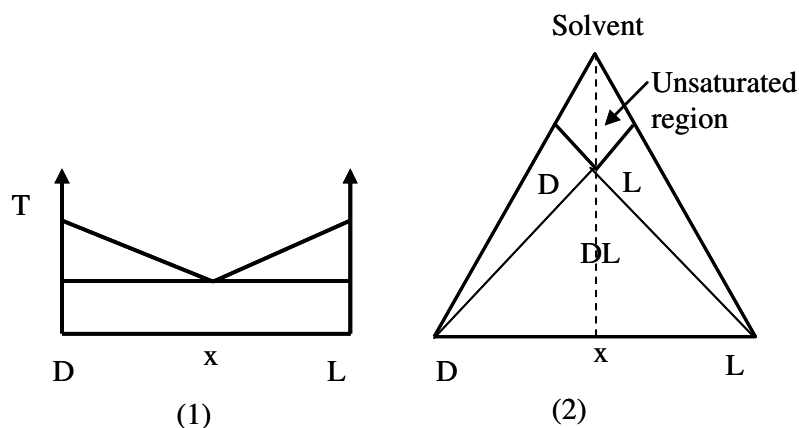


Fig 2: Model phase diagrams of conglomerates:(1) binary melting phase diagram (2) ternary solubility phase diagram; D, L-two phase regions, DL-three phase region (dashed line is just to indicate the racemic composition)

The melting point of the racemic conglomerate is always lower than the individual enantiomers and the solubility of individual enantiomers are always lower than the solubility of their racemic conglomerate. The melting point of one enantiomer decreases or solubility of one enantiomer increases with the increase in the composition of opposite enantiomer. The composition of maximum solubility or minimum melting point of mixtures is called eutectic

composition. Usually for conglomerates, due to symmetry eutectic holds at racemic mixture in both phase diagrams.

2.2.2. Racemic compounds

Racemic compounds behavior is observed in almost 90% of all enantiomers discovered[13, 22]. While forming crystal lattice, molecules have much high affinity towards the opposite enantiomer than the like enantiomer. Enantiomers distribute evenly in an order in 1:1 ratio in the crystal lattice of the racemate. Racemic compounds can be distinguished from conglomerates according to their melting point and solubility phase diagrams. A typical melting point and solubility phase diagram for racemic compound-forming substances are shown in Fig 3.

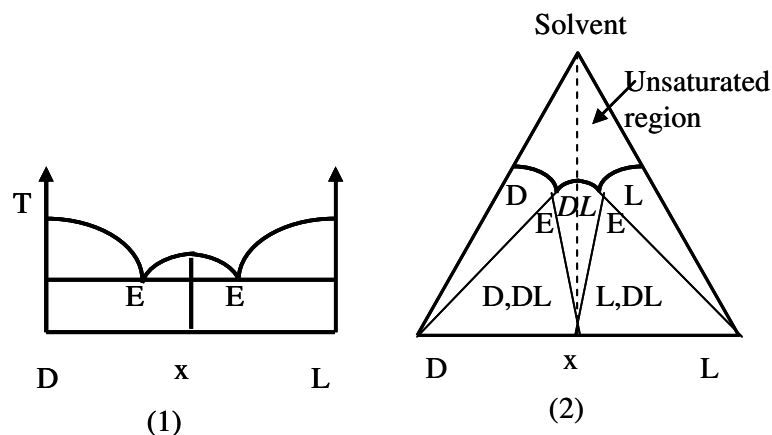


Fig3: Model phase diagrams of racemic-compounds: (1) binary melting phase diagram, (2) ternary solubility phase diagram; D, L, DL-two phase regions; D-DL, L-DL-three phase regions

The melting point of an enantiomer can either be higher or lower than the racemic compound but lowest melting point, i.e. eutectic melting would be at some other composition than 50:50 mixture. For example in Fig 3(1) the melting temperatures are decreasing from the pure enantiomers and reach eutectic composition at another composition other than racemic composition. Then again melting temperatures are increased until the racemic composition. In the same way, in solubility phase diagram also the eutectic composition stayed at some other composition of both enantiomers other than racemic composition. The solubility isotherm is symmetric on both sides of isoplethal line of 50:50 mixture of both enantiomers[23].

2.2.3. Solid solutions (pseudo racemates)

Even though pseudo-racemates constitute just 1% of racemates they are distinct from the racemic-compounds or conglomerates [24]. Here the affinity between the enantiomers and the opposite enantiomers has no big difference. In molecular level the crystal lattice is distributed unevenly with equal amounts of both enantiomers. Example melting point and solubility phase diagrams are shown in Fig 4.

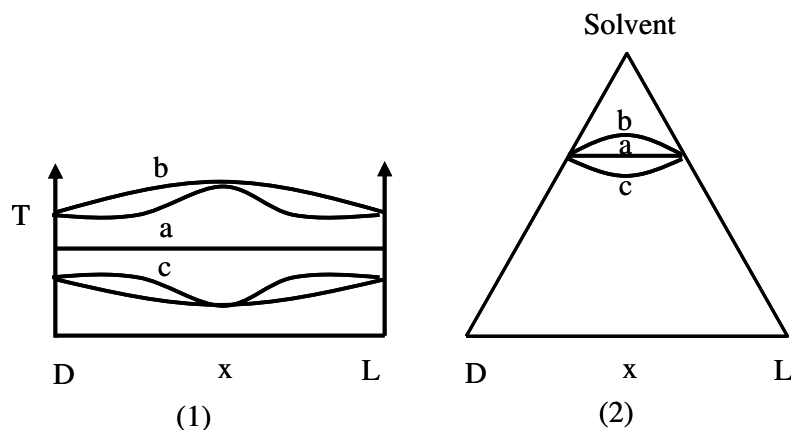


Fig 4: Model phase diagrams of solid solutions: (1) binary melting phase diagram (2) ternary solubility phase diagram (a,b,c –Roozeboom isotherms).

The enantiomers forming solid solutions, in binary melting phase diagram show variation in eutectic composition. Ideally, the melting point or solubility of one enantiomer changes (increase or decrease) or does not change at all with the addition of other enantiomer[25]. Roozeboom firstly specified different possible phase behaviors of solid solutions which are shown in Fig4.

2.3. Different production ways of enantiomers

2.3.1. Chiral pool

Many optically pure enantiomers do exist in nature as their derivatives. They present a part of complex enantiomeric organic chemical compounds which have readily available in the nature [26]. Many enantiomers which belong to several organic groups like amino acids, monosaccharides or carbohydrates etc. are obtained from their complexes by necessary modifications to the target structure [27-30]. Based on the molecular resemblance of enantiomer to its enantiopure source, it can be achieved either by simple reaction or a lengthy synthesis which involve huge loss in yield. The success of chiral pool synthesis depends on the suitable source of starting material otherwise the process may not be fruitful.

2.3.2. Asymmetric synthesis

In the manufacturing of optically active substances, asymmetric synthesis (also called stereoselective synthesis) is one of the very strong approaches. Usually this process refers to the production of a chiral product by applying various conversion steps starting from an achiral raw material[31]. In an asymmetric reaction, the combination of a substrate and a reagent forms a diastereomeric transition state. During the reaction, asymmetry will be induced only at the sites of substrate where chiral element is present. Most of the times, at the functional site, a trigonal carbon converts to a tetrahedral one to get asymmetry. This can be processed by various methods like (a) substrate controlled methods, (b) auxiliary-controlled methods, (c) reagent controlled methods and (d) catalyst-controlled methods [32, 33]. The evaluation of an asymmetric reaction can be done via measuring the desired and unwanted enantiomers composition. If the synthesis process is successful, it produces exactly the same kind of enantiomer without involving the appearance of the other unwanted enantiomer. This would reduce a lot of further processing of waste with different techniques like racemization. An increasing interest is being observed in the pharmaceutical industry despite of the complexity involved in the asymmetric synthesis [34].

2.3.3. Racemate resolution

A racemate is always produced, if there is no chiral starting material like chiral raw materials, catalyst or special solvents, during the production process of a chiral substance. As there is no special impact on the production, racemate production is a far cheaper way to approach a chiral substance than to form its enantiomer directly[13]. In industry, mostly racemate cannot be used directly for the concerned purpose so it must be separated into its enantiomers. Different types of racemate separation techniques are discussed in this chapter.

2.3.3.1. *Diastereomeric salts formation*

This separation technique for racemates is one of the very prominently used techniques in the industry[35]. In this technique a racemate is reacted with an optically active resolving agent to form two diastereomeric salts. In industry, these diastereomeric salts are separated rarely with chromatography but mostly with crystallization due to the difference in their physical and chemical properties. The separated salt is reacted with a strong acid or base to get back the desired enantiomer. This process is always executed in batch process, which is highly suitable for pharmaceutical industry[36]. Even though, despite of its simplicity in its application it has

a disadvantage like using many containers for reaction and separation processes. Each time the mother liquor must be stagnated in the industry to execute further processing, which occupies a lot of space in the plant. Environmental safety also includes problems like resolving agent recovery and unwanted enantiomer racemization which increases the cost of production and process time. Since this technique is objective for the present thesis a detailed description of this process is given in the chapter 3.

2.3.3.2. *Kinetic resolution*

It is a special kind of process in which the two enantiomers in a racemate have different conversion rates to form a product when it is reacted with a chemical reagent. In fact, in an ideal resolution one of the enantiomers readily forms the product while the other does not. Dynamically during the resolution process, an increase in the enantiomeric excess (e.e) of less reactive enantiomer can be seen. The efficiency of the kinetic resolution process can be decided based on the e.e. obtained. This reaction process may be executed either by chemical or enzymatic methods. Research is under progress for chemical catalytic processes while for enzymatic kinetic resolution there are processes which reached to the industrial level as well. Often a high enantiomeric excess in kinetic resolutions was found for the enzymatic process when compared to the normal chemical stoichiometric or catalytic processes[26]. This area of research is promising by revealing the potential of chemical catalysts or enzymes in separating the racemates[37].

2.3.3.3. *Chromatographic techniques*

Chiral chromatographic separations always depend on the difference in the distribution ability of different enantiomers between a stationary phase (chromatographic column) and a mobile phase (either single solvent or mixture of solvents-eluent). Usually for chiral separations the stationary phase would be attached with special chiral selectors. These chiral selectors interact with enantiomers and form temporary bonds which lead to the difference in the retention time of enantiomers in the column. The same can also be done with a non-chiral stationary phase with a chiral mobile phase[10, 38]. However the chiral mobile phase utilization is not much in use because of the involvement of much expensive solvents. There are different types of chromatographic techniques, based on its mobile and stationary phases applied for interaction and also for the purpose of utilization e.g. Liquid chromatography (HPLC, TLC), Subcritical or Supercritical fluid chromatography and Gas chromatography etc. Many of these techniques are mostly used for analytical purpose in the laboratory but High-performance liquid chromatography (HPLC) is under scanner for preparative scale [39]. Despite of its

complications like costly stationary phase, stability of stationary phase, using huge amount of solvents, expensive operating conditions and extra unit operations for solvent recovery, increase in demand for pure chiral substances made industry to opt for higher scale chromatographic separations with different advances like simulated moving bed(SMB)[40].

2.3.3.4. *Crystallization techniques*

Crystallization based enantioseparations are cheapest techniques among all the separation techniques[41]. This process can be directly used for the separation of enantiomers if the racemate comes under conglomerates. In the solubility phase diagram shown in Fig 2 in chapter-2.2.1, if the initial solution mixture is in the three phase region at the racemic mixture, then a specific technique called preferential crystallization allows for separation of both enantiomers sequentially in different steps[42]. This process has been successfully implemented in industrial production of L-glutamic acid. If the initial solution is in one of the two phase regions, selectively seeds of the one of the enantiomers can be introduced and pure enantiomer crystallization can be achieved. This process may also be used for racemic compound-forming systems, if the initial composition is in three phase region in Fig3. Intensive research is under progress to apply preferential and selective crystallizations for racemic compound-forming systems under special conditions [43]. A considerable amount of tailor-made additives also have good effect on the crystallization-based separations of conglomerates. Sometimes enantiomers might show considerable difference in their thermodynamic or kinetic properties with chiral solvents and ionic liquids due to special chiral interactions [44, 45]. Crystallization-based separations can also be combined with different separations techniques and form a hybrid separation process to achieve higher yields and purities with moderate costs [46].

2.3.3.5. *Other techniques*

Some more chiral separation techniques are also mentioned here. These techniques are yet under scanner for their application from lab scale to a preparative scale.

Enantioselective membrane separations: Due to the high potential for chiral separation and low operational costs, much effort is invested in the membrane-based separation process[47]. Membranes like dense polymers or liquid membranes provide a selective barrier and allow only one of the enantiomer through it preferentially. In the case of liquid membranes a chiral selector, which is non- mixable in the solvents, is used. This technique is highly promising but has practical problems like trial and error based chiral selectors for liquid membranes and poor enantioselectivity[38, 48].

Some more enantioseparation possibilities are also available like *Liquid-liquid extraction*, *Capillary electrophoresis*, *Enantioselective distillation* and *foam flotation*. Among these *Capillary electrophoresis* is available for only analytical scale. But other three are applicable for preparative scales for certain substances.

3. Classical Resolution of racemates via diastereomeric salt formation

Chapter 3

Classical Resolution of racemates via diastereomeric salt formation

3.1. Principle of Classical Resolution and formation of diastereomeric salts

In principle, Classical Resolution falls under reactive crystallization based separation processes. A racemate of a chiral substance is dissolved uniformly in an achiral solvent and reacted with an optically active resolving agent, which has equal affinity to react with both enantiomers of the racemate. Always the nature of a chiral racemate to be separated affects the reaction process of Classical Resolution. Depending upon the functional groups in racemate chemical structure, the reaction forms either a pair of dissociable diastereomeric salts or covalent compounds[35, 49].

In the case of dissociable compounds, if the racemate is a chiral acid then the resolving agent used would be a chiral base and vice versa for chiral racemic base. This reaction process would yield two diastereomeric salts (p-salt and n-salt) and there would be an increase in chiral centers in the newly formed salts. These products unlike enantiomers show different properties in their physical properties like solubility in the given solvent[50, 51]. Usually the difference in physical properties would be exploited to achieve the separation of the less soluble salt from the solution via crystallization. The quality of separation would depend on the solubility difference in the solvent used and the behavior of newly formed diastereomeric salts in the ternary phase system (two salts and a solvent). The separated less soluble salt would then possess only one enantiomer in its chemical structure. The simple hydrolysis of the diastereomeric salt yields the pure enantiomer and the resolving agent[52, 53]. Based on the process requirement, mother liquor and recovered resolving agent would be reprocessed. The explained principle of Classical Resolution is schematically shown in Figure 5.

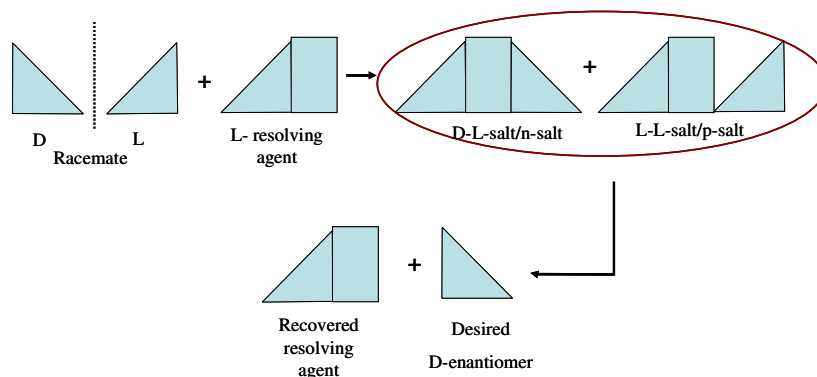


Fig 5: Schematic explanation of the principle of Classical Resolution

If the racemate is an amino acid, where two active sites are available for the acid-base reaction, it is not suggestive to react directly with a resolving agent. This could create some

internal reactions between the amino and carboxylic groups inside the amino acid itself. To avoid this kind of problem one of the active functional groups (either amino or carboxylic groups) must be derivatized by reacting with an achiral substance[54, 55]. This would give a clear path for the original acid-base reaction for Classical Resolution.

This process would also be useful in the case of neutral substances like alcohols and carbonyl compounds (ketones and aldehydes). There are a good number of examples which were executed practically where they transformed some of these neutral substances into the derivatives of either an acid or a base[56, 57]. In the same manner successful resolutions were also carried out for Werner complexes and Lewis acid-base complexes forming between racemic substrate and optically active reactant[58, 59].

The formation of covalent diastereomers is opted only for chiral substances that are non-capable of salt formation. Simple examples are the formation of diastereomeric amides or esters and separation via either chromatography or fractional crystallization[60, 61]. For example DL-decalactone was resolved with the help of (S)-phenylethylamine by forming an amide[62]. Increase in interest is observed for separation of covalent diastereomers by chromatography as it provides both diastereomers with high purity. Separated covalent diastereomers face much problem at the time of cleavage to the corresponding enantiomer when compared to dissociable compounds. The recovery of resolving agent without racemization and decomposition is the major problem[13].

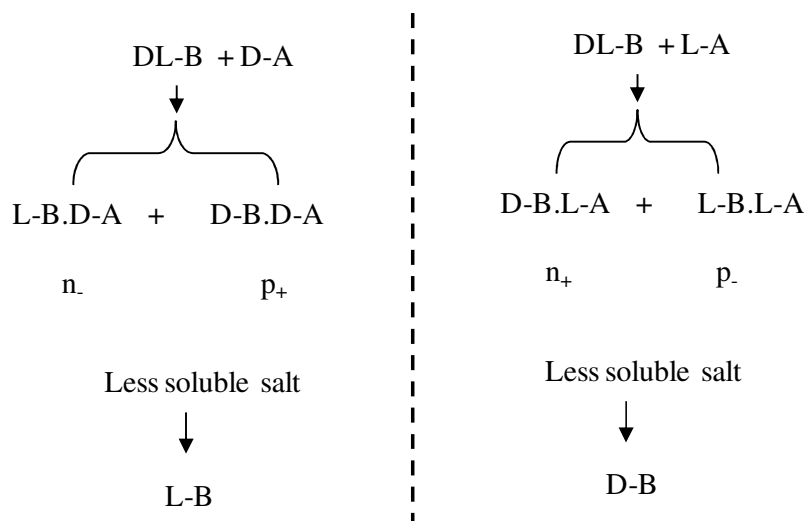
As Classical Resolution has the high applicability for racemate resolution, novel approaches were attempted for attaining both enantiomers and yield improvements. To resolve both enantiomers in pure form Marckwald discovered a new point in classical resolution [63, 64]. Efforts in the area of using non-stoichiometric amount of resolving agent to improve the yield and to reduce the amount of resolving agent were put by Pope and Peachey [66]. Both principles are explained elaborately below.

The Marckwald principle

If both enantiomers of a resolving agent (say D-A, L-A) are available, to separate both enantiomers of a racemate (DL-B), first d-form of resolving agent is used to achieve the less soluble salt D-B.D-A yields LB. The mother liquor of first separation process has the excess of D-B.D-A. The resolving agent D-A must be separated from the solution with a back reaction. The other enantiomer of resolving agent L-A should be used as a resolving agent to yield the salt D-B.L-A which yields D-B enantiomer. The procedure is shown in scheme 1.

This procedure is mirror image related to each other and can be executed for separation of both enantiomers under same conditions

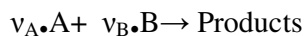
Resolution of a racemic base DL-B by acids D-A and L-A



Scheme 1: Explanation of Marckwald principle

Resolution with non stoichiometric quantities of reagents

Assume a general chemical reaction between two compounds A and B based on the stoichiometric coefficients v_A and v_B .



This represents also the formation of diastereomeric salts from a racemic chiral compound A and a resolving agent B. The requirements regarding stoichiometric feed supply can be conveniently expressed introducing the so-called stoichiometry feed ratio λ_r , defined as follows,

$$\lambda_r = \left(\frac{n_B^{\text{Feed}}}{n_A^{\text{Feed}}} \right) * \left(\frac{-v_A}{-v_B} \right) \quad \text{--- (1)}$$

Where n_B^{Feed} , n_A^{Feed} are number of moles of A, B in the feed.

If this ratio is 1, the feed is stoichiometrically composed. If $\lambda_r < 1$, less resolving agent is supplied than stoichiometrically required and unconverted racemate will remain. If $\lambda_r > 1$ unconverted resolving agent will remain. There will be also an effect on the rate of reaction (r

= $K \cdot C_A C_B$) due to changes in λ_r , which is not considered further in this work. This aspect is indeed not relevant here, due to the fact that the salt formation reactions are typically rapid.

As Classical Resolution is frequently used and very successful in an industrial scale, it appears to be important to deal more systematically with the relative amount of resolving agent. Instead of using stoichiometric amounts of both reactants (racemic acid or base and resolving agent), in some applications less resolving agent was used ($\lambda_r < 1$) [65]. This led to the formation of reduced amounts of both diastereomeric salts. Crystallization of the less soluble salt would occur if it is supersaturated in the solvent, while the more soluble salt would be undersaturated. This leads to the formation of only one salt in the solvent with low yield. The method was further extended to use only half of the required resolving agent and as the other half some other achiral acids or bases. But this approach is connected with the presence of some other salt. This concept involves the separation of a diastereomeric salt and an enantiomeric salt which could give better separation than the usual resolution. As an example the resolution of DL-tartaric acid was executed with variable quantities of cinchonidine [65]. Several similar experiments were executed also by Pope and Peachey [66, 67]. In some cases it was observed that the less soluble salt crystallized in the presence of an excess of resolving agent. This was found in the case of certain amines, where an excess of tartaric acid was used [68, 69]. In certain exceptional cases Armstrong proposed that reduced resolving agent might push the crystallization of one of the free enantiomers [70].

For this thesis the case working with more R.A was investigated in more detail, i.e. $\lambda_r > 1$. In this case unreacted R.A will remain in the solution. Less work was done up to now for this interesting case, which might lead to attractive separation enhancements.

The main steps for designing Classical Resolution are the selection of a suitable resolving agent, the molar feed ratio of resolving agent to racemic substrate (λ_r), the study of the crystallization behaviour of diastereomeric salts in a suitable solvent and identification of resolution process conditions, like concentration and temperature and effect of excess resolving agent on the crystallization of diastereomeric salts. Each of the mentioned effect will be discussed intensively further in this chapter.

3.2. Selection of resolving agent

A successful resolution of a racemate always depends on the selection of a suitable resolving agent. Selection of synthetic resolving agent rationally is not yet understood so far and the separation process is still dependent highly on the trial and error basis with different sets of

available resolving agents. Hoeve and Wynberg gave some basic qualities of a suitable resolving agent for diastereomeric resolution [71]. The criteria are not necessary to follow absolutely for the selection but they can be used as guidelines for new resolving agents design. Mostly followed characteristics for designing synthetic resolving agents are given below:

- To increase the ability to form salt a strong acidic or basic resolving agent should be chosen over weak acid or base (in many resolutions strong acids like chiral sulphonic or phosphoric acids are chosen over weak chiral carboxylic acids).
- The chiral centre of the resolving agent should be as near as possible to the functional group under reaction during the salt formation.
- Functionalities of the resolving agent should be several- this would increase selectivity and rigidity of the diastereomeric complex.
- Both enantiomers of resolving agent should be available at low prices and they must be chemically and optically stable during all steps of resolution process (they should not racemise).
- Resolving agent should not be toxic.

Based on the above mentioned guidelines, several resolving agents are screened for the racemates to be resolved in the laboratory scale. The stability of diastereomeric salts formed and separability of salts and then the recovery of resolving agent are considered in finalising a suitable resolving agent. Also efforts are under progress to design a resolving agent computationally, where the solubility ratio of two diastereomers obtained from solid-state properties act as a deciding factor [72].

3.3. Basic aspects in diastereomeric salt separation via crystallization

The second step in the Classical Resolution is separation of formed diastereomers. In the case of all dissociable diastereomers and for some covalent diastereomers crystallization is the best suitable and frequently used process. However, effective separation via crystallization processes not only depends on differences in individual salt properties but also on the behavior in the binary (both salts), ternary (two salts and solvent) phase diagram and metastable zone widths in a suitable solvent.

The different types of diastereomeric salt behavior are discussed in the following.

3.3.1. Different types of diastereomeric salt (mixtures) solid phase behaviour

In the literature very few diastereomeric salt pairs were studied systematically for their binary melting point phase behaviour and ternary solubility phase behaviour with the solvent. Ideally, (if there is no solvate formation, polymorph formation and no partial solid-solid solubility) there are three types of binary or ternary behaviour observed. They are 1) Simple eutectic, 2) Double salts, 3) Mixed crystals [13, 73].

3.3.1.1. Simple eutectic

The diastereomeric salts formed after the reaction with a resolving agent are taken as p-salt (less soluble salt) and n-salt (more soluble salt). The general binary melting point phase diagram and ternary solubility phase diagram for the simple eutectic behaving n-, p-salts are shown in Fig6. In the binary phase diagram (Fig 6(1)) the lowest melting point for mixtures is observed at only one composition of both salts at a mixture other than 50:50 of n-:p-salts. The eutectic composition is near to the low melting salt. The same trend is repeated in the solubility phase diagram shown in Fig 6(2). There exists only one eutectic composition (maximum solubility for the mixture of salts) in the solubility isotherm for different mixtures in the phase diagram. The position of eutectic can be defined via diastereomeric excess (d.e.). An example d.e. of p-salt calculation is given below

$$d.e._p = \frac{(x_p - x_n)}{(x_p + x_n)} \times 100 = -d.e._n \quad (2)$$

Where x is the composition of p-/n-salt in the mixture. Until today only 20% of the total diastereomeric salts investigated and applied show simple eutectic behavior [74]. Among all the types of diastereomeric salt (mixtures) solid phase behavior, simple eutectic is the most suitable type for a simple separation process via crystallization, because a separation is accessible direct from the racemic mixture without any additional diastereomeric enrichment step for either selective or preferential crystallization.

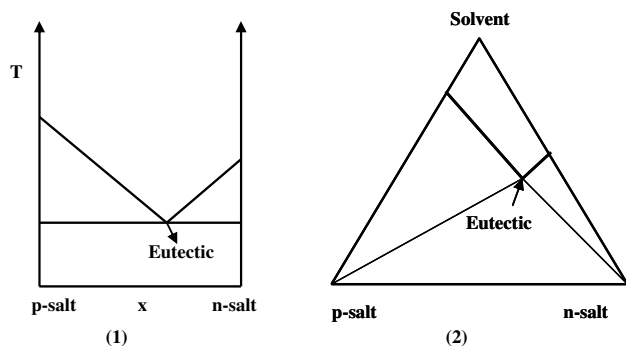


Fig 6: Model phase diagrams of simple eutectic system: (1) binary melting phase diagram, (2) ternary solubility phase diagram

3.3.1.2. Double salts

The second category of diastereomeric salts behavior is double salt formation, which involves the presence of both salts in the crystal lattice evenly at different compositions of both salts. Double salt behavior in diastereomeric salts can be considered as a racemic compound-forming behavior for enantiomers. Fig 7, gives a simple idea about the melting behavior and solubility behavior of diastereomeric double salts. The liquidus line in the melting point phase diagram and the solubility isotherm of ternary phase diagram contains two local minimum melting temperatures and two local maximum solubilities at two different diastereomeric excesses of both salts on both sides of 50:50 mixture of n-:p-salts. For double salts there could be even more eutectics at various diastereomeric excesses of both salts as there are more than one intermediate compound [73]. This type of behavior also gives a separation for the less soluble salt but reduces the yield and purity drastically by crystallizing counter diastereomer. Hence the double salt behavior of diastereomeric salts is not supportive for the separation via crystallization.

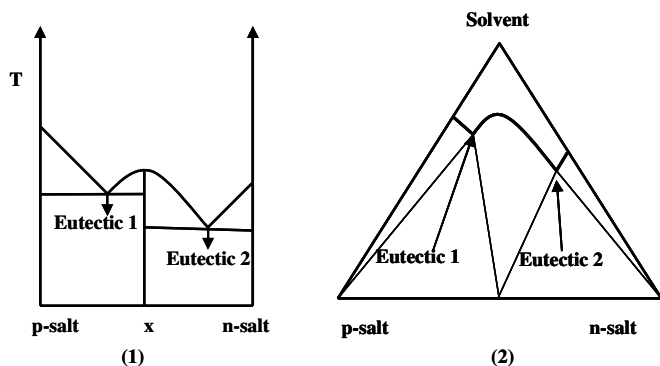


Fig 7: Model phase diagrams of double salts: (1) binary melting phase diagram, (2) ternary solubility phase diagram

3.3.1.3. Mixed crystals

The hypothetical binary and ternary solubility phase diagrams for third type of diastereomeric salts are shown in Fig 8. The molecules of both salts are present in the crystal lattice in an uneven manner. The melting behavior measurements of different mixtures of these salts show no eutectic melting peak at all and show only the total melting temperature. Hence, there exists no eutectic point at all (Fig 8(1)). The same kind of behavior can also be observed in the solubility phase diagram (Fig 8(2)). The solubility isotherm either increases its solubility continuously like a concave manner or like a convex manner. The trend can also be compared with the solid solutions behavior of enantiomers. This kind of behavior for diastereomeric salts is considered to be quite often as the number of examples is increasing. For example α -methylbenzylaminemandelate salts in water show this kind of mixed crystals trend [75]. Like double salts to separate salt pairs which show mixed crystal behavior via crystallization is also highly strenuous. Recent times, theoretical and practical study of binary and ternary phase diagrams for mixed crystals has become very interesting area of research [76, 77].

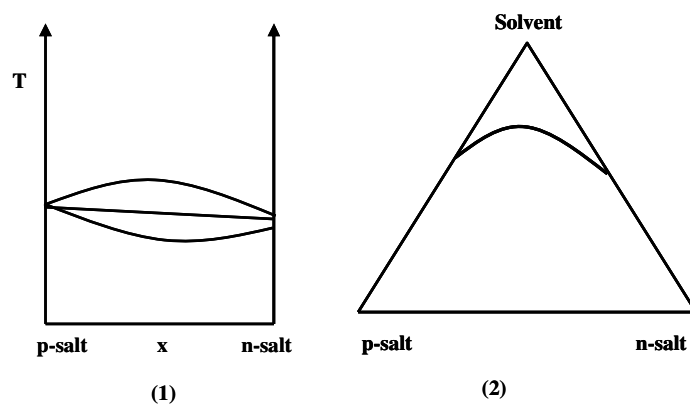


Fig 8: Model phase diagrams of mixed crystals: (1) binary melting phase diagram, (2) ternary solubility phase diagram

3.3.2. Effect of solvent

Suitable solvent selection is of prime importance for the diastereomeric salt resolution via crystallization. This has become very necessary as the solvent is not only a medium for solubilization for crystallization but also has the ability to form solvates by incorporating into the crystal lattice (e.g. hydrates in water) [78]. This solvate formation changes many parameters in the final crystallization separation of diastereomeric salts. Usually solvate formation of a substance changes the substance solubility, position of eutectic etc. Sometimes

solvate formation stabilizes the less stable diastereomeric salt crystal lattice and crystallizes the unwanted diastereomeric salt preferentially [2].

The next consideration for the solvent selection is solubility of the substance. The substance which should be separated should be of moderately soluble in the solvent and allowing a suitable crystallization process. According to Faigl et al, the resolvability has a great impact from the empirical polarity factor of the solvent [79]. Hence, for diastereomeric resolutions it is always helpful to select a solvent which is highly polar like water, methanol and ethanol. In almost all diastereomeric resolutions polar solvents played a major role. Sometimes based on the experimental requirement mixtures of solvents are also used.

3.3.3. Measurement of binary melting phase diagram

To proceed with the Classical Resolution, measurement of binary melting phase diagram which comes under the measurement of thermodynamic properties plays an important role. From the phase diagram first idea about the behavior of both diastereomeric salts (either simple eutectic or any other complicated behavior like mixed crystals or double salts) in binary mixtures can be identified. It also identifies the partial mixed crystal formation at certain parts of the phase behavior. According to D. Kozma, [80] if the composition of eutectic point is known via binary phase diagram and x-is the composition of higher melting salt in the eutectic then the efficiency of the resolution or resolvability (S) can be calculated via following formula.

$$S = \frac{(1 - 2x)}{(1 - x)} \quad \text{-- (3)}$$

He also proposed that the first idea about the eutectic composition thus resolvability can also be developed based on the melting behavior of 50:50 or any other composition of both diastereomeric salts, if the salts are non-decomposable with respect to temperature increasing. In the melting behavior of mixtures, for simple eutectic behavior, there exist two peaks. The first one indicates the eutectic melting and the second one validates the total melting of the mixture (liquidus temperature). In the case of solid solutions these two peaks merge and show only one sharp single peak. Based on the melting behavior of mixtures (example melting curve shown in Fig 9) determining the eutectic composition thus resolvability is explained below.

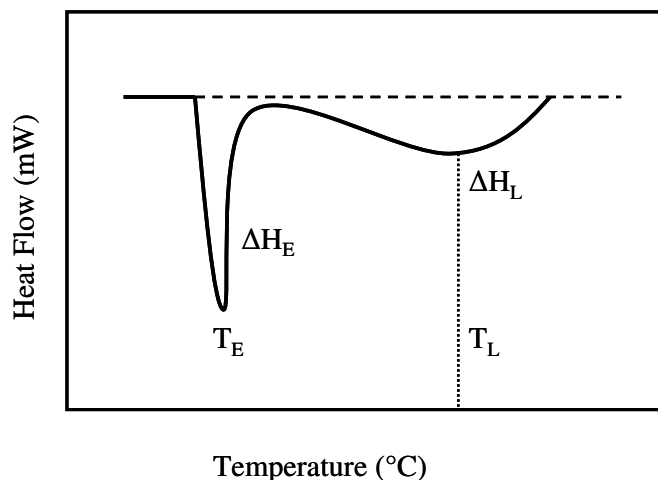


Fig 9: DSC melting behavior of 1:1 diastereomeric salt mixture

In figure 9, the eutectic melting is at T_E , liquidus temperature T_L with eutectic heat of fusion ΔH_E and the area under the second peak is ΔH_L . If x is the composition of higher melting salt in the eutectic then the heat of fusion of higher melting salt ΔH is proportional to ΔH_L which is shown in the equation below

$$\Delta H = \frac{(2 - 2x)}{(1 - 2x)} \times \Delta H_L \quad \text{--(4)}$$

The eutectic composition x_E can be found by substituting ΔH value in Schröder-Van Laar equation[81]. The final equation is given below. The value of x can be obtained by substituting ΔH value in the equation and applying different numerical methods.

$$\ln 2x = \frac{\Delta H}{R} \left(\frac{1}{T_L} - \frac{1}{T_E} \right) \quad \text{--(5)}$$

3.3.4. Solubility phase diagram

The systematic approach of crystallization based diastereomeric salt separation is completely oriented around the difference in thermodynamic properties. Among them the difference in melting points and solubility plays a vital role. Melting point phase diagram gives a first idea about the status of system like type of binary salt behaviour, possible eutectic composition etc [80]. If the materials are thermally unstable then resolution via melt crystallization is not a separation option. Usually the difference in the melting points of salt pairs also shows considerable effect on the difference in the solubility thus providing asymmetry in the ternary solubility phase diagram. The behaviour of pure diastereomeric salts and their mixtures, in the selected solvent, is necessary to plan resolution. First of all the behaviour must be a simple eutectic. The position of 2-salt saturation point (eutectic composition) should be as close to

the highly soluble salt as possible. Eutectic position decides the maximum possible yield. If the eutectic is near to the 50:50 mixture the selected separation for less soluble salt would be very low. On the other hand here salts can be separated preferentially by seeding one of the salts. A hypothetical ternary solubility phase diagram for two diastereomeric salts (n-, p-salt-simple eutectic in nature) with no solvates is shown in Fig10. Discussion about the ternary solubility phase diagrams with solvate formation was provided by Jacques et al [13]. In Fig 10(1), a single solubility isotherm at a particular temperature is shown. The phase diagram is divided based on the solubility isotherm. The area above the solubility isotherm is taken as region 1, which contains only single liquid phase unsaturated with both salts. In this region no crystallization can happen. The regions 2 are located at two separated areas for both the salts. In these triangular areas one solid phase (either n- or p-salt) and one liquid phase (saturated solution containing both salts) are present. In these areas there is only possibility for the crystallization of corresponding salt selectively (selective crystallization) [82]. In the region 3, two solid phases and one liquid phase are present. Here both salts have affinity for crystallization. To crystallize a particular salt in this region, kinetically driven preferential crystallization of one of the salt is necessary. In Fig 10(1), the two phase region area for p-salt is larger than that of n-salt as the eutectic is nearer to n-salt. This leads to the crystallization of p-salt than n-salt [83].

In Fig10(2), it is shown that when the initial composition of both salts in the solution is 50:50, then the position of initial point in the solubility phase diagram plays vital role in separation. If the initial experiment is started from the point (a) then the spontaneous crystallization would lead to the crystallization of solid at a salt composition of point (d) and leaves liquid composition at eutectic (f). If the crystallization is started at point (c) then pure solid of p-salt would crystallize but the mother liquor composition would remain at less than eutectic composition (end point (f)). This gives fewer yields than the maximum. To reach the maximum yield level, the crystallization of p-salt should start at a concentration of point (b). At the end of experiment ideally it is possible to achieve maximum yield with pure p-salt and presence of eutectic composition in mother liquor. The mother liquor can be used to crystallize with the seeds of other n-salt [84].

$$\text{Possible max.yield for p-salt at the particular isotherm by lever rule} = \frac{\overline{bf}}{\overline{ef}} \times 100 \quad \text{--(6)}$$

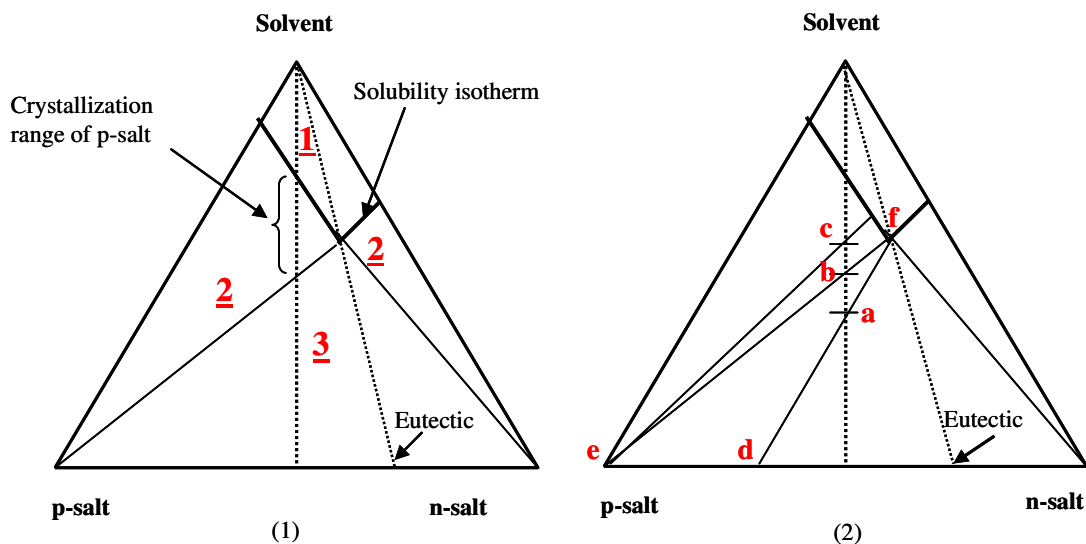


Fig 10: For diastereomeric p-, n-salts (a) Schematic explanation of simple eutectic phase behaviour with single solubility isotherm (b) general approach for separation of pure p-salt via crystallization

Usually thermodynamic properties are required to find the separation experimental conditions like temperature and concentration of solution. If the salts are thermally stable the separation experiment can be executed at the boiling temperature of the solvent to achieve maximum productivity [85]. Usually pharmaceutical substances are unstable at elevated temperatures. So the points a, b, c shown in Fig 10(2) can be reached via evaporation of the solvent in vacuum at 40°C.

3.3.5. Metastable zone width and different types of nucleation possibilities

To run successful crystallization-based resolution experiments, crystallization kinetics of the substances play a major role. In kinetics the major parts are metastable zone width for primary (homogeneous, heterogeneous), secondary (forced nucleation by seeding) nucleation, crystal growth (crystal size distribution), agglomeration and breakage of particles[86]. But to initiate a separation experiment the basic information necessary is metastable zone width for primary nucleation (also called maximum sub-cooling, beyond this region spontaneous nucleation occurs) for all the pure salts in the solvent to decide the primary or secondary nucleation for the crystallization of desired salt. Usually for a pure substance the solubility and nucleation curves are plotted in concentration against temperature plot e.g. shown in Fig 11.

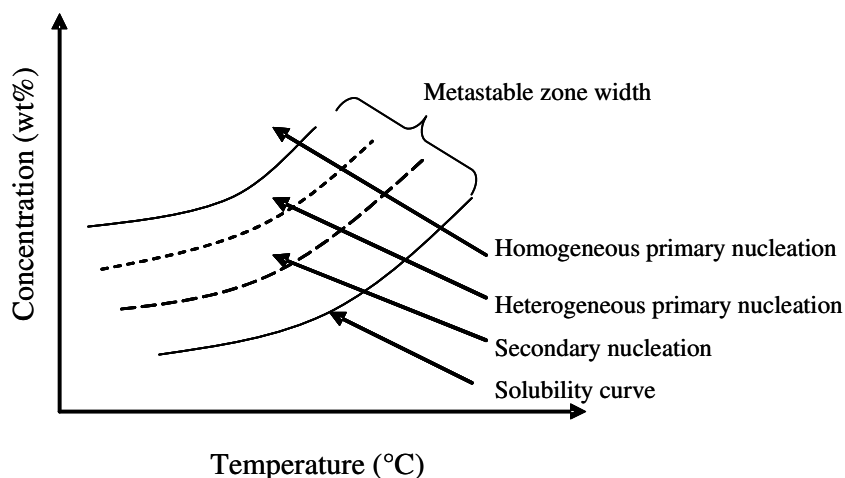


Fig 11: Solubility and different nucleation possibilities for a pure diastereomeric salt in a selected solvent

Fig 11, indicates the different stages of concentration of a solution with respect to temperature. The zone below the solubility curve is called unsaturated region. In this zone no crystallization happens at all. All the substance present would dissolve completely and form a clear solution.

If the concentration of the solution is above the solubility curve then it is supersaturated (approached either by cooling the solution or by evaporating the solvent or by both or adding an anti-solvent which gives lower solubility). Initially, up to a certain range of this supersaturation no spontaneous nucleation occurs. This region is called metastable zone width for primary nucleation. Beyond this zone (high supersaturation) spontaneous and rapid nucleation would occur. In crystallization-based separation experiments metastable zone width is the place to focus as it is the control area for regulating crystallization. In this area nucleation can only be induced by external influence. There are different types of induced nucleation like heterogeneous primary and secondary nucleation- nucleation of the substance based on the metal surfaces of reactor or surface of stirrer or scratching the walls and introducing seeds of another impurity (if the seeds of required substance is not available) respectively. Secondary nucleation- seeds of the same substance are given so that crystal growth would occur for the required substance. In diastereomeric resolution the metastable zone width for primary nucleation for both salts should be known. Further introducing seeds of the required salt would increase the nucleation of same salt either selectively or preferentially based on the process condition [87].

3.3.6. Effect of excess resolving agent

During Classical Resolution, exploiting non-stoichiometric feed ratio ($\lambda_r > 1$ or $\lambda_r < 1$) would always leave unreacted reactants in the solution (given in chapter 3.1) [88]. In case of $\lambda_r > 1$, some R.A will be left unreacted and in case of $\lambda_r < 1$ some racemate will be left unreacted. These excess reactants may have a great influence on the crystallization based separation processes. They behave as impurities in the solution and affect the yield of the final product. Crystallization of pure pharmaceutical chemicals from a solution containing impurities always faces challenges. If there is another substance (an impurity) in solution, it may influence crystallization separation in many ways. A considerable quantity of impurity can bring changes in solubility and can vary metastable zone widths in the solvent. An increase or decrease in the nucleation rates and crystal growth rates can also take place in the presence of different types of impurities. A slight quantity of impurity can enhance the chance of formation of new polymorphs and bring changes in the crystal size distribution [89]. All the above properties, influenced by impurities, are very important in the design of a crystallization process as well as for crystallizer design. Usually, the presence of an impurity increases or decreases the solubility. It may also not change the solubility of pure substance [90]. Each of the above possibilities could be useful based on the specific problem dealt with. An increase in the solubility might also increase the metastable zone width, which increases the supersaturation that can be applied and thus, higher yields can be achieved. An excess of resolving agent is sometimes used ($\lambda_r > 1$) during diastereomeric salt resolution to avoid unreacted racemate in the solution. In this case, to design an effective resolution process, it is necessary to evaluate the effect of excess resolving agent on the basic properties (solubility, metastable zone width, polymorphism etc.) of both diastereomeric salts [91]. The effect can be used for the modification of process parameters.

3.3.7. Recovery of enantiomers and resolving agent

When the both diastereomeric salts from the solution are separated successfully it is necessary to obtain individual enantiomers and recovery of resolving agent. Even though it is the last step in the Classical Resolution, care must be taken to avoid undesired racemization of separated chemical species. The method of enantiomer formation must be very simple. Usually if a chiral base like amine is resolved with an acidic resolving agent, during the final amine separation it is stirred with a diluted strong base like NaOH, Na₂CO₃ or NH₄OH. Then the amine is extracted with an organic solvent and purified acidic resolving agent can be recovered [92, 93]. Same procedure is also followed for a chiral acid and basic resolving agent recovery with an aqueous acid. Many examples are available in literature in this

context. If this process fails for the diastereomeric salts which are highly water soluble, methods like ion exchange resins can be used. Mostly in Classical Resolution only one of the enantiomer is recovered from the racemic compound via Classical Resolution which keeps the yield at low values. Racemization of unwanted enantiomer would increase the total yield.

3.4. Dutch resolutions

One more trend in practice for Classical Resolution is selection of a family of suitable resolving agents instead of a single resolving agent. This process is also called as Dutch resolution [94]. Here a mixture of multiple resolving agents having similar molecular structures is applied for example camphor sulphonic acid and bromo camphor sulphonic acid. The major advantage for this separation is nucleation inhibition of higher soluble salt by the salt impurities that are present in the solution. This could increase the less soluble salt to crystallize more. But to apply this techniques the salts (that must be separated) should have certain properties like- both salts should be crystalline, the precipitated salt during crystallization should have considerable diastereomeric excess and there must be significant difference in the solubility of the salts. Despite such complications, in many of industrial applications Dutch resolution is still used for chiral separation. Nowadays many commercial kits are available with wide variety of family of resolving agents to screen rapidly for different chiral racemates [95].

3.5. State of the art

Optical resolution via formation of diastereomeric salts and separation via crystallization is used for almost 65% of all the chiral substances as this technique can be easily adopted in the industrial environment [13].

Additionally, advantages like low initial investment for equipment for different process steps during Classical Resolutions, easy coupling option for racemization to reduce industrial waste and always superiority over other techniques in the case of enantioseparation kept Classical Resolution as the one of the major separation techniques for industrial optical resolutions.

Even though Classical Resolution is very old technology, still the selection of suitable resolving agent is trial and error basis. Different resolving agents are tried for the racemate to be resolved and best resolving agent is selected based on different landmarks like availability of resolving agent in optically pure form, low cost, easiness in diastereomers formation, crystallinity of formed diastereomeric salts, not racemising during resolution process and easiness in the final enantiomer recovery process.

Only a few examples were observed in the systematic study of ternary solubility behaviour of diastereomeric salts. Statistically the formation of simple eutectic in diastereomeric salts (around 20%) is higher than formation of conglomerates (just 5-10%) in enantiomers. Formation of solvates for one or both diastereomeric salts is also a general problem for diastereomeric salts. The other two types of behaviours (double salts and mixed crystals) are also commonly observed in the case of diastereomeric salts. Formation of mixed crystals is more often in the case of diastereomeric salt molecules which have high coefficient of geometrical similarity. Diastereomeric salts formed by various resolving agents might show different ternary phase behaviour even though resolving agent structures are similar.

Solvent selection also has a considerable effect on the diastereomers behaviour in the ternary solubility phase diagram (solvate formation, eutectic composition). Very few kinetic studies were done for diastereomeric salts as most of the separation processes depend on the thermodynamic properties (solubility, melting point difference).

The probability of separation for the less soluble diastereomeric salts from the initial data of DSC melting curves is given explicitly by D.Kozma [2, 80]. It is applicable majorly for salts with no decomposition.

Designing an effective separation process from phase diagrams is being discussed by D. Kozma and K.M. Ng et al (for Ibuprofen) but many of the crystallization based diastereomeric salt separation process are executed via random process selection [2, 96]. Type of crystallization for separation process based on the product stability also plays important role.

The application of selective crystallization is sufficient to separate less soluble salt from the diastereomeric salt mixture (if the eutectic is near to the highly soluble salt) but to achieve both salts in pure form application of selective and preferential crystallization are highly supportive. Success of selective crystallization highly dependent on the thermodynamic data (phase area for less soluble salt) while preferential crystallization becomes successful mainly based on the kinetic data (metastable zone width, type of nucleation and seeds introduction).

Classical Resolution exploiting non stoichiometric mixture of racemate and resolving agent has a strong impact on the course of the crystallization process. The unreacted reactants would act as an impurity during the crystallization of desired diastereomeric salt. Very less number of studies was observed for the effect excess resolving agent (if used during reaction) on the thermodynamic and kinetic properties of diastereomeric salts, which has considerable effect on the final crystallization based separation process as an impurity.

According to Dutch resolutions, there would be considerable increase in the yield during resolution of a racemate, if a family of resolving agents with similar chemical structure are used instead of a single resolving agent. It was also proved with family of tartaric acid family and also with camphor sulphonic acid family. But solid solution formation is still a major issue in this technique. Theoretical studies are under progress to analyse the possibility of formation of mixed crystals during Dutch resolution.

All the above coped aspects were considered throughout the present research work and studied in the case of selected model chiral racemic substances.

4. Substances selected and synthesis of diastereomeric salts

Chapter 4

Substances selected and synthesis of diastereomeric salts

4.1. Racemates to be separated

In chapter 2 mentioned separation techniques are costly and very complicated processes compared to Classical Resolution for separation of different compound-forming substances, which occupies major portion of total chiral chemicals. The present work is completely directed on the separation of compound-forming racemates into their pure enantiomers systematically. As examples two racemic compound-forming substances DL-serine and DL-phenyl glycine are selected [97, 98]. The general properties of these substances and different widely used resolving agents selected for application of Classical Resolution are discussed in this chapter.

4.1.1. Serine

Serine is a polar amino acid with three functional groups (carboxylic, amino, hydroxyl-groups) in its chemical structure shown in Fig 12 [99, 100].

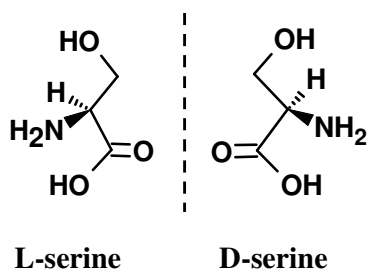


Fig 12: Chemical structure of both L-/D-serine enantiomers (MW-105.09)

The enantiomers of serine have different applications. The L-enantiomer of serine occurs in animal metabolism and plays a vital role in animal diets, whereas the D-enantiomer of serine contains no nutritional values. L-serine is also a precursor for synthesis of many substances in mammals like glycine, L-cystathionine, purines, thymidines and porphyrins. It is used as a starting material for many organic compounds like peptides and also used in cosmetics and medicines [101]. D-serine is used as an intermediate for synthesis of antibiotics like cycloserine [102]. In humans brain, D-serine works as a physiological coagonist of a key neurotransmitter receptor, the *N*-methyl-D-aspartate-type glutamate receptor [103]. Due to the variation in the applications of both enantiomers it is essential to generate both enantiomers with high purity.

The ternary phase behavior of enantiomers and racemate of serine is given in Fig 13 [1]. The phase diagram is symmetrical on both sides of isoplethal line of racemate. The solubility of enantiomers is particularly high when compared to the solubility of racemic serine. The

solubility maximum is observed between the racemic mixture and pure enantiomer at a composition greater than 99% of L-serine.

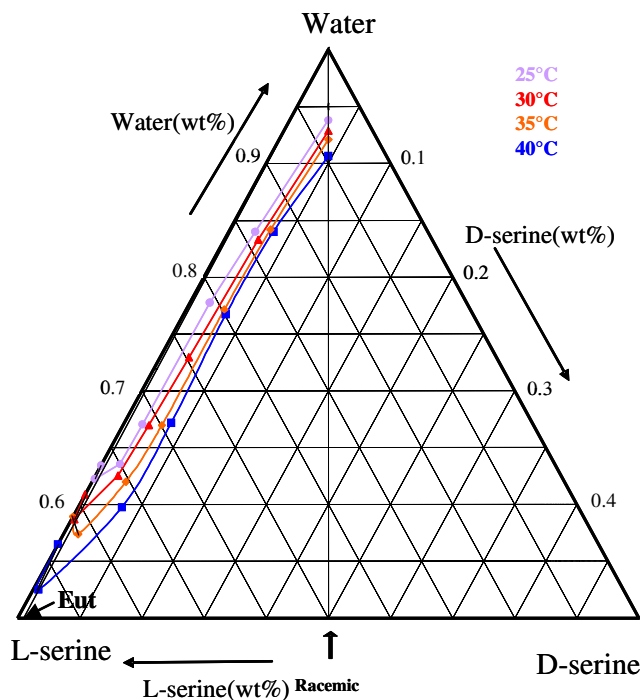


Fig 13: Ternary solubility phase diagram for serine in water[1]

4.1.2. Phenyl glycine

Phenyl glycine is an amino acid with D-phenylglycine has a significant use for the synthesis of new drugs such as aspoxicillin, cefbuperazone, and cefpyramide [104, 105]. L-Phenylglycine is a starting substance for L-aspartyl-L-phenylglycine methyl ester, which is used as a sweetener [106]. The structure is shown in Fig 14.

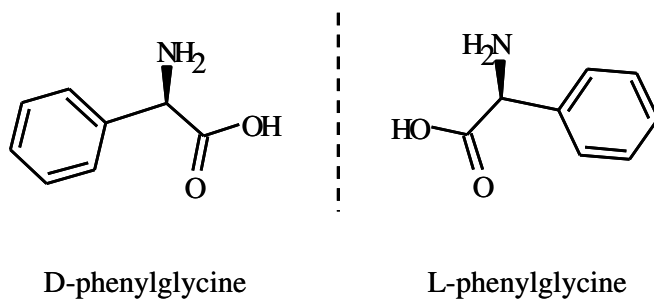


Fig 14: Chemical structure of D-/L-phenylglycine (MW-151.16)

According to literature it is clear that phenyl glycine falls under racemic compound-forming substances [107]. In our laboratory also preliminary tests like XRPD measurements and DSC melting points were measured to finalize its binary behavior. The XRPD patterns of D-/L- and

DL-phenyl glycine are shown in Fig 15. The XRPD pattern of L- and D- phenyl glycine is same at all diffraction angles in Fig 15, while DL-phenyl glycine has a different XRPD pattern compared to its enantiomers. This gives a great support that these two enantiomers show racemic compound-forming nature.

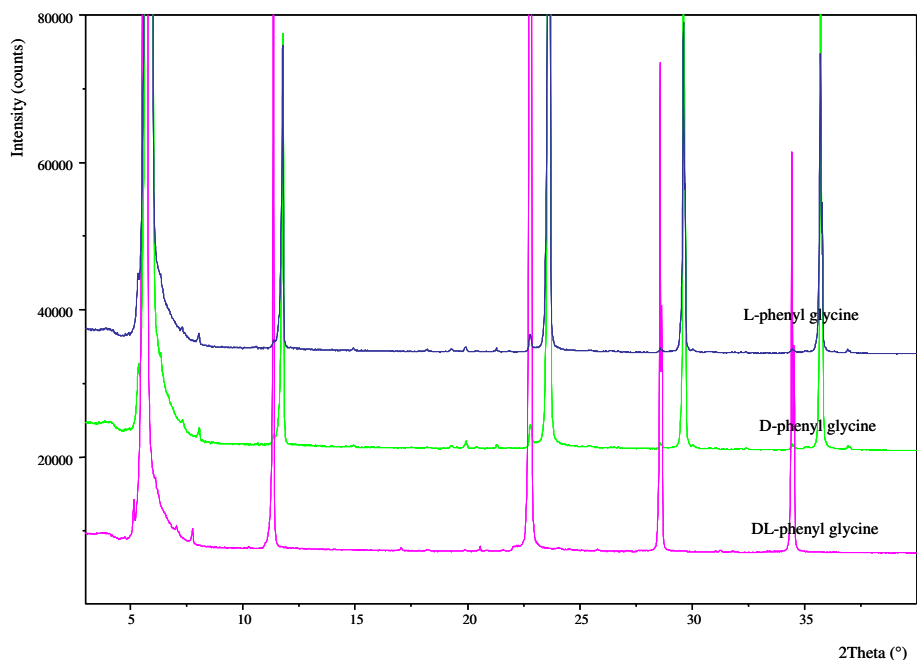


Fig 15: XRPD patterns for D-/L- and DL-phenyl glycine

4.1.3. Selected resolving agents

As stated in chapter 3.2, the first part of Classical Resolution, the selection of a resolving agent is not trivial. Especially for serine which is an amino acid, to apply Classical Resolution, alkaloids (which are active to react with carboxylic group) or chiral acids (which are ready to react with amine group) can be used. In general alkaloids such as brucine, cinchonine or quinine have a disadvantage like toxicity and availability of only one of the enantiomers [108-110]. Hence, for serine the problem is solved easily by selecting some commonly available acidic resolving agents like 2,3-dibenzoyl-D/L-tartaric acid, L(+)-tartaric acid, L(+)-mandelic acid, 2,3-ditoluyl-D-tartaric acid. These resolving agents are used quite commonly in the resolution of racemic amines [111, 112]. The both enantiomers of these resolving agents are commercially available. In the case of Phenyl glycine resolution, the optically active 1S-(+)-Camphor-10-sulphonic acid is used [113]. The chemical structures of all the resolving agents are shown in Fig 16. The general properties of these resolving agents are well given in the literatures [2, 13].

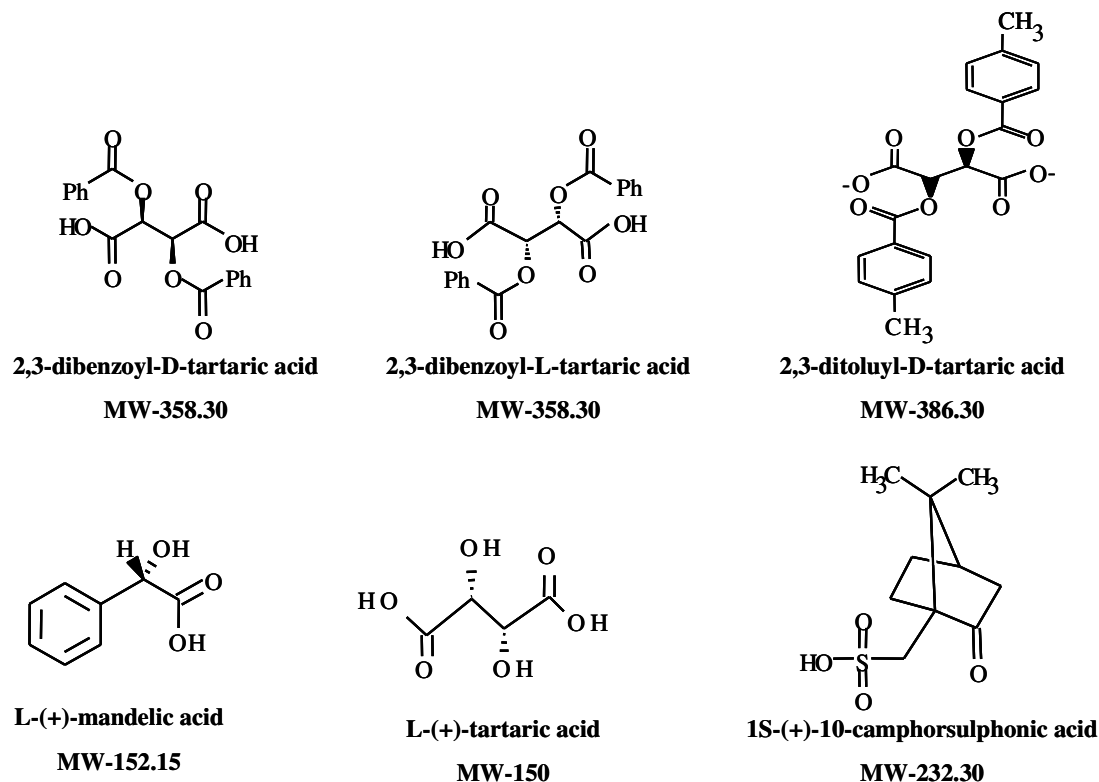


Fig 16: Chemical structures of commonly used acidic resolving agents

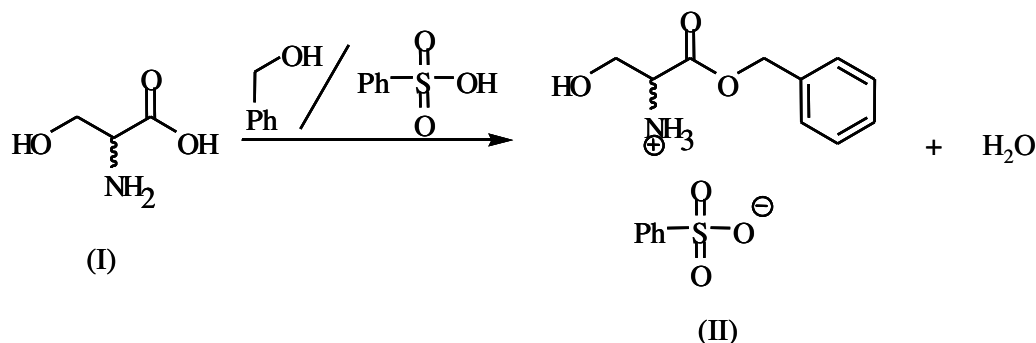
4.2. Synthesis of diastereomeric salts

4.2.1. Synthesis of serine diastereomeric salts

An in-house laboratory synthesis was executed for the diastereomeric salts of DL-serine as they are not available commercially. Serine is an amino acid having both an amino group and a carboxylic group in its chemical structure. A self-reaction between these two active functional groups might occur during the diastereomeric salt formation with the selected resolving agents. This problem can be avoided if one of these two functional groups would be derivatized by reacting with an achiral substance [114-116]. The derivatized substance can be reacted with the optically active chiral resolving agent to form the diastereomeric p- and n-salt of serine. The synthesized salts are characterized by ^1H NMR, XRPD and DSC. When the pure substances are synthesized, the materials were used to measure different phase behaviors which are necessary for crystallization process. A step by step procedure for the synthesis is shown below.

a) L-/D-serinebenzylesterbenzenesulfonate (MW-353.39)

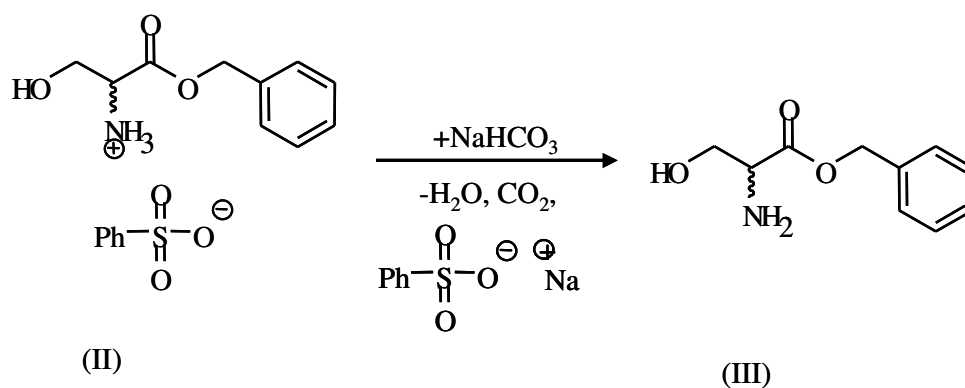
The esterification step was processed initially for the carboxylic group of L-/D-serine (I) with benzyl alcohol to form L-/D-serine benzyl ester. This is done in the presence of the strong acid benzene sulfonic acid in CCl_4 . The product from the reaction process is L-/D-serine benzyl ester benzene sulfonate (II). The reaction is shown in scheme 2 [117]. The substance (II) is commercially available. Hence the synthesis of the all serine diastereomeric salts started with substance (II) as initial reactant.



Scheme 2: Esterification of D-/L-serine

b) L-/D-serine benzyl ester

The second step of synthesis is separation of D-/L-serine benzyl ester (III) from substance (II). Here 15g (0.042 mol) of L-/D-serine benzyl ester benzene sulfonate (II) was titrated with 75ml of 5% NaHCO_3 aqueous solution at 0°C to yield L-/D-serine benzyl ester (III). The reaction procedure is shown in scheme 3.

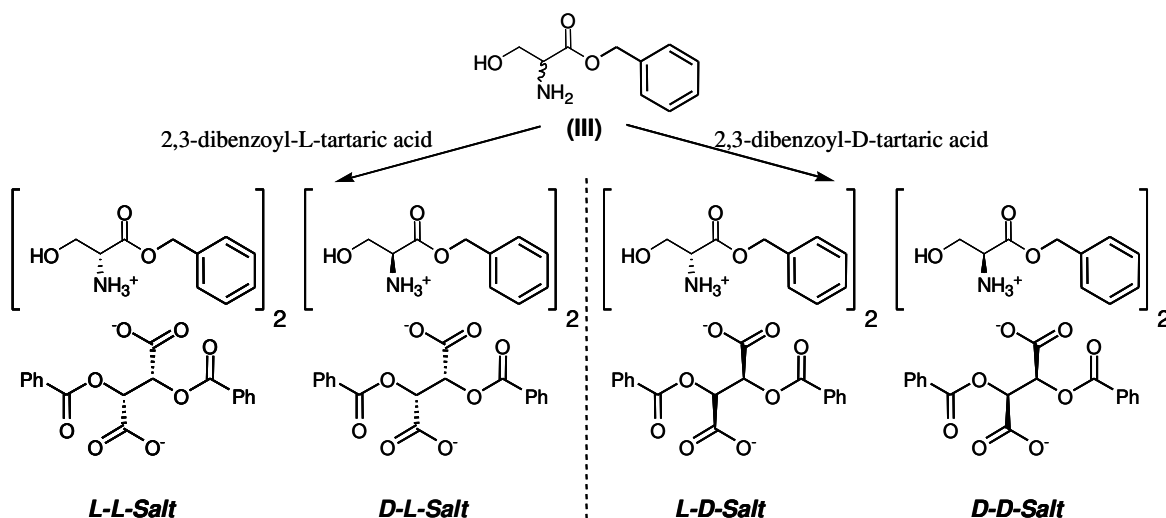


Scheme 3: Formation of D-/L-serine benzyl ester (III) (MW-195.18)

The organic matter (product) was separated from the aqueous solution by the addition of 65ml of a 4:1- chloroform: isopropanol mixture. The same extraction procedure was carried three times. Then the separated organic solution was dried over anhydrous Na₂SO₄. Finally, L-/D-serine benzyl ester was recovered by evaporation of both solvents under vacuum. The crude material obtained was used in the next step of synthesis without any further purification.

c) L-/D-serine benzyl ester- 2, 3-dibenzoyl-L/D-tartrate salts (D-D, L-D; D-L, L-L) (Pair 1 and 2)

8.27g (0.042 mol) of crude liquid of L-/D-serine benzyl ester (III) was taken in a flask and dissolved completely in 12ml of methanol. Then the solution was mixed with a solution containing 15.5g (0.043 mol, 100% excess) of 2,3-dibenzoyl-D-tartaric acid in 45ml of absolute methanol. The mixture was stirred vigorously to give a theoretical yield of 15.87g (0.021 mol) of L-/D-serine benzyl-2,3-dibenzyol-D-tartrate salts (L-D or D-D-salt). In the same manner, when 15.5g (0.043 mol, 100% excess) of 2,3-dibenzoyl-L-tartaric acid was used as resolving agent to react with substance (III) then L-/D-serine benzyl-2,3-dibenzyol-L-tartrate salts (L-L or D-L-salt) was formed. This is shown in reaction scheme 4 below.



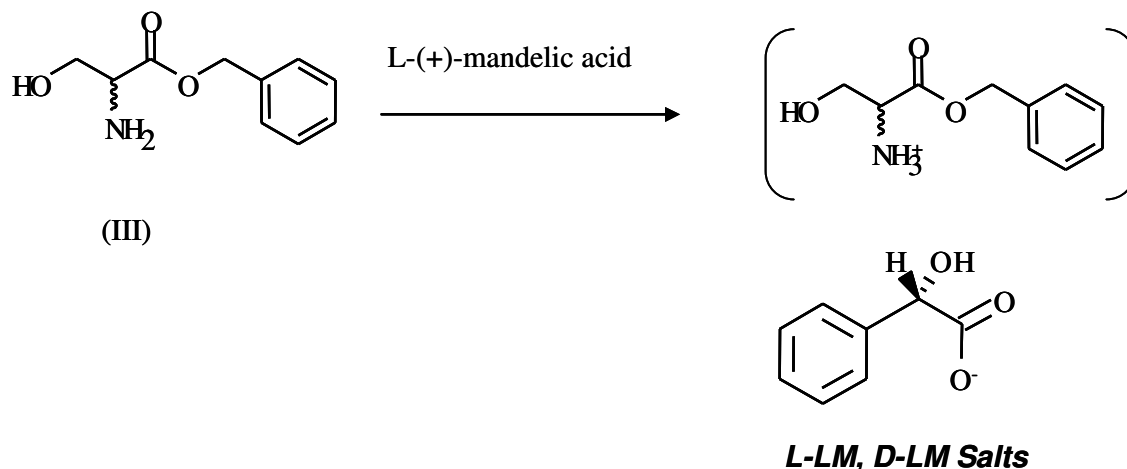
Scheme 4: Formation of L-L, D-L; L-D and D-D salts(MW-748.66)

In case of the D-L and L-D salts, they precipitated immediately during the reaction while the L-L and D-D-salts were not. The substance was recovered from methanol completely by adding an anti-solvent, diethyl ether. To get a complete precipitation of salt the solution was kept under stirring for another 48 hours. The synthesized salts were purified by repeated recrystallization steps in methanol separately[118]. Each time after recrystallization step, the

melting point of the salt was measured by using a differential scanning calorimeter (DSC-131, Setaram, France). The purification was repeated until the melting point was stable. Further, purity of the salt was also analyzed by ^1H NMR followed by DSC and X-ray powder diffraction to check the presence of impurities, solvates and crystallinity. A sample of 10mg of salt was dissolved in a sufficient amount of pure dimethyl sulfoxide-d₆ (obtained from Deutero GmbH, Germany) and the sample was tested with ^1H NMR. When the material was proved to contain no impurities and not form solvates, a small sample of salt was crushed into powder and characterized by X-ray powder diffraction (XRPD) on an X'pert Pro diffractometer (PANalytical GmbH, Germany) with CuK α radiation.

d) L-/D-serine benzyl ester- L-mandelate (L-LM, D-LM salts) (Pair 3)

8.27g (0.042 mol) of L-/D-serine benzyl ester (III) was allowed to dissolve in 12mL of methanol solvent. To this solution, 13.56g (0.089mol, 100% excess) of completely dissolved L-(+)-mandelic acid in methanol was added and stirred strongly to yield 15.05g (0.042 mol) of L-/D-serine benzyl-L-mandelate salts (L-LM or D-LM salts). This is shown in scheme 5. The same purification procedure explained in the case of L-D, D-D salts was also followed during the synthesis and characterization of pure L-LM and D-LM salts.

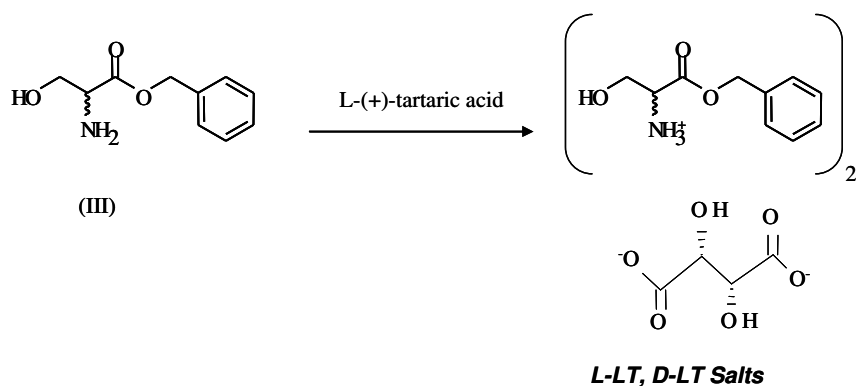


Scheme 5: Formation of L-LM, D-LM salts (MW-347.33)

e) L-/D-serinebenzylester- L-tartrate (L-LT, D-LT salts) (Pair 4)

Also during the synthesis of L-LT and D-LT salts, a completely dissolved solution of 8.27g (0.042 mol) of L-/D-serine benzyl ester (III) in 12mL of methanol was taken in a reactor. Then to this solution, 6.69g (0.045mol, 100% excess) of L-(+)-tartaric acid in 10ml of methanol solution was added and mixed completely to form 11.46g (0.021 mol) of L-/D-serine benzyl-L-tartrate salts (L-LT or D-LT) at room temperature. To gain the pure salt out

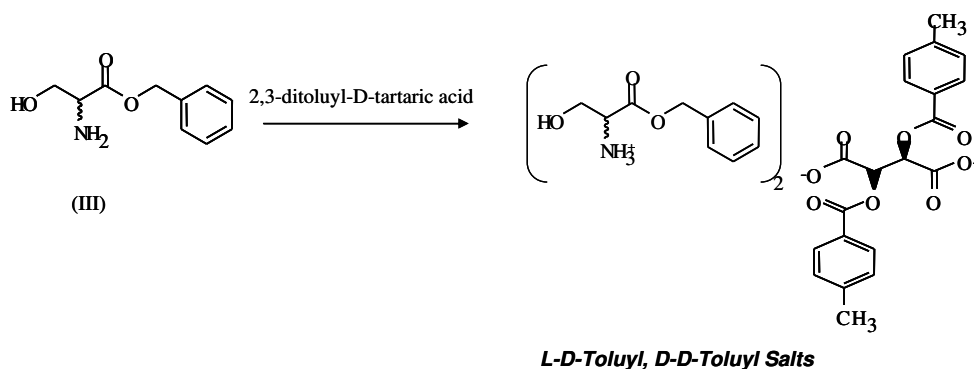
completely diethyl ether was added after half an hour. The reaction procedure is shown in scheme 6. The synthesized salts were purified via repeated recrystallizations and characterized by different analytical techniques like ^1H NMR, DSC and X-ray powder diffraction.



Scheme 6: Formation of L-LT, D-LT salts(MW-540.45)

f) L-/D-serinebenzyl ester-2,3-ditoluyl-D-tartrate (L-D-Toluyl, D-D-Toluyl salts)(Pair 5)

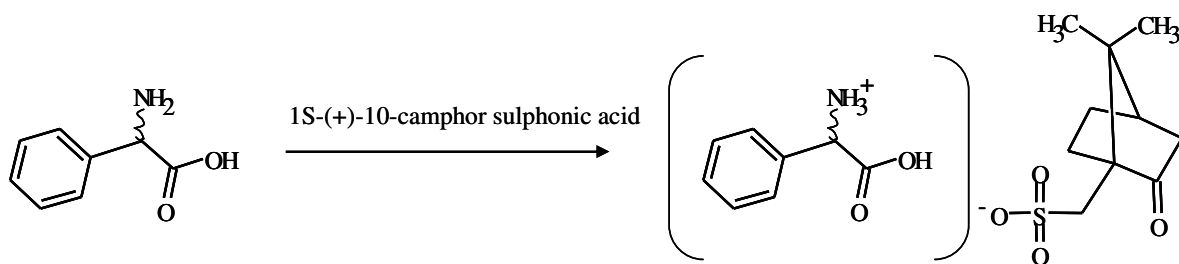
Synthesis of L-D-Toluyl and D-D-Toluyl salts were done by mixing a completely dissolved solution of 8.27g (0.042 mol) of L-/D-serine benzyl ester (III) in 12mL of methanol with a solution of 16.37g (0.042 mol, 100% excess) of 2,3-ditoluyl-D-tartaric acid in 10ml of methanol solution. Both reactants were allowed to react in methanol medium under vigorous mixing at room temperature for 24 hours to form one mole of L-/D-serine benzyl ester-2,3-ditoluyl-D-tartrate (L-D-Toluyl or D-D-Toluyl salt). To precipitate the salt completely from methanol solution, 350ml of diethyl ether was added after about 30 min of reaction time. The reaction procedure is shown in scheme 7. The precipitated pure salts were filtered from solution and purified via repeated recrystallizations. The purified salts were characterized by ^1H NMR, DSC and X-ray powder diffraction.



Scheme 7: Formation of L-D-Toluyl, D-D-Toluyl salts (MW-776.66)

4.2.2. Synthesis of phenyl glycine diastereomeric salts (Pair 6)

10g (0.066mol) of L-/D-phenyl glycine was dissolved in 20ml of methanol. It was combined with 16g (0.688 mol) of the selected resolving agent 1S-(+)-10-camphor sulphonic acid dissolved in 30mL of absolute methanol and stirred vigorously to yield 25.33(0.066mol) of L-/D-phenyl glycine-1S-(+)-camphor-10-sulphonate salts (LPG-CS/DPG-CS-salt). The reaction is shown in the scheme 8with chemical structures.



Scheme 8: Formation of LPG-CS, DPG-CS salts (MW- 383.78) [107]

Both DPG-CS and LPG-CS salts were precipitated partially after the synthesis. To achieve a complete precipitation of these salts from methanol, an anti-solvent diethyl ether was added to the solution and allowed to crystallize for 24 hours under stirring in the reactor. Later the salts were purified from impurities via recrystallization. Solvent used for recrystallization was acetonitrile (HCN). As a first guess for the purity of the substance, melting point was measured for the salt at the end of every recrystallization step by DSC. Recrystallization steps were repeated until a fixed melting point was reached. Finally, to characterize the salt purity, formation of no solvates and crystallinity, analytical tests were also done with the help of ^1H NMR and X-ray powder diffraction. When the material was out of impurities and solvates, the salts were characterized by melting point and XRPD patterns.

4.3. Summary

In the chapter 4, the basic part for the application of Classical Resolution to chiral compound-forming substances, is discussed. The selection of exemplary compound-forming substances with known properties, the search in the literature for different suitable resolving agents for the diastereomeric salt formation is given. Further, synthesis and characterization procedure for diastereomeric salts of both serine and phenyl glycine are discussed in detail with schematic diagrams.

5. Experimental techniques and analytical methods used

Chapter 5

Experimental techniques and analytical methods used

5.1. Experimental techniques

5.1.1. Melting phase diagram measurement

Attempts were made to measure melting point phase diagrams for all the pairs of diastereomeric salts synthesized [119, 120]. Equipment named differential scanning calorimeter (DSC) was used. Samples of different compositions were prepared carefully by measuring the weights of both salts into a mortar. To ensure the uniform mixing in the mortar the samples were crushed and mixed completely. To make the salts distribution even better the mixture was dissolved in appropriate solvents like methanol, acetone or ethanol accordingly for respective salt pairs. The dissolved salt mixture was recrystallized by evaporating the solvent completely and they were once again mixed and crushed to a uniform mixture. A quantity of 10-15mg were taken into the aluminum crucible and allowed for melting in the DSC with a heating and cooling program. Initially the sample was allowed to be at a constant temperature. Then a strong heating rate of 5K/min was given up to certain range of temperature. In the third step a low heating rate of 2K/min was used till the end of melting to increase the accuracy in the melting temperature. Finally the sample was cooled to room temperature with a cooling rate of 10K/min. A continuous purge gas flow of about 8ml/min pure helium was used throughout the experiment.

5.1.2. Solubility measurements

Theoretical calculation of solubility data is often not so accurate for practical experimental designs. Therefore, the required data can be obtained only by solubility measurements. There are several types of static methods available for the determination of solubility in the laboratory [121]. In these methods the temperature, pressure and composition (when equilibrium is reached) of the system are kept constant. If the solubility of the substance is approximately available, the exact value can be obtained by taking an excess of solute concentration in the solution (Isothermal excess method) [120, 122]. The sample present in the solution is dissolved at high temperatures completely and allowed to recrystallize at the desired temperature. The process is continued until the equilibrium concentration is attained. If no approximation of solubility is available, then small amounts of solute are added to the solvent in the intervals of time until some non-dissolved crystals remain in the solution for a long time i.e. till the equilibrium is attained in the solution (Successive solute addition). The equilibrium approach for the solubility measurements is shown in the Fig 17 for both processes.

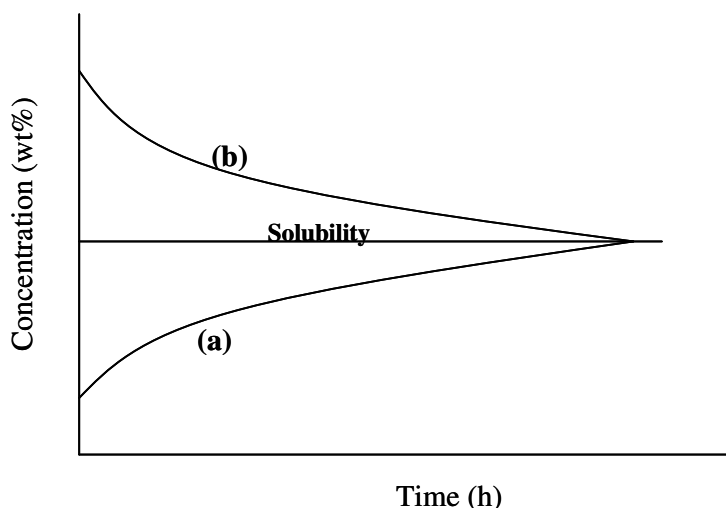


Fig 17: Determination of the time necessary to reach equilibrium at particular Temperature for solubility measurements (a) Successive solute addition method (b) Isothermal excess method.

Solubility experiments were also done by the successive solute addition method to the solvent at isothermal conditions at all the selected saturated temperatures. Small glass sample holders (5mL) were prepared with defined composition and concentration of pure salt or mixture of salts in the selected solvent. Magnetic stirrer was used to keep uniform mixing in the solution. It was operated at 500 rpm in the vessel. This glass vessel was immersed in a double walled thermostatted apparatus. Known amounts of pure or salt mixtures were added to the system until undissolved solute remains in the solution. Same conditions were maintained in the solubility equipment for 48 hours to confirm equilibrium condition in the sample vessel. Next the solid and liquid phases were separated via vacuum filtration and they are further analyzed for concentration and composition. The solubility (solute concentration in wt%) was calculated via gravimetric method [123]. In this method the solution was taken into an empty flask (weighed before and after solution addition) and allowed for solvent evaporation. When the solvent evaporated completely with time, the flask with left over solute was also weighed. Finally solubility of solute in the solvent is calculated with the formula given below:

$$\text{Solubility (wt\%)} = \frac{\text{wt(Solute)}}{\text{wt(Solute)} + \text{wt(Solvent)}} * 100 \quad \text{-- (7)}$$

A small amount of liquid phase was taken in a HPLC vial and was diluted with methanol. The collected liquid phase sample was analyzed with HPLC. In addition the liquid sample was analyzed with the refractometer for measuring the concentration of solute dissolved in the solvent. The solid sample left on the filter was analyzed with XRPD for the quality of the crystals. The equipment used for the solubility measurements is shown in Fig 18. To ascertain the reproducibility of solubility data, each solubility data point was repeated twice with Isothermal excess method as well.

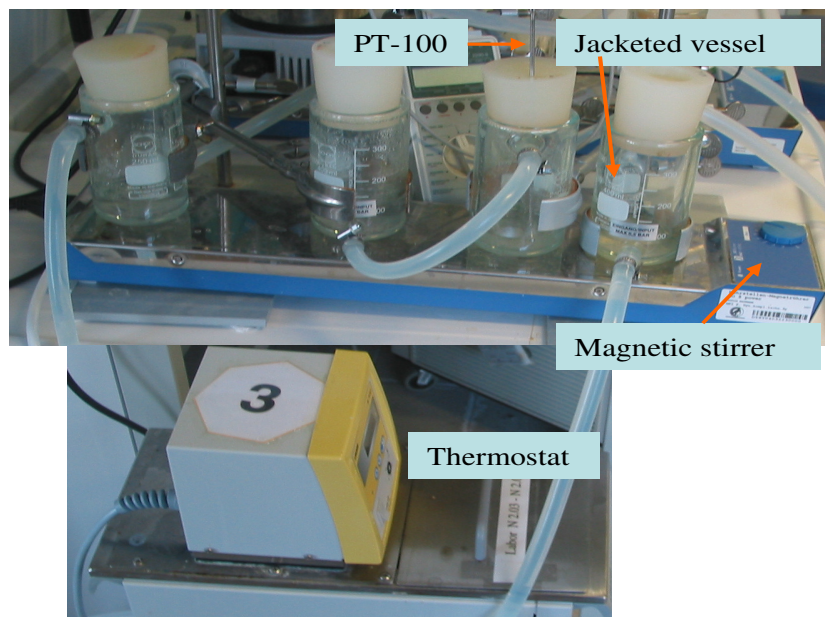


Fig 18: Conventional isothermal solubility measurement equipment

HPLC analysis

An HPLC method was developed to analyze quantitatively both *p*- and *n*-salts in liquid samples from solubility and resolution experiments. A Crownpak CR 150 × 4.6 mm column and a mobile phase of 1.63 g perchloric acid in 1 L water at a pH of 2 were applied. The flow rate was 0.3 mL/min and the pressure 46 bar.

XRPD analysis

Solid phase samples were analyzed by X-Ray Powder Diffraction on a PANalytical X'Pert Pro diffractometer with Cu K α radiation and were compared with reference patterns. The sample was analyzed on a Si sample holder and scanned from a diffraction angle 3-40° with step size of 0.017° and counting time of 50s per step.

5.1.3. Metastable zone width measurements

There are number of parameters that affect metastable zone width such as solubility, cooling rate that generates supersaturation, properties of solvent and impurities [124]. Depending upon the above parameters effect on supersaturated solutions, nucleation takes place after a definite degree of supersaturation. It is possible to determine the metastable zone width for each type of nucleation mentioned in the chapter 3.3.5. Here, in the present experimental work, the metastable zone width with respect to primary nucleation is determined. This can be measured for a saturated solution at a defined temperature. The metastable zone width measurements are performed on the basis of Nyvlt's polythermal method [125, 126]. In the present work Crystal 16 from Avantium Technologies was used for clear point (solubility) and cloud point (metastable zone width for primary nucleation) measurements (Fig 19) [127].

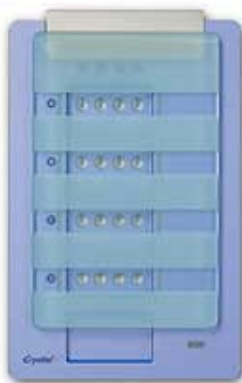


Fig 19: Crystal 16 (from Avantium technologies)

Solution samples of 1mL with different known concentrations of pure (p- and n-) salt in methanol were taken into four glass vials and placed in the slots of Crystal16. Magnetic stirrer was inserted in each sample and was operated at 700 rpm to homogenize the solution inside the vial. A heating program of temperatures between 0-55°C with a heating rate of 0.0075K/min (as low heating rate as possible to meet isothermal solubility condition) was applied for determination of clear points (saturation temperature for particular concentration of salt in methanol). As the metastable zone width is dependent on cooling rate, different cooling rates were applied to the same sample within the temperature range 55-0°C. The cooling rates 0.04, 0.05, 0.06, 0.07 K/min were selected randomly, and applied to the samples in all four samples to check their effect on the cloud point (nucleation point) temperature of the particular salt in methanol. For each cooling rate and for particular concentration of salt in methanol, the difference between saturation temperature and the nucleation temperature (ΔT)

was determined. These ΔT values were plotted against the cooling rate and a linear regression was calculated. The regression line was extrapolated to “zero cooling rate”. The intersection point with the Y-axis (at zero cooling rate) gives the maximum achievable subcooling (ΔT_{Max}) i.e. metastable zone width for primary nucleation of the salt in methanol. The complete metastable zone curve for primary nucleation was plotted in the concentration vs. temperature plot with the data obtained for different concentrations of pure salts in methanol. The metastable zone width can be expressed either as maximum subcooling at a constant concentration (ΔT_{max}) or as maximum supersaturation at a constant temperature (ΔC_{max}) [128]. The same process was repeated for all pure salts in methanol separately.

5.1.4. Resolution experiments

With the help of thermodynamic and kinetic data of salt pairs determined, different resolution experiments were designed and implemented to separate less soluble salts from the counter diastereomeric salt. For example L-D salt from L-D, D-D salt pair, D-L salt from D-L, L-L salt pair and then DPG-CS from DPG-CS, LPG-CS salt pair. In the case of L-D, D-D salt pair attempts were made to achieve both salts in pure form. Design procedure of the separation experiments for serine diastereomeric salts are explained in chapter section 6.1.5 and for phenyl glycine salts are explained in chapter section 6.6.3. A typical schematic diagram of the equipment used for all the separation experiments is shown in Fig 20 [129].

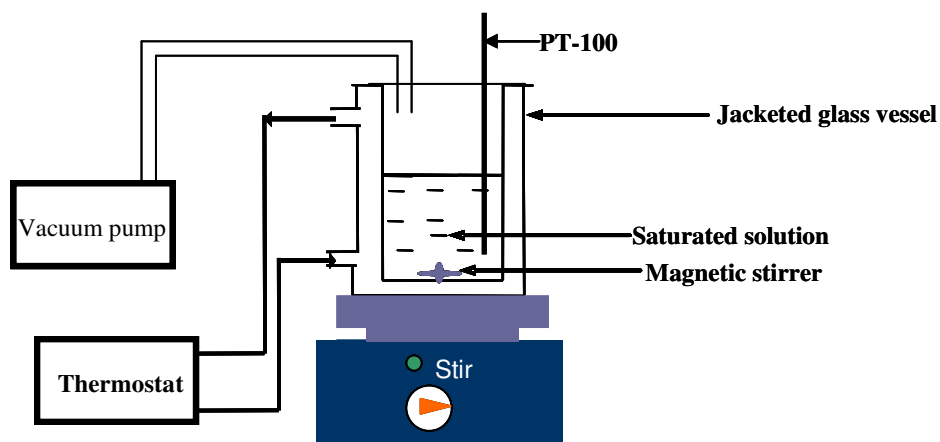


Fig 20: Schematic diagram for equipment used for the resolution experiments

Resolution experiments for serine salts (Pair 1 and 2):

Three types of crystallization based separation experiments were planned for separation of serine salts. The first one was evaporative crystallization and the second one was cooling crystallization coupled with addition of anti-solvent. Both were used for selective separation of less soluble L-D salt from L-D, D-D salt pair. The mother liquor from the selective

separation experiments was used for the preferential crystallization of more soluble D-D salt. Detailed explanation of experimental procedure for all the three types of experiments are given below.

a) Evaporative crystallization at constant temperature

According to the basic results obtained for L-D, D-D salts, initially evaporation based separation experiments were planned for separation of both salts in methanol at 40°C. To execute the evaporative crystallization experiment, 100g of clear solution was taken into a reactor with a maximum capacity of 250mL. The initial concentration of the solution was 10wt% of solute and composition of the solute was 50:50 mixture of both L-D, D-D salts. The solution was prepared according to the solubility data in methanol at 35°C. In the reactor the solution was allowed to be at 40°C to mitigate the presence of undissolved crystals. Uniform distribution in the reactor was maintained by a stirrer at a stirring speed of 150rpm. Methanol evaporation was started at 40°C under vacuum of about 320mbar to increase the supersaturation in the solution. The concentration of the solution was monitored in two ways, first by refractive index measurement and second was measurement of weight of the evaporated methanol. The refractive index of solution with pure diastereomeric salt and equimolar mixture of both diastereomeric salts in methanol at equal concentration was found to be same. Therefore, the calibration of refractometer was done for different concentrations of pure D-D salt in methanol at 40°C. The results of calibration are given in the Appendix 1. When the solution concentration reached the required supersaturation, application of vacuum was stopped and seeds of L-D salt of about 0.5g were introduced into the reactor and the system allowed to crystallize. During the experiment liquid phase samples were collected in regular intervals of time for HPLC analysis to check the solute composition change in liquid phase with respect to crystallization process time. As the crystallization was running, to increase the supersaturation methanol was evaporated under vacuum again until the limiting concentration (say 26wt%) drawn from the solubility phase diagram. When the limiting concentration was reached then the evaporation of methanol was stopped and experiment was allowed to reach equilibrium. The crystallized substance was collected via filtration. Filtered solids were washed with ethanol and dried. Solid purity was analyzed with ¹H NMR, HPLC and XRPD.

b) Cooling crystallization coupled with addition of anti-solvent

Initially based on the phase diagram the resolution approach for diastereomeric salts was evaporative crystallization but later the approach was changed to cooling crystallization coupled with anti-solvent crystallization based on the results obtained during evaporative crystallization.

Experiment:

A saturated solution sample of 10wt% of solute in methanol at 35°C, with a solute composition of 50:50 of L-D, D-D salt pair was used as a feed for the separation experiment (stoichiometric reaction is given in Appendix 2). The solution sample weights were 2.5g of L-D salt and 2.5g of D-D salt in 45g of methanol. To ensure the complete dissolution of solute, the initial temperature of solution was maintained at 40°C. The experiment was also performed in the equipment shown in Fig 20. Uniform distribution in the solution was maintained with a magnetic stirrer at 500 rpm stirring speed. The separation experiment was started by cooling the solution to 15°C with a cooling rate of 0.25K/min. 0.1g of pure L-D salt seeds were introduced into the solution at a temperature of 25°C, inside the metastable zone width thus the crystallization starts. When the solution temperature reached to 15°C, 45g of milliQ water was added to the solution to reach the solvent composition in solution to 50:50 methanol: water. The solution was allowed for further crystallization at 15°C for another 30mins to attain equilibrium. In the third step of resolution experiment, another 60ml of water was added to the solution to increase the anti-solvent composition to 70% i.e. final solvent composition in the solution was 30:70 methanol: water. The solution was allowed to crystallize for further 90-100 min to reach equilibrium. At this point of time, the experiment was stopped and the crystallized solid phase was filtered. The quality of solid phase was analyzed with XRPD and HPLC, while the mother liquor filtered was used for further experimentation to separate highly soluble D-D salt preferentially. Throughout the experiment tenure at all steps, the liquid phase samples were collected continuously at constant time gap for the determination of composition and concentration of liquid phase via HPLC and refractometer.

Table 1: Overview of experimental conditions for separation of serine salts

Experiment	Initial amount of Solute taken (g)						
	L-D salt	D-D salt	2,3-dibenzoyl-D-tartaric acid	L-L salt	D-L salt	2,3-dibenzoyl-L-tartaric acid	Methanol
L-D, D-D separation experiment	2.5	2.5	0				45
L-D, D-D with excess R.A- separation experiment	2.5	2.5	1.4				45
D-L, L-L separation experiment				2.5	2.5	0	45
D-L, L-L with excess R.A- separation experiment				2.5	2.5	1.4	45

R.A: Resolving Agent

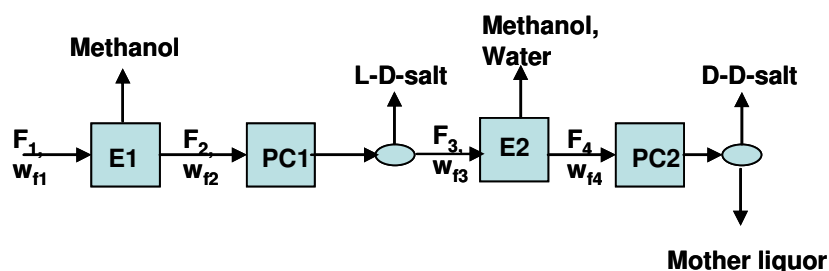
Same procedure was followed for different number of experiments for the salt pairs L-D, D-D salts and D-L, L-L salts without and also with excess resolving agents (excess R.A calculation is given in Appendix 2 and chapter 6.1.3). The initial quantities of substances taken for different separation experiments for above salt pairs are shown in Table 1.

c) Preferential crystallization of counter-salt

The purpose of planning of this experiment was to enhance the pure product yield with repeated crystallization steps. Here, the first two parts (cooling and anti-solvent crystallization) were performed described above (part b). The additional point in this experiment was- at the end of anti-solvent crystallization, a sequence of solvent evaporation (initially methanol then water at 40°C to increase supersaturation) and crystallization of one of the salts preferentially at 10°C was done for two times. Each time solids crystallized were separated and the mother liquor was reused for the further crystallization experiment.

In the first preferential crystallization experiment, 40g of methanol was evaporated and allowed for crystallization of L-D salt in the presence of 0.05g of L-D salt seeds for about 50 min. At the end of the crystallization solids were separated and analyzed with XRPD.

The mother liquor from preferential crystallization-1 was again utilized as a solution for preferential crystallization-2. Solution was vacuum evaporated to remove methanol completely and 25g of water. The solution was allowed to crystallize preferentially for D-D salt at 10°C for another 40 min. The seeds of highly soluble D-D salt were introduced. After the crystallization experiment the solids were once again filtered, dried and analyzed with XRPD for the purity analysis. During each crystallization step, liquid samples were taken regularly and analyzed with HPLC. The procedure followed is shown in scheme 9.



Scheme 9: Schematic representation of preferential crystallization experiments planned for L-D, D-D salts (F: feed to the concerned unit operation, w_f : weight fraction of solute in solution, E1, E2: evaporators; PC1, PC2: preferential crystallizers)

Resolution experiments for phenyl glycine salts (LPG-CS and DPG-CS) (Pair 6):

d) Cooling crystallization coupled with addition of anti-solvent

For LPG-CS and DPG-CS salts there is a possibility to use evaporative crystallization as well as cooling crystallization coupled with addition of anti-solvent. As the research did not go very deep for resolution of LPG-CS and DPG-CS salts, the first experimental approach used for separation of less soluble salt and also effect of excess resolving agent on the separation are explained here.

Experiment:

A sample of 20wt% of solute in methanol, with a solute composition of 50:50 of LPG-CS and DPG-CS salts (located in the two phase region of DPG-CS for the isotherm at 5°C) was used as a feed for the separation experiment. The feed contains 4g of LPG-CS salt and 4g of DPG-CS salt in 32g of methanol. To avoid problems like undissolved crystals in the solution, the

solute was completely dissolved at higher temperature than the saturation temperature i.e. at 30°C. The resolution experiment was performed in the same equipment shown in Fig19. Magnetic stirrer was maintained at 500rpm. The experiment was started by cooling the solution to 0°C with a cooling rate of 0.25K/min. 0.22g of pure DPG-CS salt seeds were introduced into the solution when the solution temperature was 5°C i.e. in the metastable zone. The supersaturation in the solution was also increased by addition of 32g of anti-solvent acetonitrile. Then the solvent composition in the solution was 50:50methanol: acetonitrile. For the next 30 min solution was allowed for crystallization to reach equilibrium. Next step in the resolution experiment was adding another 43g of acetonitrile to increase supersaturation further in the solution. Final composition of the solvent in the solution was 30:70 methanol: acetonitrile. The crystallization experiment was allowed to run for another 45mins to reach equilibrium. At this point of time, the experiment was stopped and the crystallized solid phase was filtered. The solid phase was analyzed with XRPD and HPLC for purity check. Throughout the experiment, before and after all the three steps (cooling and two times anti-solvent addition) liquid phase samples were collected continuously at regular intervals of time to check the solution composition change in the liquid phase via HPLC.

Table 2: The solution preparation and experimental conditions for LPG-CS, DPG-CS separation

Experiment	Initial amount of Solute and Solvent (g)				Solution initial temperature (°C)	Solution final temperature (°C)	Anti-Solvent (g)	
	DPG-CS	LPG-CS	10-(+)-camphor sulphonic acid	Methanol			1 st part	2 nd part
(1) without excess resolving agent	4	4	0	32	25	0	32	43
(2) with excess resolving agent	4	4	0.9	32	25	0	32	43
(3) with excess resolving agent	4	4	2	32	25	0	32	43

Same procedure was followed for different separation experiments for the salt pairs LPG-CS, DPG-CS and with various concentration of excess resolving agent (10(+)-camphor sulphonic acid) in the feed. Total experimental quantities taken for separation experiments with and without excess resolving agent are given in Table 2.

5.2. Analytical methods used

5.2.1. Differential Scanning Calorimetry (DSC)

Differential Scanning Calorimetry (DSC) is a thermoanalytical technique which is used to measure thermal transitions in chemical substances. Different properties of materials like glass transitions, phase changes, solvate formation, melting, crystallization, product stability etc can be analysed with this technique [130, 131]. A typical diagram of main part Differential Scanning Calorimeter is shown in Fig 21. In this device, two heating plates are provided to keep the sample and reference crucibles (made of high thermal conductivity material like aluminium). Both are allowed to heat with same heating rate uniformly under the presence of inert gas helium.

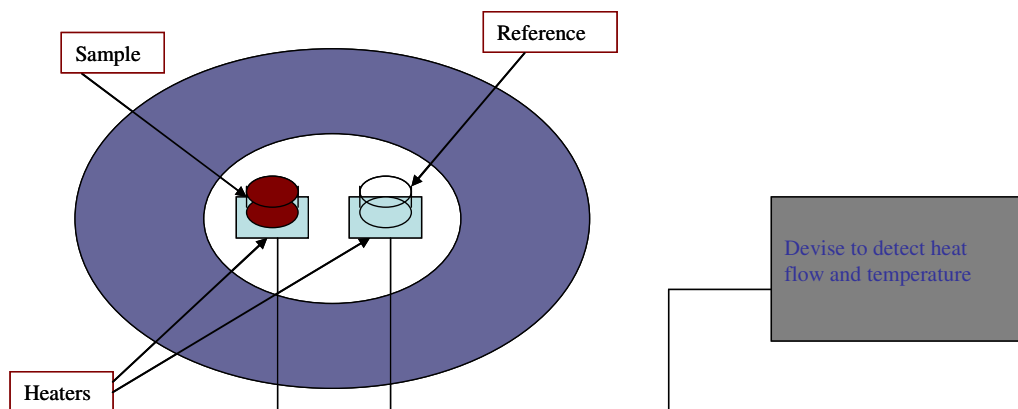


Fig 21: Block diagram representing a typical differential scanning calorimeter

The fundamental principle underlying in this technique is, while maintaining a constant rate of temperature increase for sample and reference, the phase transitions in the sample leads to heat flow fluctuations accordingly and no changes in heat flow to reference. Release of more or less heat depends on the endothermic or exothermic nature of the phase transition process. If the sample is melting, more heat flow is necessary due to endothermic melting process and for exothermic phase transition like liquid phase to solid (crystallization) needs less heat flow to maintain the same rate of temperature increase. These heat flow fluctuations between the sample and the reference would be detected by DSC and allows the system to calculate the amount of heat absorbed or released during phase changes with respect to rate of temperature change. In Fig 22 is shown a simple DSC heat flow curve with respect to temperature (thermogram) indicating various phase transition temperatures like glass transition

temperature (T_g), crystallization temperature (T_c) and melting temperature (T_m) [132]. In the present work the differential scanning calorimeter DSC 111, Setaram, France) was used to observe the melting behaviour of pure and mixtures of different diastereomeric salts.

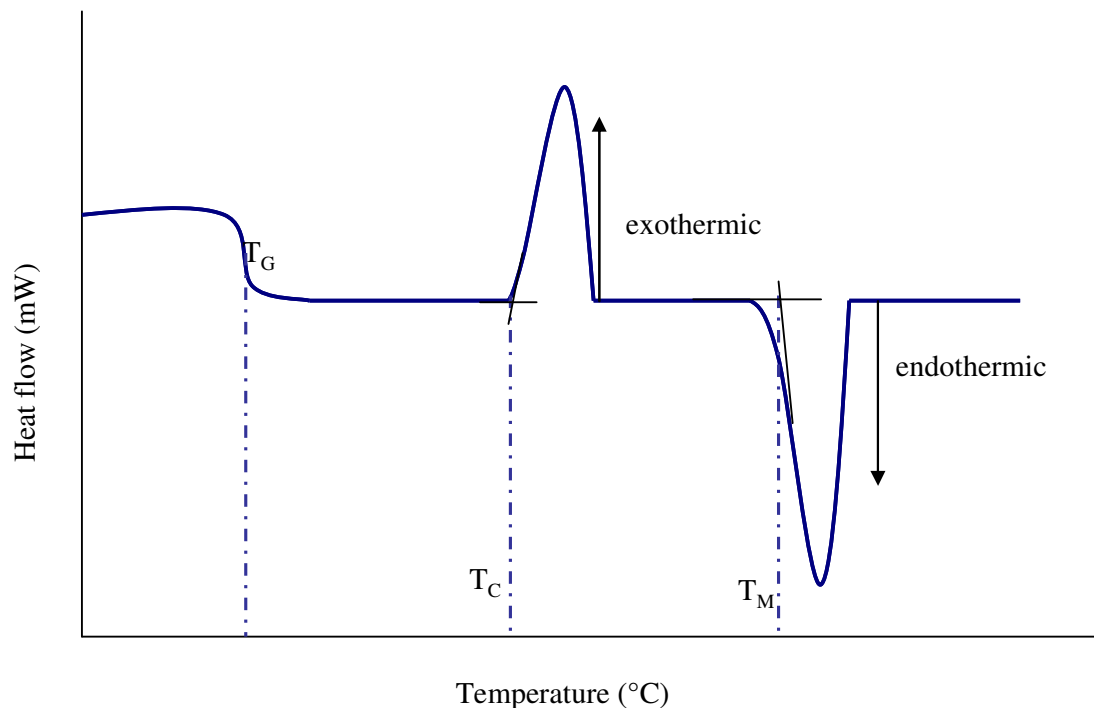


Fig 22: DSC thermogram representing different phase transitions

5.2.2. Nuclear magnetic resonance (NMR)

NMR spectroscopy is one of the most powerful tools for determination of the structure of both organic and inorganic species [133]. The working principle of NMR depends on the charge possessed by nuclei of different elements. In the nuclei of an element the number of protons, neutrons are odd, then the nucleus has either a half integer spin (eg: $I = 1/2, 3/2, 5/2$ etc) or an integer spin (eg: $I = 1, 2, 3$ etc). When a magnetic field is applied externally, the nuclear magnetic moment of a nucleus will align in only $2I+1$ ways that either with or against the applied field. In case of a single nucleus with $I=1/2$ and a positive magnetogyric ratio γ (which relates the magnetic moment μ and the spin number I for a specific nucleus), the possible transitions between the two energy levels is only one. The energetically preferred orientation is the magnetic moment aligned parallel with the applied field with a spin $m=+1/2$, and the higher energy anti-parallel orientation with spin $m=-1/2$. The spin states, oriented parallel to the external field are lower in energy while the spin states whose orientations oppose the external field are higher in energy. It is possible to introduce a nucleus with lower

energy orientation to "transition" to an orientation with a higher energy by irradiating the nucleus with a correct energy of electromagnetic radiation (as determined by its frequency). This energy absorption during the transition gives the basis for the NMR method [134]. The energy of NMR transition depends mainly on magnetic-field strength and the magnetogyric ratio γ of an atom. The local environment around a given nucleus in a molecule will slightly perturb the local magnetic field exerted on that nucleus and affect its exact transition energy. This effect on transition energy with respect to position of atom in the molecule makes NMR to be very useful for determining the structure of molecules. A block diagram representing NMR spectrometer is shown below in Fig 23. Bruker AVANCE 600 spectrometer at 600.13 MHz is used in the present work.

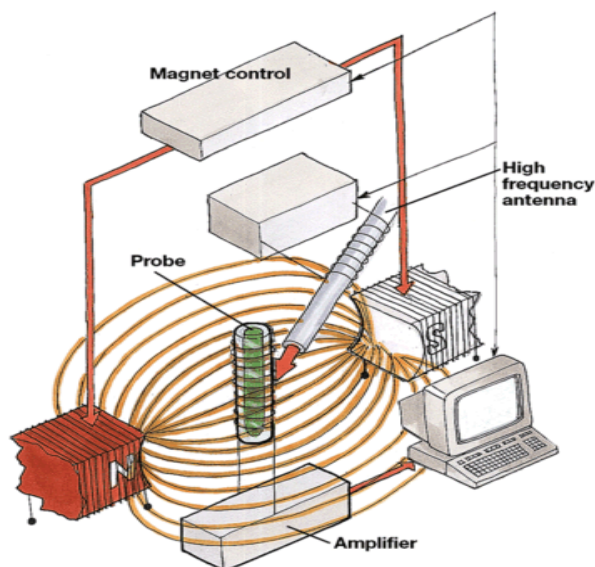


Fig 23: A typical block diagram of Nuclear Magnetic Resonance Spectrometer [135]

5.2.3. X-ray powder diffraction (XRPD)

X-ray powder diffraction is an instrumental technique which is used extensively in chemical industry and also for research purpose because of simplicity in sample preparation and rapid measurement [136]. XRPD provides reliable information for fast identification of a substance. It is very useful in analyzing the solid phase behavior of different minerals and chemicals with respect to crystallinity, polymorphism, solvate presence or any mixtures with more than one substance etc [137-139]. When X-ray beam interacts with the three dimensional planes of a non-amorphous crystal lattice of substance, the beam is partially transmitted, absorbed, refracted, scattered and part of it is diffracted. These X-rays are diffracted differently by different substances based on the molecular arrangement in the crystal lattice. XRPD gives

different patterns for enantiomers and the racemate of a chiral compound-forming substance and also for each of the specific behavior (like polymorph or solvate) [45, 140].

In general the distances between adjacent planes of different orientation of a crystal are unique for each substance and even for different polymorphs of the same substance. When an X-ray beam interacts with the sample and is diffracted, the distance between the planes of atoms can be calculated by applying Bragg's law, which is expressed in the equation below as;

$$n\lambda = 2d \sin \theta \quad \text{-- (8)}$$

λ :wavelength of incident wave (m), n : an integer value, 2θ : theta: diffraction angle ($^{\circ}$), d :lattice distance (m)

The characteristic set of d -spacings generated from the X-ray scan provides a distinctive "pattern" of the sample. Thus the pure substance can be distinguished from the other polymorphs or solvates formed in the system by showing different reflexes in the measurement. A simplified sketch of XRPD equipment is shown in Fig 24. In this equipment the X-ray tube and the detector both move through the angle theta around the stationary sample holder.

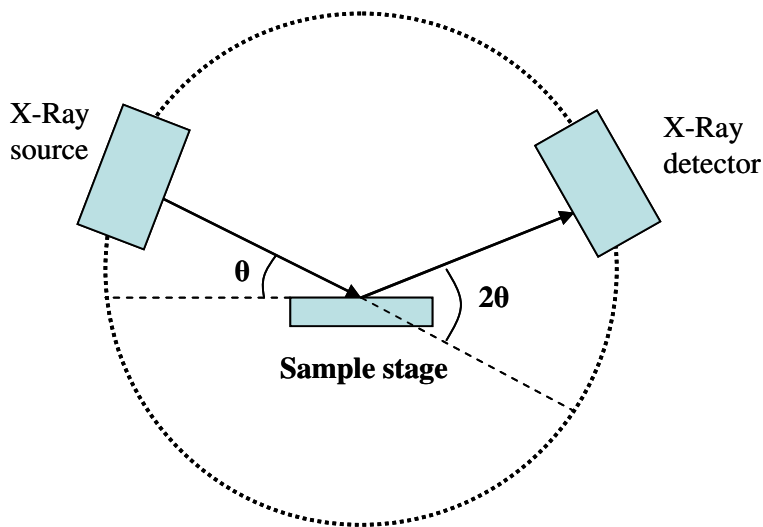


Fig 24: The geometry of an XRPD unit

5.2.4. High Performance Liquid Chromatography (HPLC)

High performance liquid chromatography is a well-known analytic technique frequently used in many pharmaceutical and biological industries [141], which can be used not only to

separate a mixture of compounds but also to quantify and purify the individual components of the mixture.

In HPLC technique, a small quantity of diluted sample which needs to be analyzed is injected into the stream of solvent or solvent mixture (mobile phase). The stream is then passed through a stationary column strongly packed with different solid materials (like ceramics at high pressures) with a pressure pump. Here the substances in the sample would show different physical and chemical interactions with the material present in the column, which leads to the change in their flow velocity with respect to column length. The time when the specific compound of the sample leaves the column is called the retention time. When the substance elutes from the column it is detected by an UV- detector which provides the characteristic data identity like retention time for analyte. A typical HPLC device is shown in Fig 25.

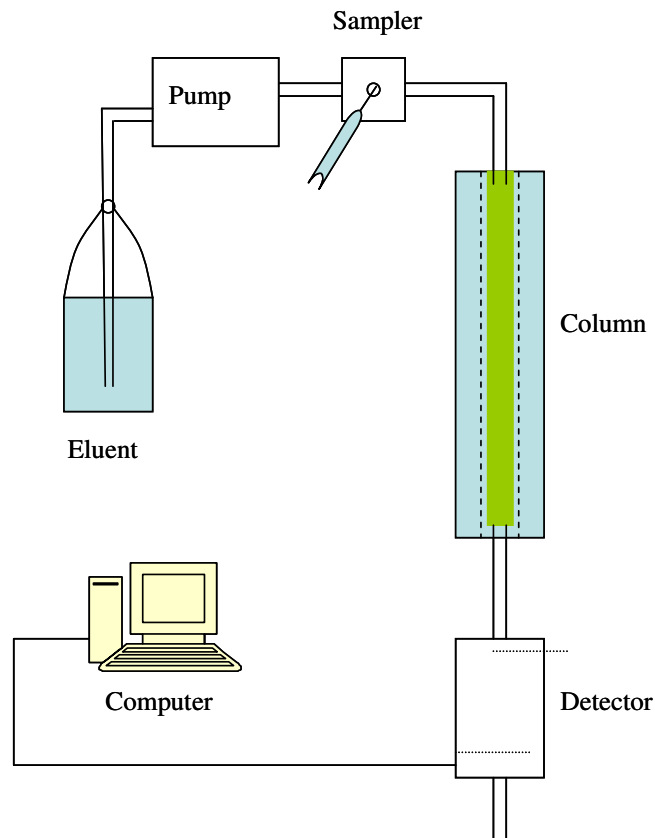


Fig25: HPLC setup

If the sample contains enantiomers, then to separate them it is necessary to use either a chiral stationary phase or a chiral mobile phase [142]. In the present work to separate diastereomeric salts a special chiral stationary phase Crownpak CR was used.

5.2.5. Refractometer

Refractometer can be used for the rapid measurement of solution concentration in terms of Refractive Index (n). Refractive Index of a substance is the ratio of the velocity of a ray of light in vacuum to its velocity in a medium. When a ray of light with constant wavelength passes from high dense medium to another less dense medium (for e.g. from liquid medium like water to gas medium like air shown in Fig 26(a)) at an angle other than perpendicular, it changes its angle. This can be explained with the Snell's law;

$$\sin \beta = \frac{n_1}{n_2} \cdot \sin \alpha \quad \text{-- (9)}$$

α : incident angle, β : largest possible angle of refraction, n_1 , n_2 : refractive index of medium 1, 2 respectively.

When the incident angle α is increased to an angle called critical angle the ray no longer passes into the less dense medium, further increase of α would lead to the total reflection. At critical angle $\beta=90^\circ$ then $n_1=n_2/\sin \alpha$. The reflection is a function of incident light wavelength and temperature of the medium. In this work a Refractometer Mettler-Toledo RE40, shown in Fig 26(b) was used. Sodium light of constant wavelength 589.3nm was used and a constant temperature was maintained while measuring the sample. The measuring principle is based on the light from the source that passes through the prism and reaches the sample. Then this light partially refracts and reflects. An optical sensor records the reflected light. The dark and light areas are divided by a boundary which gives the critical angle. By this the refractive index (n_1) can be measured [143].

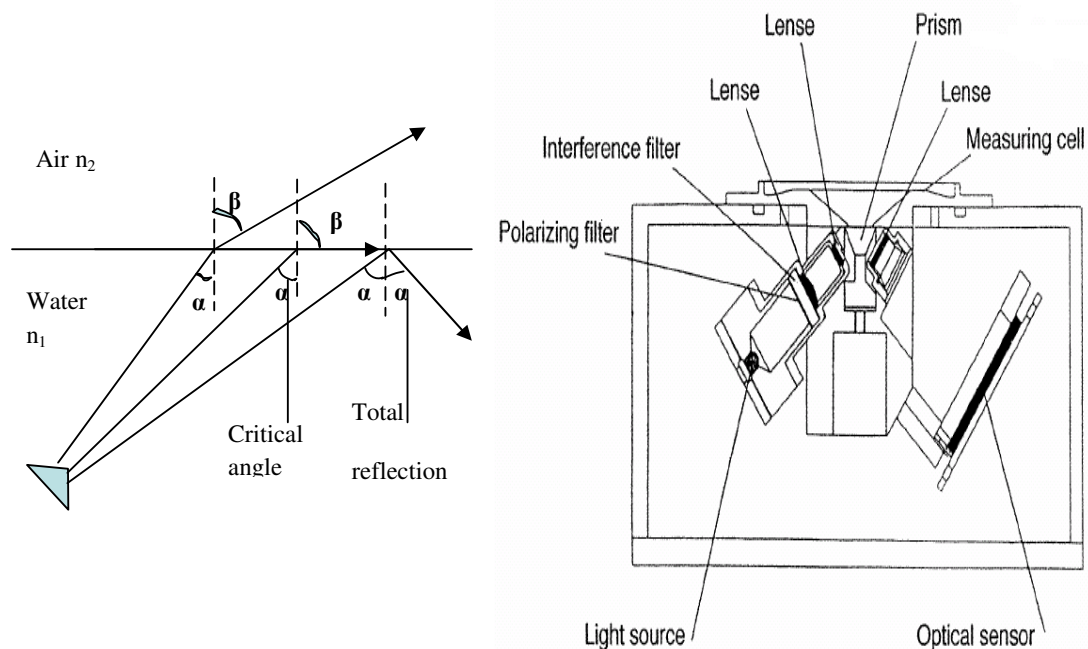


Fig 26: (a) The total angle of reflection, critical angle and reflection of light from water to air (b) Setup of the measurement system RE40 [27].

5.3. Summary

Present chapter gives an overall idea about the different experimental techniques applied for all the salt pairs generated. The fundamental techniques that were used to determine the basic information like thermodynamic data (binary melting and ternary solubility phase diagrams) and kinetic data (metastable zone width for primary nucleation) for designing a crystallization based separation process are given very elaborately. The process followed during separation experiment for different serine salts and phenyl glycine salts are also discussed. Finally the analytical techniques used throughout the research work (DSC, HPLC, NMR, XRPD and Refractometer) are discussed along with their working principle.

In the succeeding chapter 6, the achieved results are discussed.

6. Results and discussion

Chapter 6

Results and discussion

All results obtained in this present work are discussed in a systematic manner. Initially the synthesis results of serine diastereomeric salt pairs with different resolving agents are presented (Table 1). The salt pairs are L-D, D-D salts, L-L, D-L salts, L-LM, D-LM salts, L-LT, D-LT salts and L-D-Toluyl, D-D-Toluyl salts (chapters 6.1-6.5). Some unexpected experiences seen during the synthesis of some serine salts are also shown in the subchapter 6.5. In chapter 6.6 the synthesis and resolution results of phenyl glycine salts LPG-CS, DPG-CS salts are discussed. Table 3 reminds the names of the salt pairs 1-6 and their abbreviations.

Table 3: List of salt pairs

Salt pair	Substancename
1	L-/D-serinebenzylester- D-2,3-dibenzoyl tartrate (L-D, D-D)
2	L-/D-serinebenzylester- L- 2,3-dibenzoyl tartrate (D-L, L-L)
3	L-/D-serinebenzylester- L-mandelate (D-LM, L-LM)
4	L-/D-serinebenzylester- L-tartrate (D-LT, L-LT)
5	L-/D-serine benzyl ester- D-2,3-ditoluyl tartrate (L-D-Toluyl, D-D-Toluyl)
6	L-D-phenyl glycine-(+)-10-camphor sulphonate (LPG-CS, DPG-CS)

As discussed above, these six salt pairs are well suited to address specific problems in Classical Resolution. The results for the salt pairs are explained in the order of thermodynamic (binary and ternary systems) and kinetic data. With regard to these data the feasibility of salt pair resolution is analyzed. The separation experiments are performed for selected salt pairs (pair 1, 2 and 6) and presented with detailed explanation at the end of respected sub-chapters. To make the explanation simple, all the thermodynamic, kinetic data and the resolution experiments of all salts are quantified in weight percent (wt%) instead of mole percent (mol%).

6.1. Results of L-D, D-D salts (pair 1)

A step by step procedure is followed to explain the results of L-D, D-D salt pair. Initially characterization results of both salts followed by basic thermodynamic and kinetic data of both salts in suitable solvents are presented and discussed. Afterwards, the crystallization based separation process design and experimental results are discussed.

6.1.1. Characterization of L-D, D-D salts

After the synthesis of L-D and D-D salts, purity was analyzed initially with ^1H NMR followed by XRPD and DSC melting point measurements. ^1H NMR and XRPD results are shown in Fig 27. As both salts split into ions in the solvent the ^1H NMR spectrum is identical for both L-D and D-D salts. The analysis of the ^1H NMR spectrum is ^1H NMR (400 MHz, d₆-DMSO) δ 3.62-3.72 (m, 4H), 3.81 (t, 2H), 5.15 (q, 4H), 5.62 (s, 2H), 7.31-7.39 (m, 10H), 7.46 (t, 4H), 7.61 (m, 2H), 7.91 (d, 4H). According to the results from ^1H NMR, no indication for the presence of a methanol solvate (possible from synthesis) or any other type of impurities is observed.

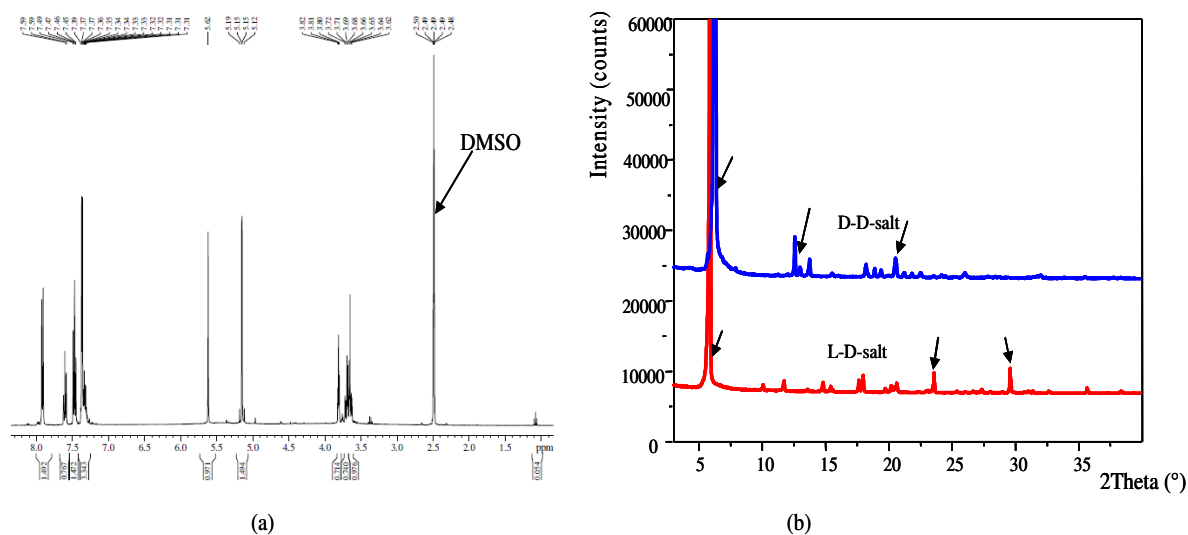


Fig 27: (a) ^1H NMR and (b) XRPD patterns for both L-D and D-D salts (main peaks characterizing the individual salts are indicated by arrows)

Hence both salts are chemically pure and do not form solvates. Significant and diverse XRPD patterns are observed for L-D and D-D salts. The peaks which denote the difference between the two salts are indicated by arrows in Fig 27(b). From the XRPD results, the two salts can be considered that they are perfectly crystalline. These patterns are used as reference for future analysis of the material during the separation process.

6.1.2. Binary melting behavior

The appropriate DSC-curves for pure and a selected mixture of both salts are shown in Fig 28. The onset points of the melting curves are taken as the melting temperature of the pure substances, whereas for the mixtures, the onset of first recognized peak is taken as the eutectic melting and the peak maximum of the curve is taken as the end of melting of the mixture since there are no perfectly separated peaks for the eutectic and the final melting.

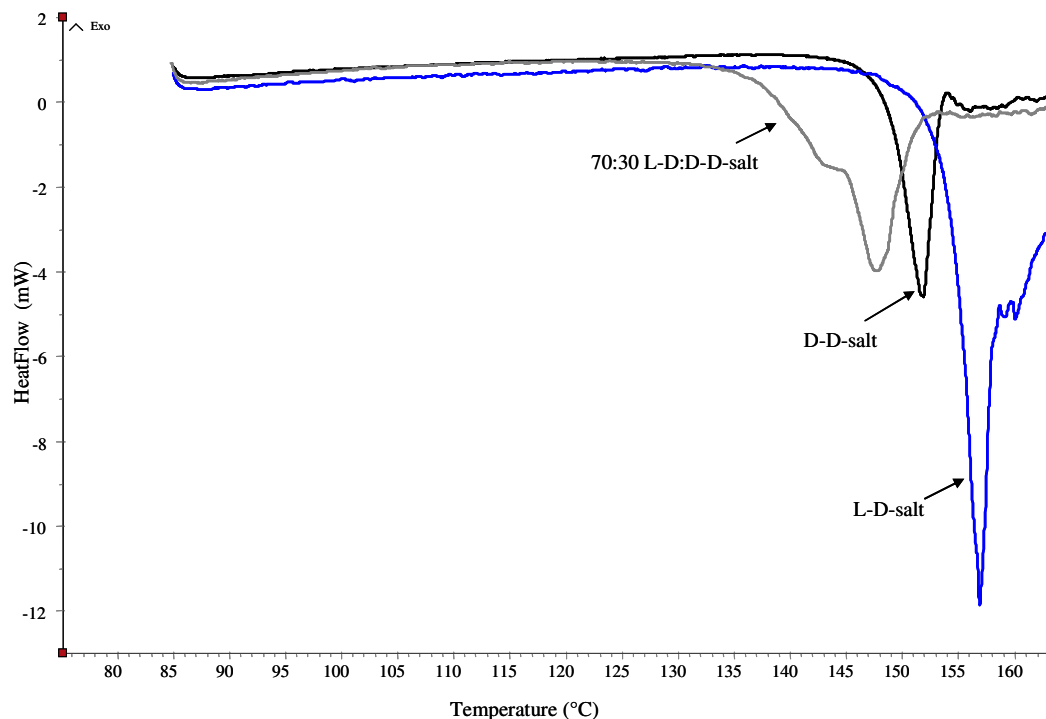


Fig 28: Melting curves for L-D, D-D-salts and a 70:30 mixture of both salts (sample masses: 8-10 mg)

From the melting curves, it is clear that the melting points and melting enthalpies of both L-D and D-D salts are different for each other. The melting temperature of L-D-salt is 152.4°C and D-D-salt is 148°C. In the thermograms of both salts, melting peaks do not reach back to base line since the material is decomposing during melting. Therefore the accurate determination of melting enthalpy was not possible. Due to the thermal instability at higher temperatures, decomposition with melting also eliminated the possibility of using melt crystallization for the separation of both diastereomeric salts [144]. According to the melting peak area for both diastereomeric salts in Fig 28, melting enthalpy of L-D- salt is far higher than that of D-D-salt. If compared, the solubility of D-D-salt expected to be far higher than that of L-D-salt in a

particular solvent, due to the solubility dependency on the melting enthalpy and melting point of solute.

A series of XRPD patterns of pure L-D, D-D and various mixtures of both salts are shown in Fig 29. The XRPD patterns of these selected mixtures are matched with the reference XRPD patterns of pure D-D-and L-D-salts. The peaks in the XRPD pattern present at various angles for both pure salts are appeared together in the XRPD patterns of mixtures. Further no additional peak is observed. This behavior suggests that both salts together behave like simple eutectic and no double salts (intermediate compounds). No indication of solid solutions in the system could be observed.

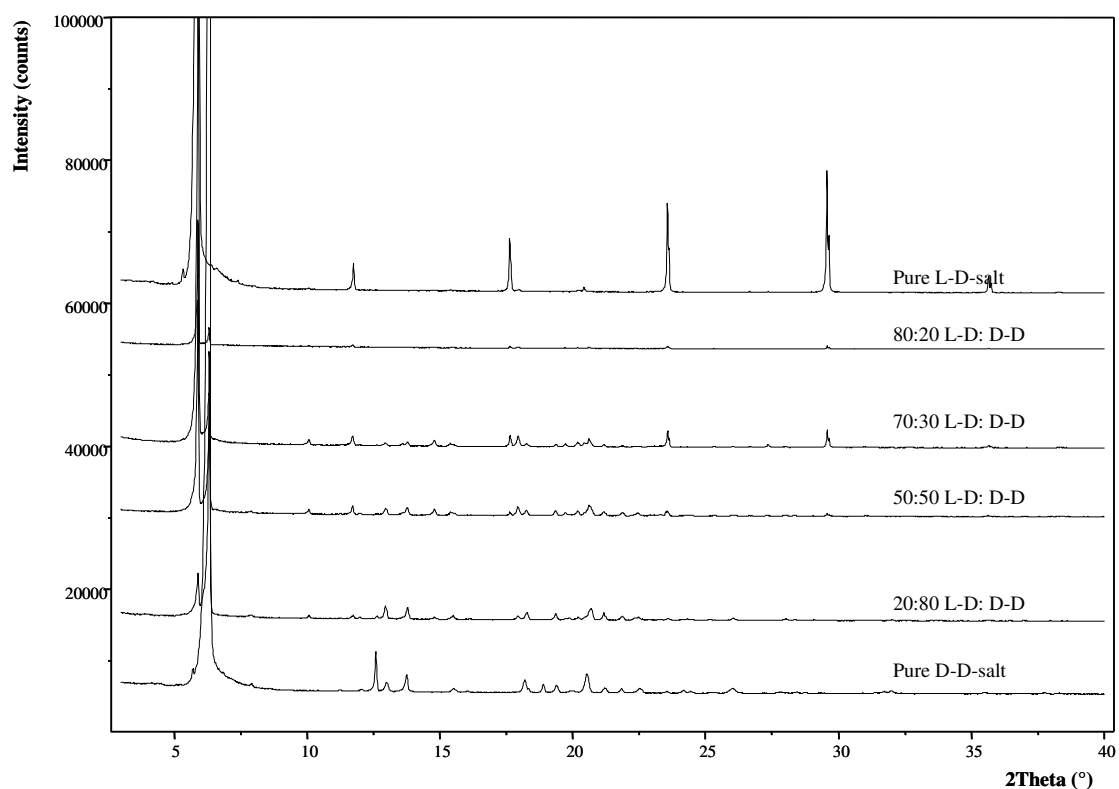


Fig 29: XRPD pattern comparison of different mixtures of L-D and D-D-salts with the pure single salts

6.1.3. Ternary solubility phase diagram

As the material rejects the melting-based crystallization separation process, the resolution of both salts was approached via crystallization from the solution. Solubilities in different solvents like methanol, acetone, water and ethanol have been measured. Solubility results of both salts in these solvents are given in Table 4. The solubility of both L-D and D-D salts is increasing in the solvent order from ethanol, water, acetone to methanol. As expected from

the melting point and expected melting enthalpy values, the solubility of D-D salt is higher than that of L-D salt. Solubility of both salts in methanol is far higher than that of in other three solvents.

To achieve a better separation via crystallization solvent selection plays a crucial role[145]. Solvent selection for better resolution is done based on - ratio of solubility of highly soluble salts to less soluble salt in selected solvents (if the ratio is high there is a high possibility for separation of both salts). In the present work according to the solubility ratio shown in the Table 4, with highest solubility ratio methanol is the most suitable solvent for better separation. On the other hand, due to the low solubility and solubility ratio one of the other three solvents can be selected as anti-solvent. Water is most suitable as anti-solvent due to lowest solubility and solubility ratio.

Table 4. Solubilities of pure D-D and L-D-salts in selected solvents at 25°C

Solvent	Solubility of diastereomeric salts (wt %)		Solubility ratio (D-D to L-D)
	L-D-salt	D-D-salt	
Methanol	3.08	16.11	5.2
Acetone	0.97	3.27	3.4
Water	0.47	1.22	2.6
Ethanol	0.20	0.95	4.8

Solubility phase diagram in methanol

In methanol both diastereomeric salts have considerably higher solubility and the highest solubility ratio compared to other solvents at 25°C. Based on this information methanol was selected as main solvent for diastereomer separation. The ternary solubility phase diagram of both salts in methanol is shown in the Fig 30. In Fig 30(1), solubility isotherms at temperatures 15°C, 25°C and 35°C are given. As can be seen, due to the difference in solubility there is a strong asymmetry in the ternary solubility phase diagram. The solubility of the L-D-salt is much lesser than the solubility of the D-D-salt at all the temperatures. This makes clear that during the resolution starting from a 50:50 composition of the salts, the L-D-

salt crystallizes out first leaving (in optimal case) the diastereomers at a eutectic composition in the liquid phase. In all the solubility isotherms, only one maximum solubility point is observed for the mixture of salts, which shows that there is only one two-salt-saturation composition (2-salt point composition in the diastereomeric mixture). Thus both L-D and D-D salts fall under simple eutectic system which is highly supportive for the separation via crystallization. The composition of the two-salt-saturation point for solubility isotherm at 15°C is 17:83 L-D:D-D salts, for 25°C 20:80 L-D:D-D salts and for 35°C 22:78 L-D:D-D salt. There is a slight variation in the eutectic composition of both salts with respect to temperature. As the temperature is increasing, the eutectic composition is moving towards the 50:50 composition of both salts. From the data in Fig 30(1), it can be observed that the solubility dependency on temperature is more significant for D-D salt than L-D salt in methanol. The solubility of pure L-D salt at 15°C is 1.72wt% and at 35°C 4.62wt%. On the other hand the solubility of pure D-D salt at 15°C is 13.86wt% and at 35°C 21.23wt%. In the case of L-D salt, for a temperature gap of 20K, ~3wt% increase is observed whereas for D-D salt an increase of 7.5wt% is observed. This difference in solubility increase rate with respect to temperature might have effect on the eutectic position at that particular temperature.

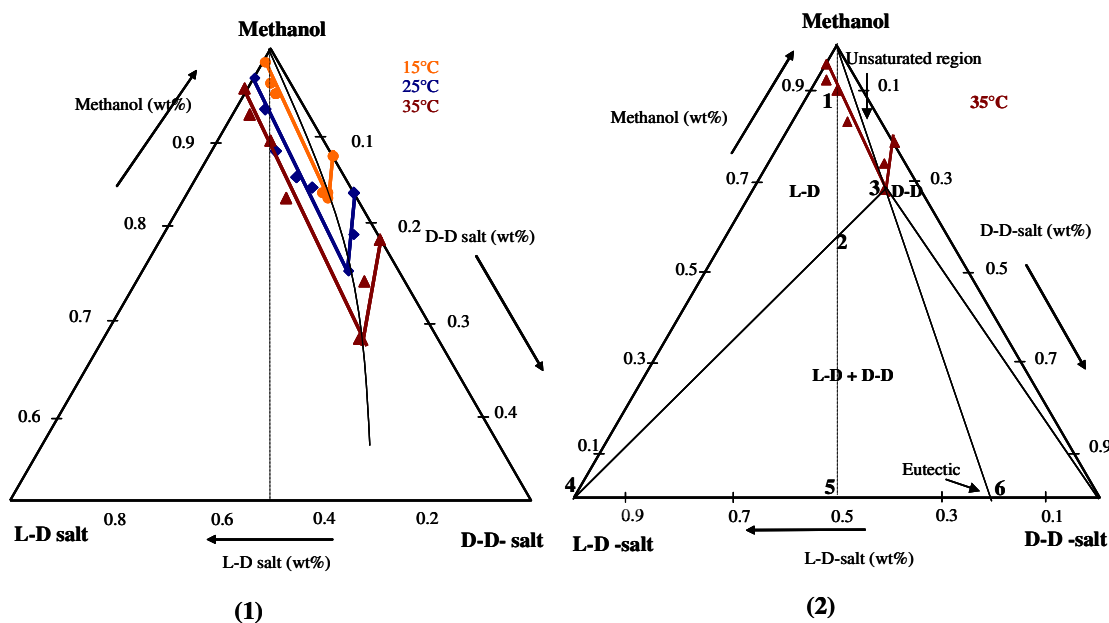


Fig 30: Ternary solubility phase diagram of both L-D- and D-D-salts in methanol (1): Upper 50% of the solubility phase diagram (2): Full ternary phase diagram

This kind of thermodynamic effect has a strong effect on the selection of type of crystallization experiment. In this particular case the eutectic composition is moving towards

D-D salt when the temperature is reduced, it is important to include cooling step in the separation experiment for L-D, D-D salts to increase final yield.

In Fig 30(2), the solubility isotherm at 35°C is taken in a 100% ternary phase diagram to explain the possibilities for maximum yield from a single isotherm. The separation strategy from a racemic mixture of DL-serine and accordingly a 50:50 diastereomeric salt mixture is the crystallization within the two phase region of L-D salt (solid L-D + saturated liquid). Interestingly, due to the huge difference in the solubility of L-D and D-D salts and the position of eutectic composition close to the corner of D-D salt, the two phase region for L-D salt is extremely wide compared to the two phase region of D-D salt (solid D-D + saturated liquid). From this it follows that the crystallization of D-D-salt is not likely, which will allow far high yields with high diastereomeric purities for the L-D-salt. Noteworthy, D-D-salt might be obtained from the 50:50mixture within the three phase region via preferential (cooling) crystallization conditions.

A separation strategy from the solubility phase diagram can be derived for the maximum L-D salt separation from 50:50 mixture of both salts. For a solution at point 1 (solubility for 50:50 mixture of both salts at 35°C) in Fig 30(2), the maximum yield of the pure L-D-salt can be achieved by reaching the solution position to the concentration at point 2 by evaporation of methanol and crystallizing of L-D salt till the eutectic composition at point 3. The maximum possible yield can be calculated by the lever rule [80] [(length of segment 23/ length of segment 43)*100], which is 15.7%. Since solubility increases with temperature, maximum yield also increases with temperature. The maximum possible yield for the L-D-salt would be theoretically 37.5% (segment 56/ segment 46) in the binary system if melt crystallization would be applied. A series of batch processes with a recycle should be helpful to improve the separation process with an increased yield [146].

Solubility phase diagram in water

Ternary solubility phase diagram for both L-D and D-D salts is also measured in water. The results are shown in Fig 31. Solubility isotherms at temperatures 25°C and 35°C are presented in the upper 10% of the solubility phase diagram. According to the solubility isotherms at both temperatures, in water also strong asymmetry is observed in the phase diagram. The solubility of the L-D-salt is lower than the solubility of the D-D-salt at both the temperatures. Like in methanol, here in water also only one solubility maximum composition is observed in the solubility isotherms, which shows the two salt saturation composition (eutectic

composition) at 20:80 L-D:D-D salts. Thus, L-D and D-D salts also showed simple eutectic behavior in water as solvent. On the other hand, unlike in methanol there is no considerable change in the eutectic composition with respect to temperature. This might be due to the very low solubility in water and also there is no considerable change in the solubility increase with respect to temperature for both salts. Thus, the change in eutectic composition is also solvent selective. Due to the very low solubility for both salts, water can be used as an anti-solvent for the crystallization based resolution experiment.

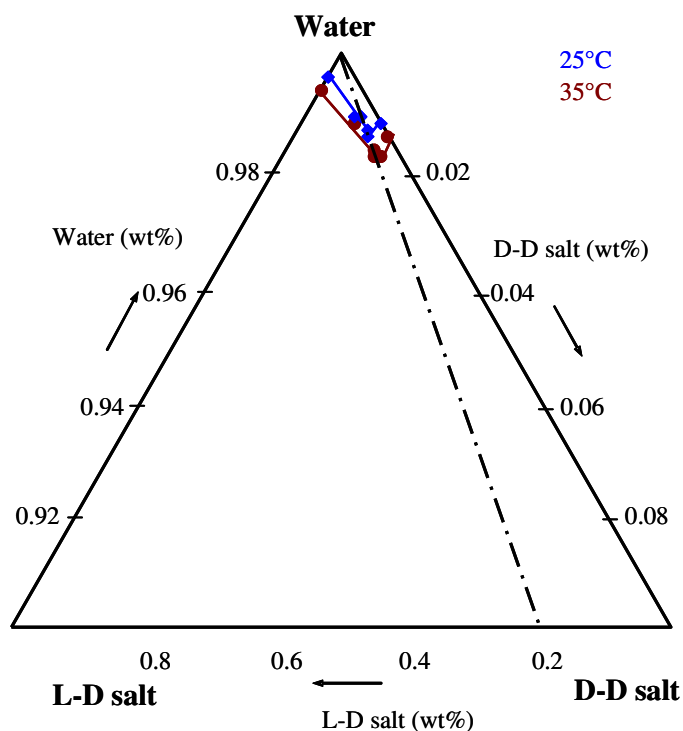


Fig 31: Ternary solubility phase diagram for L-D, D-D salts in water (upper 10%)

Effect of anti-solvent water on the solubility of pure diastereomeric salts in methanol

In Fig 32 the effect of water on the solubility of L-D and D-D salts in methanol at 25°C and 5°C are shown. At these two temperatures solubility of pure L-D and D-D salts are very different in methanol and water. If the content of pure methanol is reduced by water addition there is a drastic decrease in the solubility of both pure salts and minimum solubility found for pure water. At both temperatures for these two salts there is no significant solubility variation after a composition of 70:30 water: methanol to pure water. If an anti-solvent based supersaturation is planned for resolution, a final solvent composition of 70:30 water: methanol would be a good option and it can be used in the resolution experiment.

As the use of anti-solvent in crystallization is more prone to the formation of polymorphs, solvates and hydrates [147], the solid samples of excess solute obtained after solubility measurements were analyzed by XRPD to check for the appearance of any new phases. The XRPD patterns of all four salts are identical to the reference patterns. This confirms the absence of polymorphs, solvates or hydrates within the operating temperature range and solvent composition.

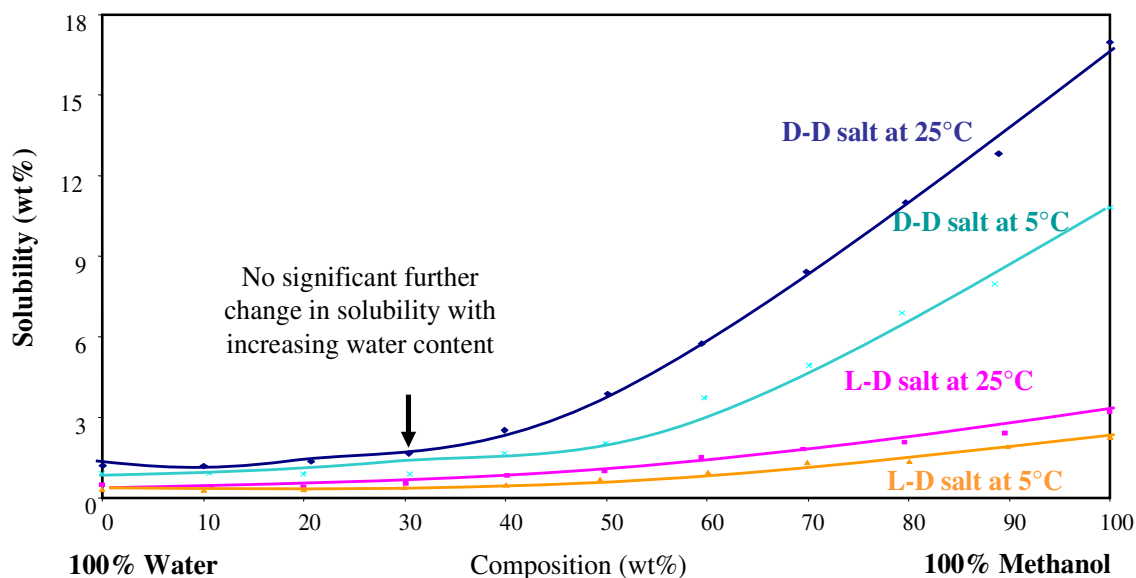


Fig 32: Solubility change for L-D and D-D salts according to the change in anti-solvent content in methanol

Effect of excess resolving agent on the solubility of L-D, D-D salts

The results of solubility measurements for L-D and D-D salts and then the 50:50 mixture in methanol in various stoichiometric feed amounts ($1 \leq \lambda_r < 2.2$) are shown in Fig 33. In this figure, the first point on the blue line shows the saturation temperature (solubility temperature) of pure L-D salt in methanol i.e. $\lambda_r = 1$. The other three solubility results are for samples with an ascending order of increase in λ_r value (i.e. excess resolving agent concentration: Eq-1 in chapter 3.1).

The saturation temperature of L-D salt in methanol initially increased (decrease in solubility) with an increase in λ_r (addition of excess of resolving agent) and reached a maximum at a particular value of λ_r (or concentration of excess of R.A) and then the saturation temperature decreased as the λ_r (the excess of R.A concentration) further increased. This means, initially

the excess of R.A has a reducing effect on solubility at lower concentrations and when it exceeds a certain concentration it has an increasing effect.

In the same manner, the solubility results for D-D salt are plotted in pink in Fig 33. Here a similar influence like for the L-D salt but an extended effect on the solubility is observed. Initially at low values of λ_r (i.e. < 1.3) the saturation temperature increased (decreased the solubility) of D-D salt in methanol slightly, and then decreased saturation temperature (increased the solubility) very steeply with slight increase further in λ_r value (excess R.A concentrations). The effect of resolving agent on the 50:50 mixture of both salts is shown in maroon color. The effect of resolving agent on the solubility of 50:50 mixture and L-D salt are alike. There is a slight decrease in solubility initially and followed by an increase in the solubility of 50:50 mixture with respect to λ_r value increase.

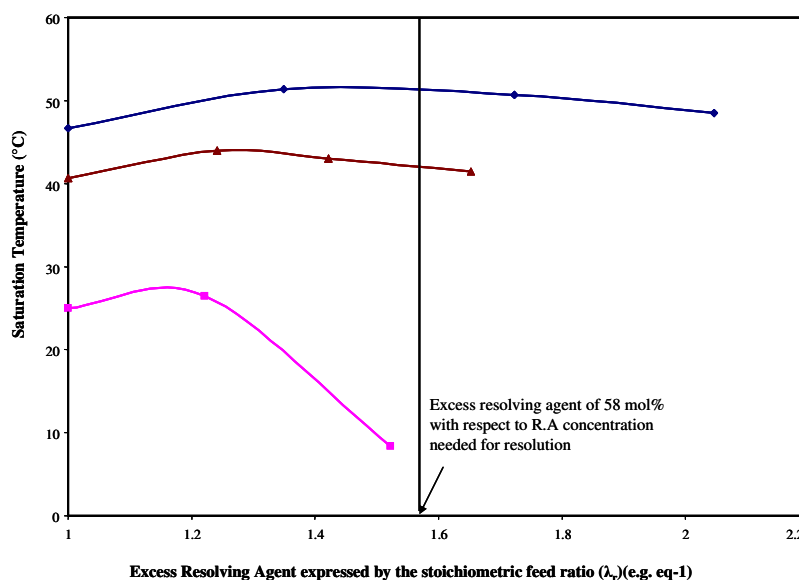


Fig 33: Effect of excess of resolving agent (R.A) (2,3dibenzoyl-D-tartaric acid) on the solubility of L-D salt (blue color), D-D salt (pink color) and 50:50 mixture of L-D: D-D salts (red color) in methanol

If the above results are compared with each other, significant difference in the effect of resolving agent on the solubility of both L-D and D-D salts can be observed. The effect of 2,3-dibenzoyl-D-tartaric acid on L-D salt solubility has more tendency to decrease the solubility at lower concentrations while D-D salt solubility is affected very little and then the increase in solubility is very high. This suggests that certain percentage of excess resolving agent could increase the crystallizing ability of L-D salt and also decreases the ability of D-D salt crystallization upon supersaturation. Thus it could be effective to use $\lambda_r > 1$.

The amount of excess resolving agent, which was taken later for the experiment, can be calculated from Fig 33. The saturation temperature of 50:50 mixture of L-D and D-D salts is at about 41°C, while the last point in the figure also has a saturation temperature close to 41°C. Correlation between these two points leads to the determination of optimum amount of excess resolving agent, since the amount of excess resolving agent present in the solution should not change the saturation temperature of the solution. Based on these considerations for the experiments described below a λ_r value of 1.58 i.e. an excess amount of 58mol% resolving agent with respect to the equimolar amount of resolving agent was selected. A detailed calculation if the conditions for the experiment carried out is given in Appendix 2 and used in the resolution experiment described in section 5.1.4 and 6.2.4.

6.1.4. Metastable zone width for primary nucleation

The metastable zone width for primary nucleation results for both L-D and D-D salts are shown in Fig 34. The figures are plotted with temperature as X-axis and concentration of the solute (wt%) in the solution as Y-axis. Fig 34(1) is for L-D salt in methanol. At various temperatures the solubility of L-D salt in methanol was measured and plotted as solubility curve (the blue line) while the line above (pink line) shows the metastable zone width for L-D salt in methanol for particular concentration and temperature. For example the solubility of L-D salt in methanol at 50°C is around 8.7 wt%. The maximum possible subcooling (ΔT_{max}) defining the metastable zone width for primary nucleation is around 13K. In between these two curves if the seeds of L-D salt are provided then in ideal case only crystal growth would occur without any nucleation for L-D salt.

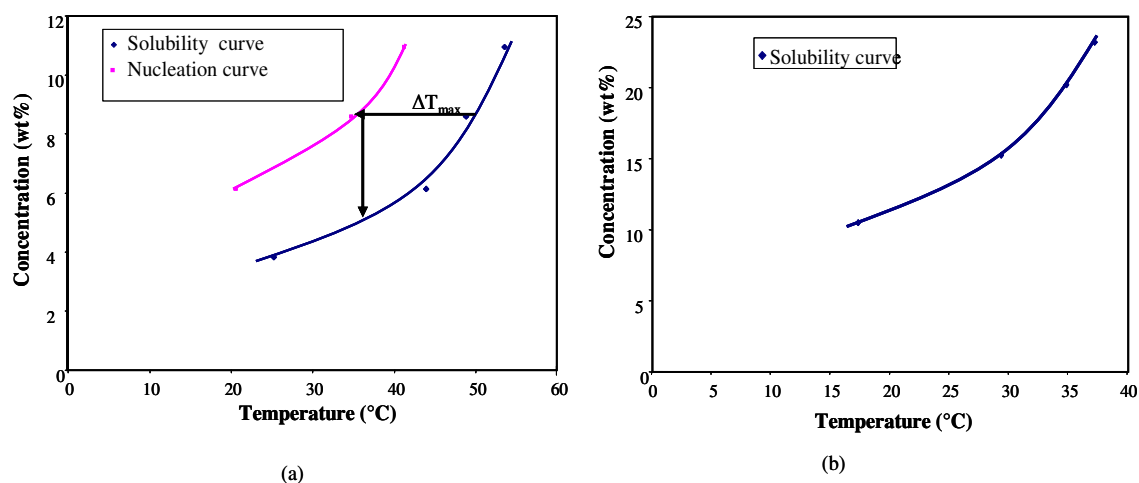


Fig 34: Metastable zone with for primary nucleation for a) L-D, b) D-D salt in methanol (Maximum possible subcooling(ΔT_{max}) from extrapolation to zero K/min cooling rate)

On the other hand in Fig 34(2) the solubility curve is only visible in particular temperature range (17-45°C) in methanol. In this required range solubility of D-D salt varied from 10 -24 wt%. But during experimentation cooling the solution to the temperature -5°C also showed no nucleation in methanol at all the D-D salt concentrations. This means there is a better possibility for L-D salt to crystallize homogeneously than for the D-D salt if both salts are taken in the solution at equal composition. But there could be heterogeneous nucleation for D-D salt in methanol while L-D salt crystallization [148]. The assumption, no heterogeneous nucleation of D-D salt, is considered for all the separation experiments. The initial saturated solution of 50:50 mixture of both L-D, D-D salts at 35°C (saturated solution of 10wt% from Fig 30) is taken for separation experiment then the seeds for the L-D salt can be given in between the temperatures 5°C - 30°C as it is the metastable zone width of L-D salt.

6.1.5. Resolution experiments for (L-D, D-D) salt pair 1

The thermodynamic data presented in chapter 6.1.3 were used to design different variants for a resolution procedure of separating less soluble L-D salt with high purity. These are a) evaporative crystallization b) cooling and anti-solvent crystallization. Further there is described the preferential crystallization of highly soluble D-D salt. Finally an overall evaluation of resolution is given.

a) Evaporative crystallization experiment design and results

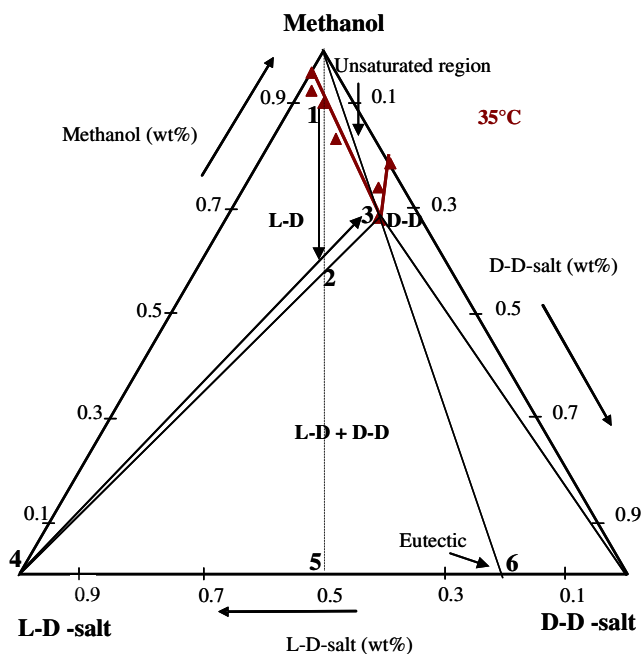


Fig 35: Evaporative crystallization based resolution experiment design for L-D, D-D salts

The separation procedure is designed based on the evaporation of solvent and crystallization of L-D salt. The resolution process design is explained with the help of Fig 35 (redrawn from Fig 30(2) and explained in chapter 6.1.3). In the Fig 35, the solubility isotherm at 35°C in methanol is given. The initial feed composition of the process is at point 1 which is 50:50 mixture of L-D: D-D salts with a concentration corresponding to the solubility in methanol at 35°C. The solution at point 1 is allowed to reach the point 2, by evaporating methanol slowly under vacuum. When the concentration of the solution reaches point 2 seeds of pure L-D salt would be introduced into the solution so that pure L-D salt crystallizes (of about segment 23) and finally the solution composition reaches to point 3 in Fig 35 which is eutectic composition (~ 22:78 L-D: D-D salts). At this point the solids are separated from the solution and analyzed. The mother liquid will be used for the further separation experimentation for highly soluble D-D salt preferentially. Due to the practical difficulties to follow the above explained procedure the operating parameters like reaching supersaturation at point 2 was modified. Seeds of L-D salt were introduced even before the solution reached point 2.

Results for evaporative crystallization of salt pair 1:

The critical problem faced during the execution of resolution experiments was monitoring the concentration of solution accurately during the evaporation of methanol so as to stop the supersaturation exactly at point 2. It was found that considerable amount of methanol escaped through the vent of vacuum pump without getting condensed in the collecting flask. So the seeds of L-D salts were introduced well before the point 2 so that crystallization of L-D salt starts perfectly. Due to the difficulty monitoring of the solution concentration, the experiment had to be stopped well before the planned point to avoid the crystallization of eutectic mixture.

The solids obtained in the experiment were analyzed with different analytical techniques. The XRPD result for solid phase obtained from the evaporative crystallization experiment is shown in Fig 36. The reference patterns of pure L-D and D-D salts are also given in the Fig 36 to evaluate the product. The XRPD of the product shows crystalline behavior. However, the pattern is completely different from the expected product L-D salt. There are no peaks from the highly soluble D-D salt as well. The crystallized product is neither one of the pure salts nor the mixture of both salts. It is certain that the substance is either a new polymorph of L-D salt or it might be completely other substance. To find the exact chemical structure of the product, the crystallized solid was further analyzed with ¹H NMR. Fig 37 depicts the ¹H NMR spectrum of the crystallized solid phase.

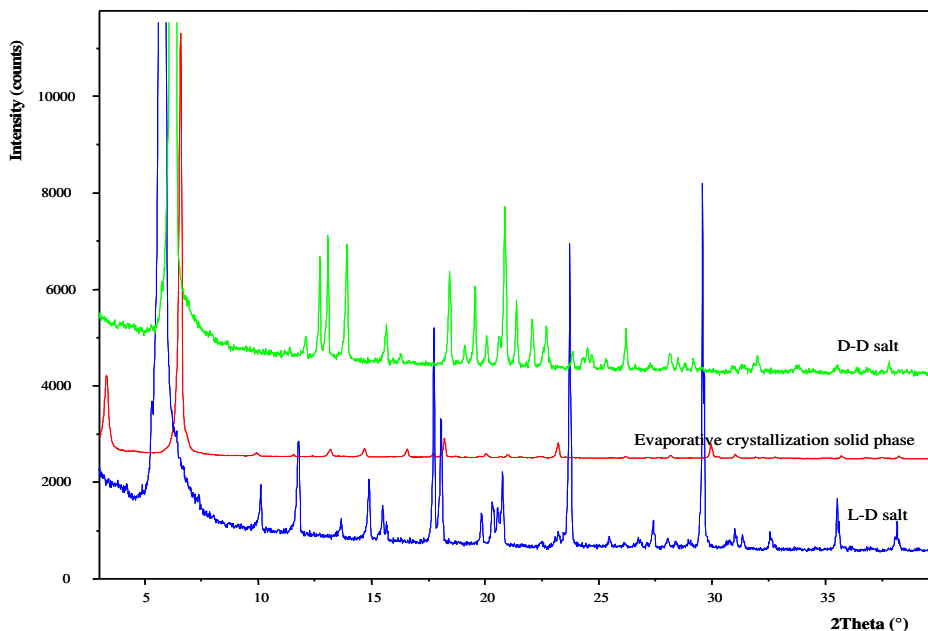


Fig 36: XRPD analysis for solid phase crystallized during Evaporative crystallization based resolution experiment for L-D, D-D salts

The analysis of ^1H NMR spectrum is ^1H NMR (400 MHz, d_6 -DMSO) 3.60-3.82 (m, 9H), 5.15 (q, 2H), 5.62 (s, 2H), 7.30-7.39 (m, 5H), 7.45-7.90 (m, 10 H). The ^1H NMR result of product is thoroughly compared with the ^1H NMR results of pure L-D and D-D salts (shown in Chapter 6.1.1) and confirmed that the crystallized material is not one of the pure L-D, D-D salts. The newly crystallized substance has only one cation molecule (L-serine benzyl ester) with one anion molecule (2,3 dibenzoyl-D-tartrate), whereas there were two cations and one anion present in the chemical structure of both L-D and D-D salts. Further the product has two molecules of methanol into its structure and thus it is a solvate. The result ascertains that the L-D salt is not so stable at higher temperatures or the newly formed substance is the stable form at higher temperatures. This behavior have to be analysed further with a strong observation during the experiment with some in-situ experimentation in presence of some spectroscopic instruments [149]. Analysis was tried with Raman spectroscopy but the laser destroyed the substance at lower temperatures and the new form was crystallized.

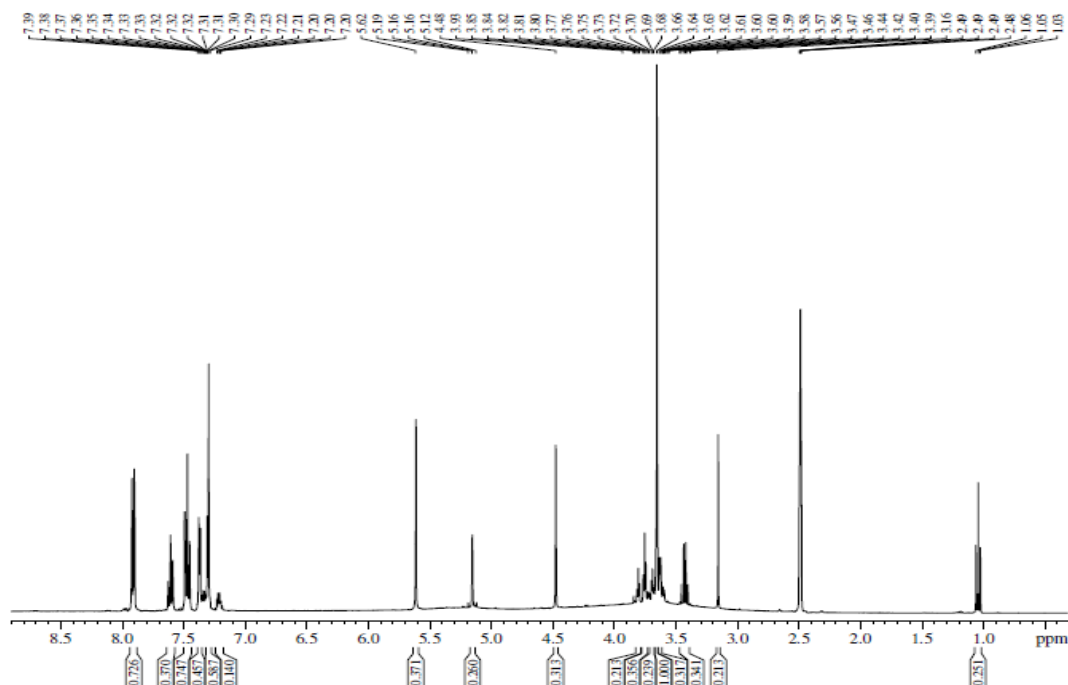


Fig 37: ^1H NMR analysis for solid phase crystallized during Evaporative crystallization based resolution experiment for L-D, D-D salts

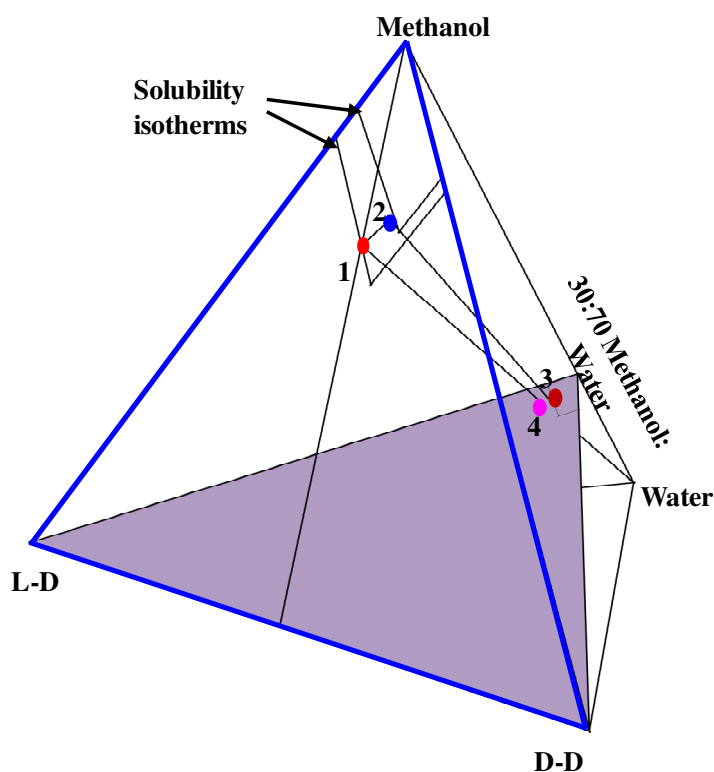
b) Cooling and anti-solvent crystallization experiment design and results

Usually diastereomeric salts are unstable at higher temperatures [13]. They might also undergo chemical degradation when temperatures are elevated. This problem is also evident in the present diastereomeric salt pairs L-D, D-D salts. To overcome this problem in the present work there is a necessity of a design based on lower temperatures like cooling the solution to enhance the supersaturation. To further increase supersaturation an anti-solvent addition is also another option [150]. Several anti-solvents were tried and finally water was selected as an anti-solvent (according to the solubility results in chapter 6.1.3) and also water has non-azeotropic behavior with methanol.

In the design of resolution experiment two issues are considered from the basic solubility data to enhance the yield or to reach the maximum with less effort. First one is the change in eutectic composition with respect to temperature (detected and discussed chapter 6.1.3) and the second one is composition of water in the final solution as anti-solvent (as derived already in subchapter 6.1.3 -effect of water as anti-solvent) .

The resolution process design is explained with the help of Fig 38. The initial composition taken for the separation process can be at point 1 in Fig 38, which is a saturated solution of

the equimolar mixture of both L-D and D-D salts in methanol. Due to the eutectic composition change towards the pure D-D salt with temperature reduction (explained in chapter 6.1.3) initially the solution can be cooled to a lower temperature say 35 to 15°C and further to 0°C (lower limit 0°C is taken due to the water utilization as anti-solvent) which is at point 2. During cooling seeds of less soluble L-D salt have to be provided to get perfect selective crystallization of desired L-D salt. Metastable zone width results (explained in chapter 6.1.4) were used to define the seeds introducing temperature. The seeds of L-D salt were given at a temperature of 25°C. When the solution reaches point 2, there is still further possibility to increase yield by increasing supersaturation via addition of anti-solvent water. With regard to the solubility results shown in chapter 6.1.3, 70 wt% of the anti-solvent composition in the final solvent is the optimum limit that can be used in this experiment.



- 1-2 : Cooling from 35 C-15 C
- 2-3: Anti-solvent crystallization
- 1-4: Overall composition change

Fig 38: Resolution by cooling and anti-solvent crystallization for L-D, D-D salts

Thus the final composition of the solvent in solution would be 70:30 water: methanol. This can be approached in either one step or different number of steps by adding small quantities of water to the solution. Thus the solution reaches point 3 from point 2 in Fig 38. In Fig 38,

the segment between point 1 and 4 denotes the overall composition change of all substances (includes liquid and solid phases) in the reactor. The difference between points 3 and 4 denotes the amount of pure L-D salt crystallized during the resolution. Same resolution procedure is also used for the determination of effect of excess resolving agent on the separation process.

After filtration further the mother liquor can be used for the preferential crystallization of highly soluble D-D salt via evaporative and cooling crystallization. The procedure followed for preferential crystallization is explained in the chapter 5.1.4(C).

Resolution results for (L-D, D-D) salt pair 1:

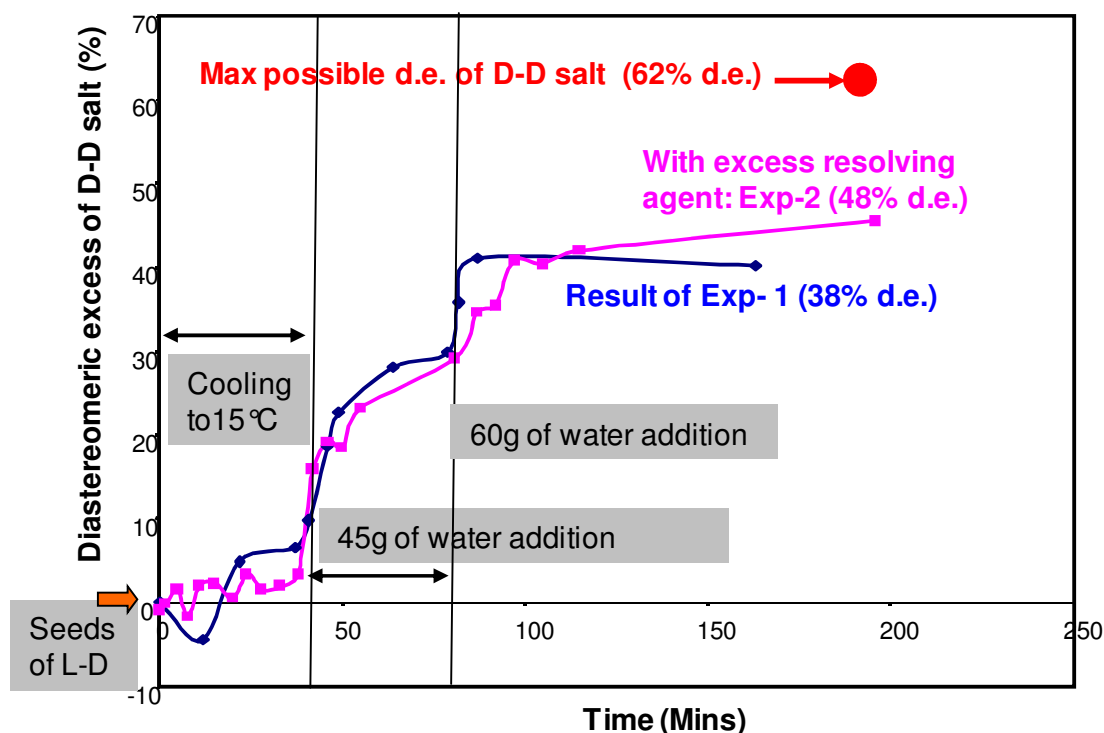


Fig 39: Liquid phase (HPLC) analysis of resolution experiments for L-D, D-D salt

Two same type of resolution experiments (explained above) were executed for L-D, D-D salt pair for the separation of less soluble L-D salt. First experiment was separation of L-D salt from a 50:50 mixture of L-D, D-D salt mixture without excess resolving agent and the second experiment was with excess resolving agent of 58wt% (with respect to necessary equimolar resolving agent) in the initial solution. The course of resolution experiments are discussed with the HPLC results obtained with respect to time in Fig 39. In both experiments there is an identical change occurred in the liquid phase composition. The diastereomeric excess after

seeding is unstable for some time but as the crystallization of L-D salt proceeded there is a stable increase in the diastereomeric excess (d.e.) of D-D salt in the liquid phase. Finally a d.e. of 48% of D-D salt (i.e. a final composition of 26:74 of L-D: D-D salts) is observed at the end of the experiment with excess resolving agent. On the other hand for the experiment without excess resolving agent a d.e. of 38% of D-D salt (i.e. a final liquid phase composition of 31:69 L-D: D-D salts) is obtained, i.e. there is an increase of 10% diastereomeric excess of D-D salt in the final liquid phase in the experiment with excess resolving agent. Thus excess resolving agent enhanced the solubility of D-D salt and reduced the solubility of L-D salt and increased the supersaturation of L-D salt to crystallize more as explained in chapter 6.1.3.

Table 5: Purity and Yield analysis of resolution experiments for L-D, D-D salts

Experiment	Initial amount of Solute, R.A and Solvent taken (g)				Purity (HPLC)	Solid phase (XRPD)	Amount of L-D salt crystallized (gm)	Yield based on L-D salt as basis (%)
	L-D salt	D-D salt	R. A	Methanol				
without resolving agent	2.5	2.5	0	45	97.6% L-D salt	L-D salt	0.95	38
with excess resolving agent	2.5	2.5	1.4	45	99.1% L-D salt	L-D salt	1.2	48

The solid phases obtained from the experiments were collected, dried and weighed directly without any further purification. The purity analysis and yield comparison for both experiments are given in Fig 40 and Table 5. As expected from the above explanation for both experiments there is a considerable difference in the final yield of both experiments. The experiment with excess resolving agent gave a yield of 48% i.e. 1.2g of L-D salt crystallized out of 2.5g of initial substance in solution. But in the case of experiment without resolving agent there is only 0.95g of L-D salt crystallized out of 2.5g of intake to the initial solution which leads to 38% of yield. The outcomes of both experiments are also highly pure with > 97.5% of L-D-salt (HPLC analysis). The XRPD patterns of both products shown in Fig40 exactly resemble L-D salt pattern. There is no specific extra peak from either D-D salt or from excess resolving agent as possible impurities.

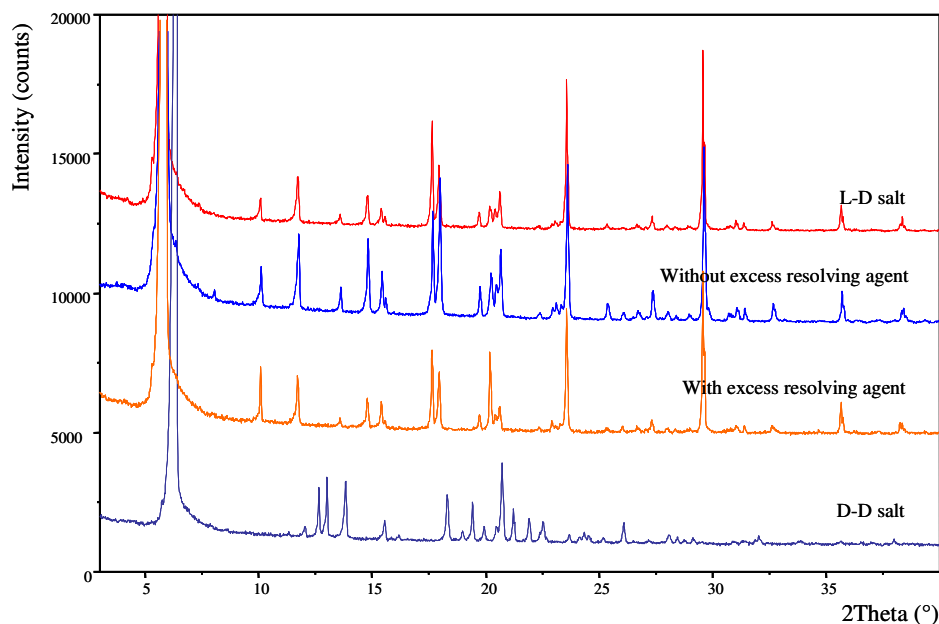


Fig 40: XRPD solid phase analysis for both resolution experiments for L-D, D-D salts

Preferential crystallization for D-D salt:

The mother liquor from the above cooling and anti-solvent crystallization experiment was used for the further separation of the other salt in two sequential steps. The experiment procedure followed in the lab and quantity of solvent evaporated is already given in the experimental section 5.1.4(c). The results for both preferential crystallization experiments are shown in Figs 41 and 42. Fig 41 gives the liquid phase composition change with respect to duration of the experiment and Fig 42 gives the solid phase XRPD analysis for both experiments.

Fig 41(1) belongs to the preferential crystallization of L-D salt. As the final composition in the liquid phase did not reach the maximum possible diastereomeric excess (say 66% d.e of D-D salt) during the first cooling and anti-solvent crystallization, the solution was allowed to crystallize again for L-D salt. According to Fig 41(1), when the seeds of L-D salt were given initially slight crystallization of L-D salt (increase in the d.e of D-D salt in liquid phase) is observed. After 5 min, crystallization of D-D salt started (decrease in the d.e. of D-D salt in liquid phase) until the 15th minute. Then spontaneous crystallization of L-D salt is observed (increase in the d.e. of D-D salt in liquid phase) till the end of the experiment. After the solid phase separation a dry cake of 0.49g was obtained from the experiment. The solid phase analysis via XRPD and HPLC also supports the liquid phase HPLC analysis. XRPD of preferential crystallization-1 for L-D salt, given in Fig 42, showed peaks from both L-D and

D-D salts. HPLC analysis of this solid phase gave a composition of 20:80 L-D: D-D salts. This means crystallization of eutectic composition occurred in the preferential crystallization-1 experiment.

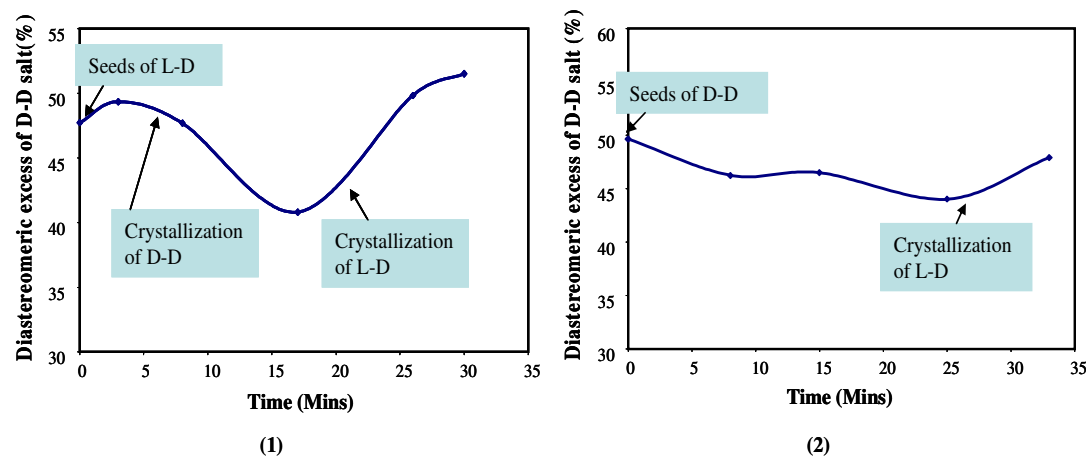


Fig 41: Liquid phase composition change during preferential crystallization experiments (1) L-D salt (2) D-D salt

In Fig 41(2), the results of liquid phase composition with respect to time are shown for the preferential crystallization experiment-2 (for D-D salt). In the Fig 41(2), after seeds of D-D salt were added to the solution, there is a decrease in the d.e of D-D salt in the liquid phase for about 25 min. During this time preferential crystallization of only D-D salt can be seen. After 25th minute, there is an increase in the d.e. of D-D salt in the liquid phase, hence there is also crystallization of L-D salt in the solution. A dry cake of 0.2g was recovered from the solution. The solid phase XRPD and HPLC analysis also supported the above liquid phase analysis. In Fig 42, XRPD pattern for preferential crystallization-2 (for D-D salt) solid phase possesses peaks from D-D salt strongly and very tiny peaks from L-D salt. HPLC analysis of the solid phase gave a composition of 6:94 L-D: D-D salt.

From the above results, it is clear that even though the eutectic composition is near to one of the diastereomeric salts it is possible to separate highly soluble salt preferentially with moderate purity.

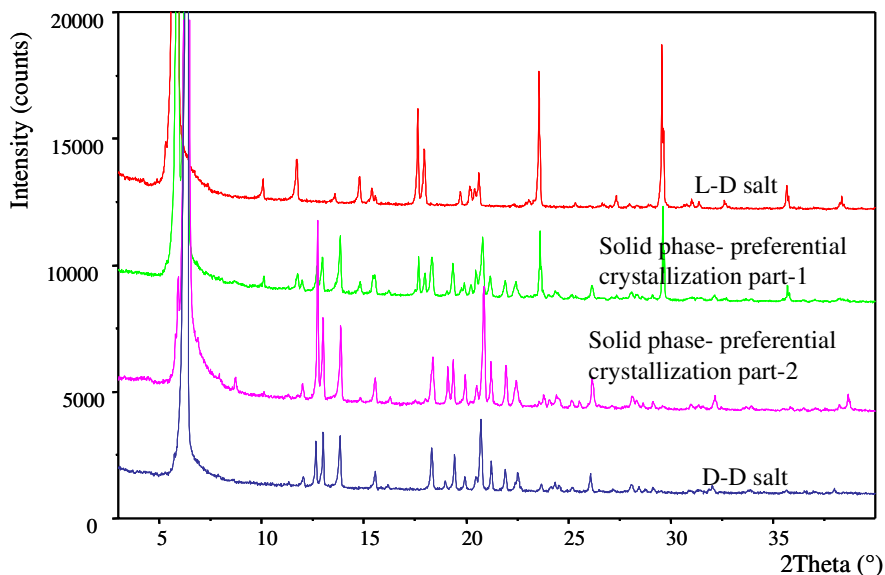
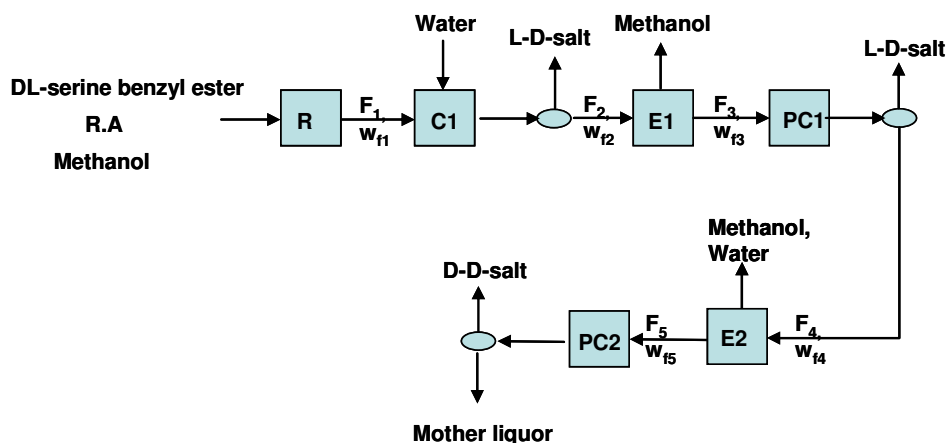


Fig 42: XRPD solid phase analysis for preferential crystallization experiment-1 (for L-D salt) and 2 (for D-D salt)

c) Entire process description for resolution of (L-D, D-D) salt pair 1:



Scheme 10: Overview for formation and resolution of L-D, D-D salts; R-reactor; C-selective crystallizer; E-evaporator; PC-crystallizer for preferential crystallization; F-feed to the concerned unit operation; w_f -weight fraction of solute

The total process followed for the resolution of L-D salt selectively and D-D salt preferentially by Classical Resolution is explained via the block diagram shown in the scheme 10. Initially, reactants D-/L-serine benzyl ester and 2,3dibenzoyl-D-tartaric acid were allowed to react to form L-D and D-D salts in reactor R. A 50:50 mixture of both salts with saturated solution of 10wt% at 35°C was used as a feed for the crystallizer 1, where selective crystallization of L-D salt was executed by cooling and anti-solvent crystallization. The solid

crystallized (L-D salt) was filtered and mother liquor was sent to the evaporator E1 to increase the supersaturation in the solution by evaporating methanol. The supersaturated solution was further allowed for crystallization of L-D salt preferentially in PE1 crystallizer. The solid phase crystallized (mixture of L-D and D-D salt) and the mother liquor was separated. The solute concentration in the mother liquor was again increased by evaporating methanol and water in the evaporator E2. The solution was further used to perform preferential crystallization of D-D salt in PE2 crystallizer. The solid phase obtained was separated and dried. All the solid phase obtained during the three crystallization experiments were analyzed with XRPD and HPLC.

Individual mass balance and quality of product from each crystallization experiment is given in Table 6. Exact values are not given in the table for the initial quantities taken for PE1, PE2 crystallization experiments, due to the loss in the masses of solvent and solute during the filtration and inter reactor transport. The results show that there is a considerable increase in the total yield from 38% to 48% (38+10) due to the preferential crystallization of counter salt (D-D salt). Very low yield for D-D salt accomplished during preferential crystallization due to the initial salt composition in the solution is at the side of L-D salt.

Table 6: Mass balances for resolution experiments for L-D, D-D salts

Experiment	Amount of solute and solvent for the crystallization experiment (g)				Purity (HPLC)	Solid phase (XRPD)	Amount of salt crystallized (g)	Yield based on initial pure L-D / D-D salt as basis (%)
	L-D salt	D-D salt	Methanol	Water				
Selective crystallization for L-D salt	2.5	2.5	45	105	97.6% L-D salt	L-D	0.95	38
Preferential crystallization for L-D salt	~ 0.9	~ 2.4	5	105	79.3% D-D	L-D and D-D	0.47	--
Preferential crystallization for D-D salt	~ 0.67	~ 2.0	0	80	94% D-D	L-D and D-D	0.2	10

~: used for the approximation of the value

The resolution of salt pair 1, by cooling and anti-solvent crystallization based on the results in Table 6, was proven to be successful to attain both salts in pure form. The yield can be improved with more intensified tests for preferential crystallization of highly soluble salt.

6.2. Results for L-L and D-L salts (pair 2)

Successful resolution for the L-D, D-D salts was the main basis for the research on the salt pairs D-L and L-L salts. D-L salt is an enantiomer of L-D salt and L-L salt is enantiomer of D-D salt. Exact synthesis procedure was followed for these two salts like L-D and D-D salt pair. Here D-L and L-L salts are also investigated for their basic thermodynamic and kinetic data and finally separation process to check the repeatability of similar kind of behavior like L-D and D-D salts. The preferred option for a resolution process is starting from a 50:50 mixture of both salts, as this composition is usually obtained from chemical synthesis. This is also an investigation on the theory suggested by Marckwald [13]. The salt pair L-D, D-D is used to separate naturally occurring L-serine by crystallizing L-D salt from the mixture. In the case of D-L, L-L salt pair the unnatural D-serine can be obtained by crystallizing D-L salt from the mixture.

6.2.1. Characterization of D-L and L-L salts

As expected the ^1H NMR spectrum of both D-L and L-L salts is identical due to the splitting of salt into ions in DMSO-d₆. ^1H NMR spectra for both salts is shown in Fig 43(a). The analysis of the ^1H NMR spectrum is ^1H NMR (400 MHz, d₆-DMSO) δ 3.62-3.72 (m, 4H), 3.81 (t, 2H), 5.15 (q, 4H), 5.62 (s, 2H), 7.31-7.39 (m, 10H), 7.46 (t, 4H), 7.61 (m, 2H), 7.91 (d, 4H). No trace of any other material like impurity is found in the NMR data. There is also no presence of any solvent like methanol or ethanol (washing solvent) in both salts. Hence both D-L and L-L salts are chemically pure with no solvate formation.

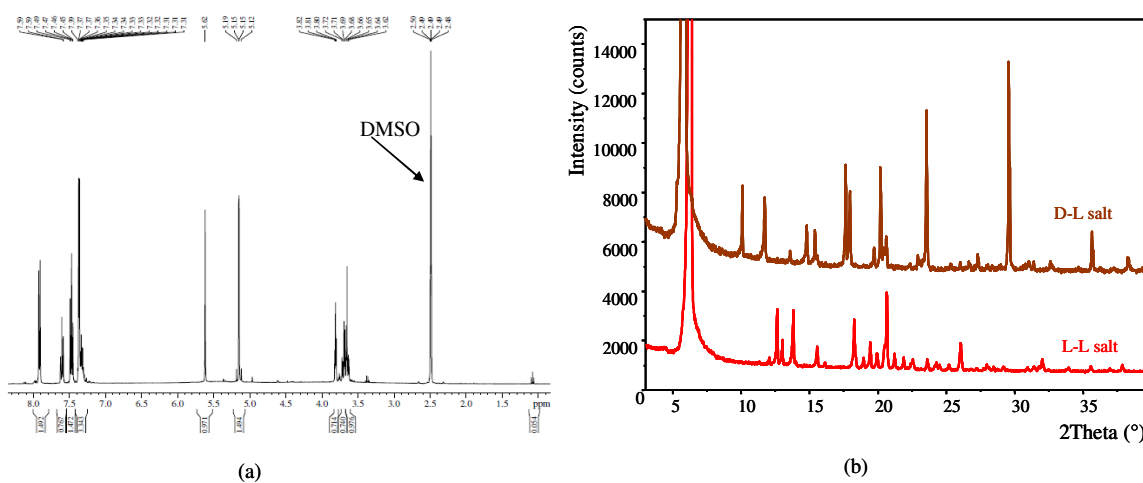


Fig43: (a) ^1H NMR and (b) XRPD patterns for both D-L and L-L salts

The crystallinity was observed with the XRPD analysis. The XRPD results are shown in the Fig 43(b). According to the patterns for both D-L- and L-L-salts, both have distinct XRPD patterns and they also represent perfect crystalline behavior. As expected the XRPD pattern of D-L and L-L salts resemble exactly like L-D and D-D salts respectively as they are enantiomers to each other. These patterns are used as a reference for future product analysis.

6.2.2. Thermodynamic data

Binary melting point phase diagram

The melting behavior was checked for both D-L, L-L salts and for their mixtures. Just like L-D and D-D salts, both D-L and L-L salts were also decomposing upon melting. The melting curves for D-L and L-L salts are given in the Appendix3. The onset point was taken as melting temperature for pure salts and for mixtures the onset of first recognized peak was taken as eutectic melting and the peak maximum of total melting curve is taken as melting temperature of the mixture.

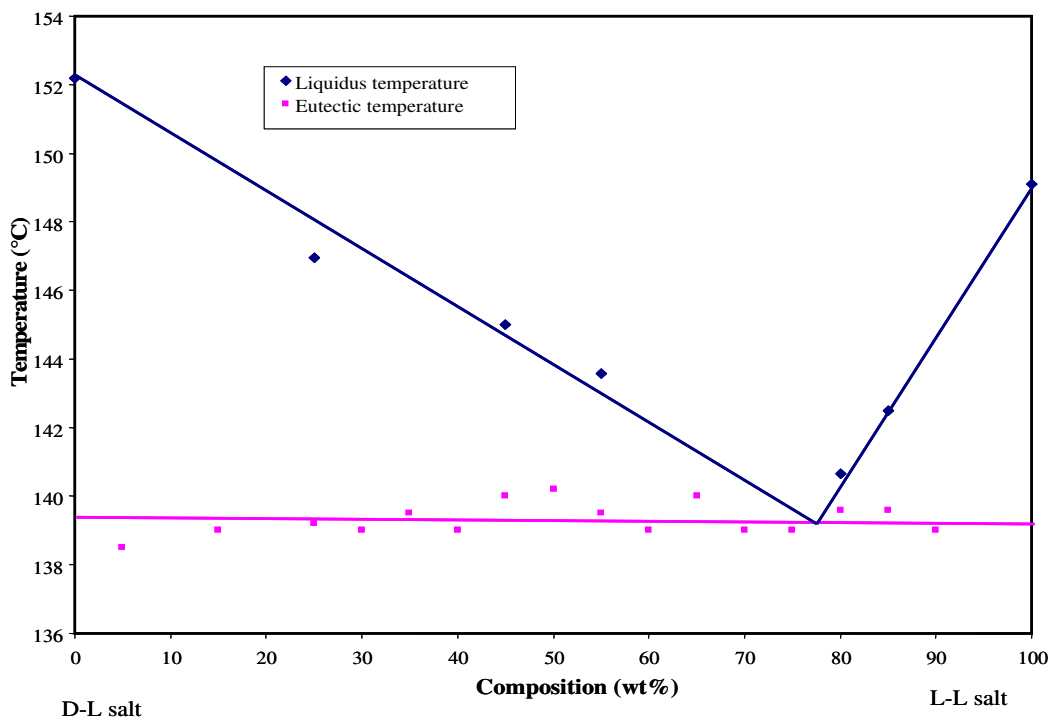


Fig 44: Binary melting point phase diagram for both D-L- and L-L-salts (the eutectic composition was derived from the DSC-experiments)

The binary melting point phase diagram for both D-L and L-L salts is shown in Fig 44. The melting temperature for L-L salt is 148°C and for D-L salt is 152.5°C. The eutectic temperature is repeated for all measurements at ~ 139°C. A guide line to the eye is drawn

through the liquidus temperatures of different mixtures. A mixture of ~20:80 D-L:L-L is taken as eutectic composition as there is a strong single peak in the DSC-melting curve. Decomposing during melting decreased the accuracy of calorimetric measurements and subsequently made it impossible to determine accurate binary phase diagram. The liquidus lines cannot be calculated theoretically via Schröder-Van Laar equation as no melting enthalpy could be determined [151]. The diastereomeric salts show a simple eutectic nature where eutectic is present on the L-L-salt side. However, on the basis of the asymmetry in the binary melting phase diagram with different melting temperatures for both salts, asymmetry in the solubility phase diagram can be anticipated.

The XRPD analysis for all measured mixtures with the reference D-L and L-L patterns are shown in Fig 45. The 50:50 mixture of both D-L and L-L salt and all the other mixtures (enriched with one of the diastereomeric salt) include just the XRPD peaks that are present in the corresponding individual pure salts without the appearance of any new peaks. This behavior is evident in the case of salts which behave simple eutectic.

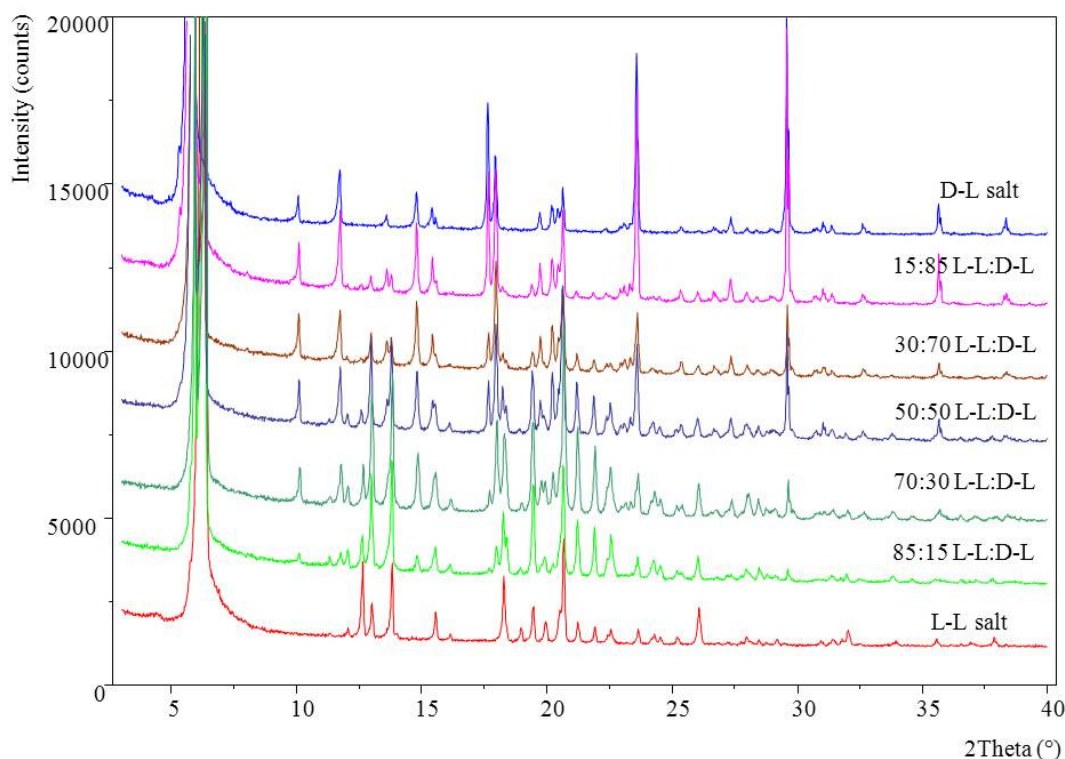


Fig 45: XRPD patterns of reference D-L and L-L salts and mixtures of different composition

The XRPD pattern results for D-L and L-L salts also strongly support the concept of a simple eutectic behavior in the binary mixtures. No indication of solid solutions or double salts in the system could be observed.

Ternary solubility phase diagram

For salt pair D-L and L-L salts no investigation was done in the case of solvent selection. As these two salt pairs are behaving exactly like their enantiomers L-D and D-D salts, directly methanol was selected as a main solvent and water was selected as an anti-solvent. Solubility phase diagrams in both solvents to check the repeatability of eutectic composition in the ternary phase as well.

Solubility phase diagram in methanol:

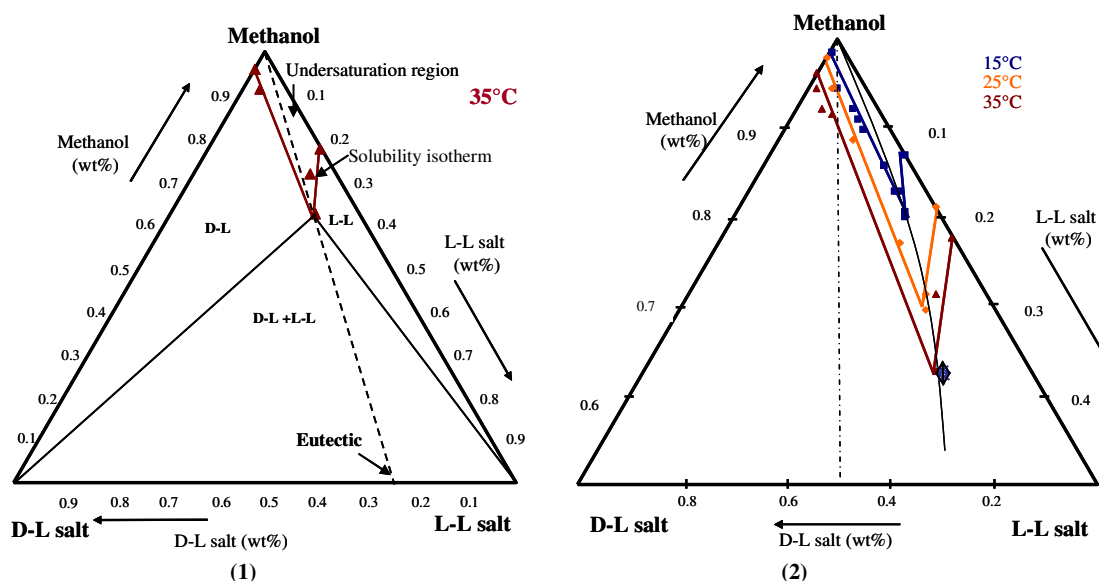


Fig 46: Ternary solubility phase diagram for D-L and L-L salts in methanol (1): Full ternary phase diagram (D-L, L-L, D-L+L-L: existence regions of the respective salts in the phase diagram) (2): Upper 50% of the solubility phase diagram

The expected simple eutectic behavior was therefore checked by measuring the ternary solubility phase diagram in methanol. In Fig 46(1) the solubility isotherm for D-L and L-L salts at 35°C is shown. As expected there is a clear asymmetry in the solubility isotherm. In the phase diagram the solubility of the mixture is increasing with increasing composition of the other salt and reached to a maximum solubility (two-salt saturation) at around 56% diastereomeric excess (d.e.) at a composition of 77:23 L-L:D-L salts. Thus only one two salt saturation point is observed in the ternary system of D-L and L-L in methanol. The solid phase XRPD results (shown in Appendix 4) also consistently indicated that no special solid state behavior like solvate formation or mixed crystals and double salts formation in the

ternary system. Thus D-L and L-L salt system also showed the simple eutectic behavior and emphasizes that the separation of both salts via crystallization is feasible.

In the same way explained in Chapter 6.1.4 for L-D and D-D salts, from the present D-L and L-L salt pair, the unnatural form D-serine can be obtained by separating D-L salt from the 50:50 diastereomeric salt mixture via crystallization within the two phase region of D-L salt (solid D-L + saturated liquid). The two phase region, which facilitates crystallization, is extremely wide for D-L salt compared to the two phase region of L-L salt in the phase diagram due to the solubility difference and eutectic position. Thus the crystallization of L-L-salt is not likely, which will result in high yield at high diastereomeric purities for the D-L-salt.

To ascertain the ternary solubility behavior, solubility isotherms at temperatures 15°C, 25°C and 35°C are also measured and shown in Fig 46(2). In the Fig 46(2), for each temperature, maximum solubility (two salt saturation point) is observed at only one composition for the mixture of salts. Just like for L-D, D-D salt pair explained in chapter 6.1.3, in the case of D-L and L-L salt pair solubility phase diagram, there is also considerable change in the eutectic composition with temperature. The eutectic composition at 15°C is at 17:83 D-L: L-L, at 25°C is at 20:80 D-L:L-L and at 35°C is at 23:77D-L:L-L salt. The eutectic composition is moving towards the 1:1 composition of D-L and L-L salt with temperature increase. This change is also expected due to the variation of the solubility increase rate with increase in temperature for D-L and L-L salt in methanol. If the separation experiment includes a cooling step there would be considerable increase in the yield of D-L salt due to the eutectic shift.

Solubility in water:

Ternary solubility phase diagram results for both D-L and L-L salts in water are shown in Fig 47. Solubility isotherms at temperatures 15°C and 35°C are presented in the upper 10% of the solubility phase diagram. As expected, strong asymmetry is observed in the solubility isotherms. Just like the behavior observed in methanol by these two salts, in water also only one solubility maximum is observed for the mixtures for both the solubility isotherms. The solubility maximum (two salt saturation point) is at 20:80 D-L: L-L salts. There is no other kind of behavior like mixed crystals or double salts are observed. Thus D-L and L-L salts also showed simple eutectic behavior in water. The observed eutectic shift with temperature in methanol is not seen in water for both salts. Due to the very low solubilities for both salts water can be used as an anti-solvent for separation experiments.

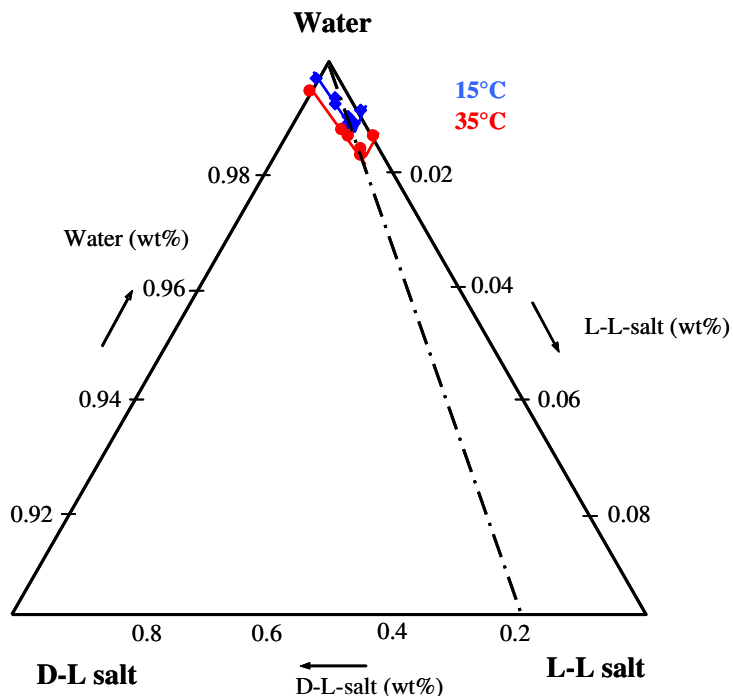


Fig 47: Ternary solubility phase diagram for D-L, L-L salts in water

Effect of water as anti-solvent in methanol

The solubility change with anti-solvent water in methanol was also measured for D-L and L-L salts at 15°C. The results are presented in Fig 48. Same kind of effect that was observed for salt pair L-D, D-D is also repeated in the solubility of D-L and L-L salts in methanol water mixtures. It can be seen from Fig 48, that there is a drastic fall in the solubility of L-L salt in methanol as the anti-solvent water content is increasing. In the case of both D-L and L-L salts also there is a continuous decrease in solubility from pure methanol to till 70:30 water : methanol and further no considerable change is observed. The solid phase analysis was also done with XRPD to cross check the possibility of formation of polymorphs and/or solvates. The XRPD patterns showed exactly as that of reference patterns. Thus, there are no polymorph, solvates or hydrates formation within the operating temperature range and solvent composition. During resolution for the salt system D-L, L-L in methanol also water is a very good option as an anti-solvent with an end solvent composition of 70:30 water: methanol.

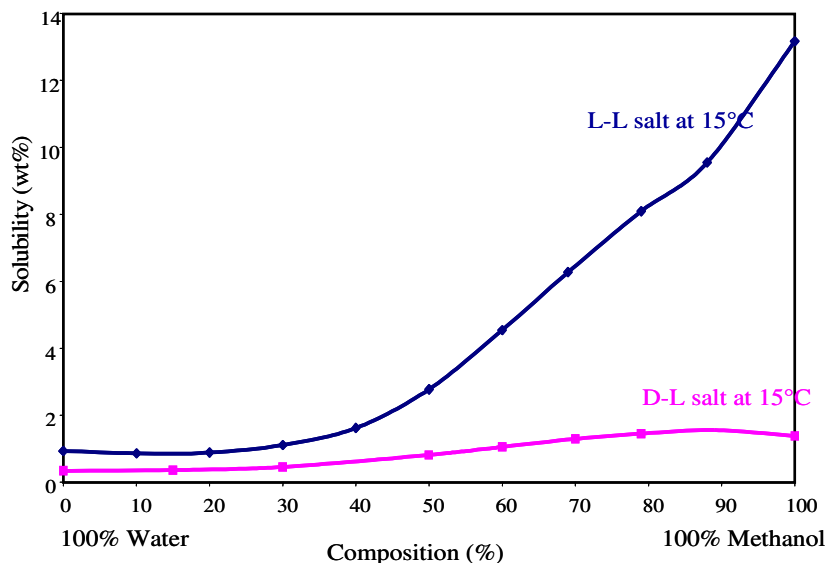


Fig 48: Solubility change for D-L, L-L salts according to the change in anti-solvent composition

6.2.3. Kinetic data

In Fig 49 (1)& (2), the results for metastable zone width for primary nucleation of D-L and L-L salts in methanol are shown respectively. With the help of the solubility data presented in solubility phase diagram in chapter 6.2.2, the solubility curve is drawn for both salts in the figures 49 (1) & (2) (blue lines). The experimental results obtained for metastable zone width for primary nucleation for various known concentrations of both pure D-L and L-L salts in methanol (mentioned in the experimental section chapter 5.1.3) are considered for nucleation curve determination. The results of nucleation curve obtained are shown in a pink line in the Fig 49(1)&(2). Just like L-D salt in chapter 6.1.4, in the case of D-L salt also there is a defined metastable zone with for primary nucleation. For example, a saturated solution of D-L salt at 55°C with concentration of 10wt% in methanol can be crystallized without any seeds at a temperature of 42°C at zero cooling rate. The maximum subcooling (ΔT_{max}) is 13°C. If seeds are provided in this zone during experiment, pure D-L salt crystal growth would be maintained.

On the other hand for L-L salt in methanol, shown in Fig 49(2), for the given solubility curve at all saturation points, there observed no nucleation in the given temperature range. Thus the metastable zone width for L-L salt is beyond the expected temperature range i.e. (L-L salt saturated solution needs to be cooled even below 0°C to crystallize spontaneously). Hence, if a 1:1 saturated mixture of mixture of both D-L and L-L salts are cooled to a lower

temperature, there is a huge possibility for homogeneous crystallization of D-L salt but not for L-L salt. Just like for L-D, D-D salt pair shown in chapter 6.1.4, during the separation, if the initial saturated solution (10wt%) of 50:50 mixture of D-L and L-L salt in methanol at 35°C is taken then the seeds D-L salt can be given at around 5°C -25°C.

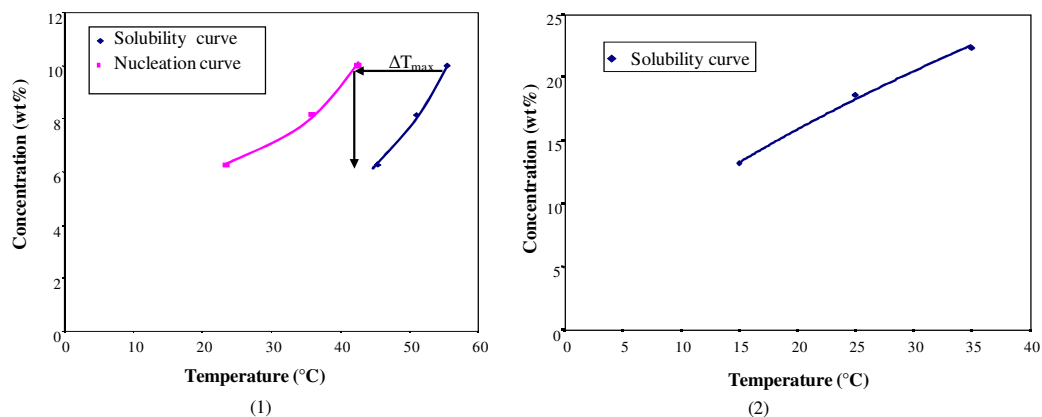


Fig 49: Metastable zone widths for primary nucleation in methanol for (1) D-L salt (2) L-L salts

6.2.4. Resolution experiments for D-L, L-L salt mixture

The salt pair D-L and L-L is also resolved by the same cooling and anti-solvent crystallization separation experiment as these are exact enantiomers of L-D and D-D salts respectively. Here no trials were done for evaporation crystallization based separation experiment. The resolution experiment with excess resolving agent was also repeated with the same amount of 58% excess 2,3dibenzoyl-L-tartaric acid. The results of both resolution experiments with and without excess resolving agents are compared each other in the following.

Resolution results for D-L, L-L salt pair:

The resolution results for D-L and L-L salt pair are shown in Figures 50 and 51 and Table 7. Fig 50 shows the composition change in the crystallizer during the separation experiments with excess resolving agent (squares) and without excess resolving agent (diamonds). The result clearly explains that in both experiments D-L salt started crystallizing at the same time. During the course of both experiments at all the points for the same time, the diastereomeric excess of L-L salt is considerably higher in the presence of excess resolving agent when compared to its absence. Thus the excess resolving agent has shown clear lowering effect on the solubility of D-L salt. At the same time it increased the solubility of L-L salt by decreasing its crystallizing ability. The difference in the diastereomeric excess of end points

of both experiments gave a good indication for the potential increase in yields of D-L salt in the presence of excess resolving agent.

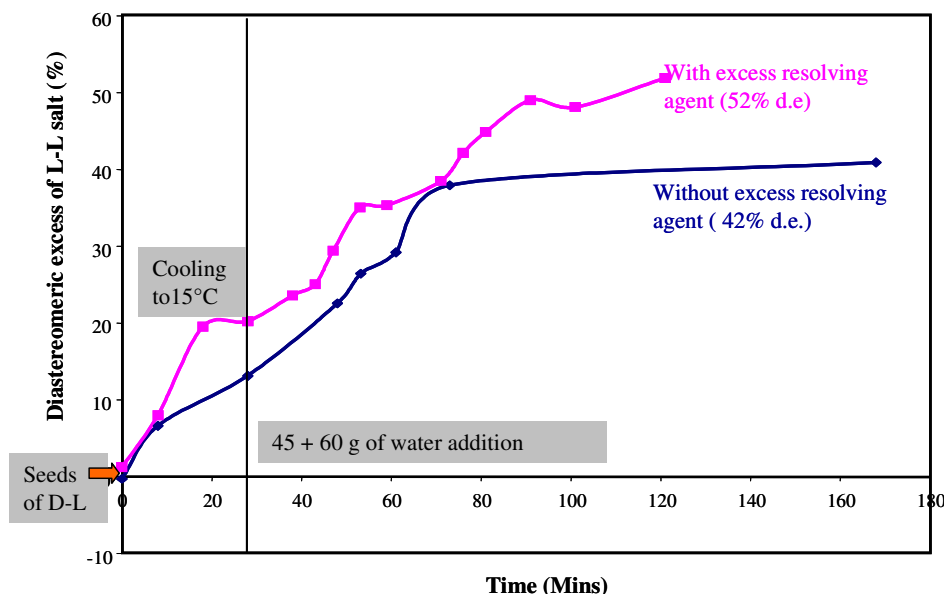


Fig 50: Liquid phase (HPLC) analysis of resolution experiments for D-L, L-L salts

The solid phase analysis of the filtered and dried product of both experiments is shown in the Fig 51. The XRPD of both products resemble exactly the D-L salt XRPD pattern. No indication from the other diastereomeric L-L salt, the excess resolving agent or other solid forms is found in the product. The purity analyzed by HPLC is specified in Table 7 as higher than 98% and 99% respectively.

Table 7: Purity and Yield analysis of resolution experiments for D-L, L-L salts

Experiment	Initial amount of Solute, R.A and Solvent taken (g)				Purity (HPLC)	Solid phase (XRPD)	Amount of D-L salt crystallized (g)	Yield based on D-L salt as basis (%)
	D-L salt	L-L salt	R. A	Methanol				
without resolving agent	2.5	2.5	0	45	>98% D-L salt	D-L salt	1.05	42
with excess resolving agent	2.5	2.5	1.4	45	>99% D-L salt	D-L salt	1.31	52

The difference in diastereomeric excesses at the end of experiment indicates that there is considerable impact of excess resolving agent on the resolution. The experiment without

excess resolving agent crystallized 1.05g of dry cake which leads to a 42% yield. On the other hand it was 1.31g of dry cake with 52% yield for the experiment with excess resolving agent. The yield obtained for D-L salt (from salt pair D-L, L-L) is slightly higher compared to the yield obtained for L-D salt in the previous salt pair (L-D, D-D salts).

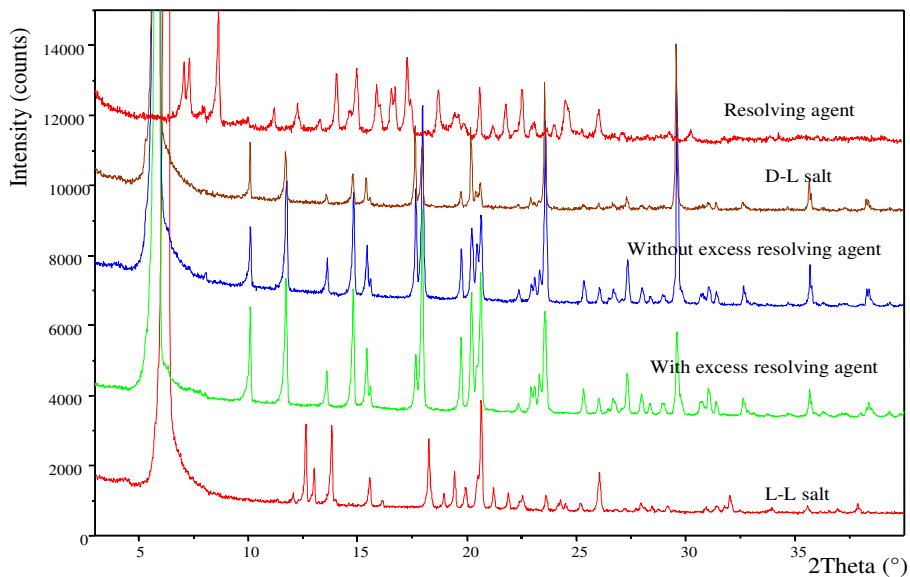


Fig 51: XRPD solid phase analysis for both resolution experiments for D-L, L-L salts

The resolution of less soluble D-L salt from the salt pair 2 was also successful. Additional resolving agent in the solution increased the yield for D-L salt by a significant percentage. This salt system could be attempted for preferential crystallization of L-L salt to increase the yield further.

6.3. Results for D-LM and L-LM salts (pair 3)

In comparison to the tartrates salt shown above mandelic acid is a monoacid resolving agent, which will form naturally an equal stoichiometry (one mole of acid requires one mole of base) with the monobasic serine benzyl ester. Furthermore mandelic acid is very well known substance used as resolving agent in laboratory and industrial relevant scales[76].

6.3.1. Characterization of D-LM and L-LM salts

It is obvious for D-LM and L-LM to have identical ^1H NMR spectra (shown in Fig 52(1)) as they also split into ions in d6-DMSO. The ^1H NMR results are analyzed and presented. ^1H NMR (400 MHz, d6-DMSO) 3.65-3.74 (m, 2H), 3.79 (t, 1H), 4.77 (s, 1H), 5.19 (t, 2H), 7.20-7.40 (m, 10H). No extra peak in the ^1H NMR spectra specifies that there is no impurity or any trace of other solvents from the synthesis. The XRPD solid phase characterization results for pure D-LM, L-LM salts are shown in Fig 52(2).

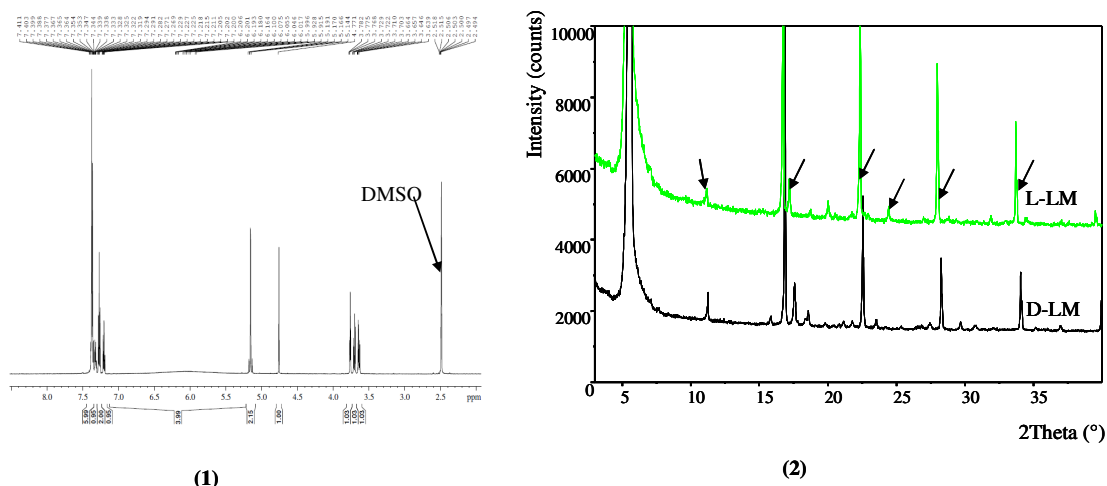


Fig 52: (1) ^1H NMR and (2) XRPD patterns for both D-LM- and L-LM-salts

The strong XRPD patterns for both salts strengthen that the salts formed are crystalline. Interestingly both D-LM and L-LM-salts are showing an obvious similarity of the main peaks. The signals are slightly shifted against each other (e.g. peaks at $17.4^\circ/17.5^\circ$, $28^\circ/28.1^\circ$ and $33^\circ/34^\circ$ for L-LM/D-LM).

6.3.2. Binary mixtures behavior analysis of D-LM, L-LM salt

The similarity between the XRPD patterns for D-LM and L-LM is also repeated for all mixtures of both salts which are shown in Fig 53. In the mixtures some new peaks (showed in the rectangular box) other than the peaks present in the both pure salts occurred. As the

similarity is very high between these two salts it is a strong indication for solid solution behavior [77, 152].

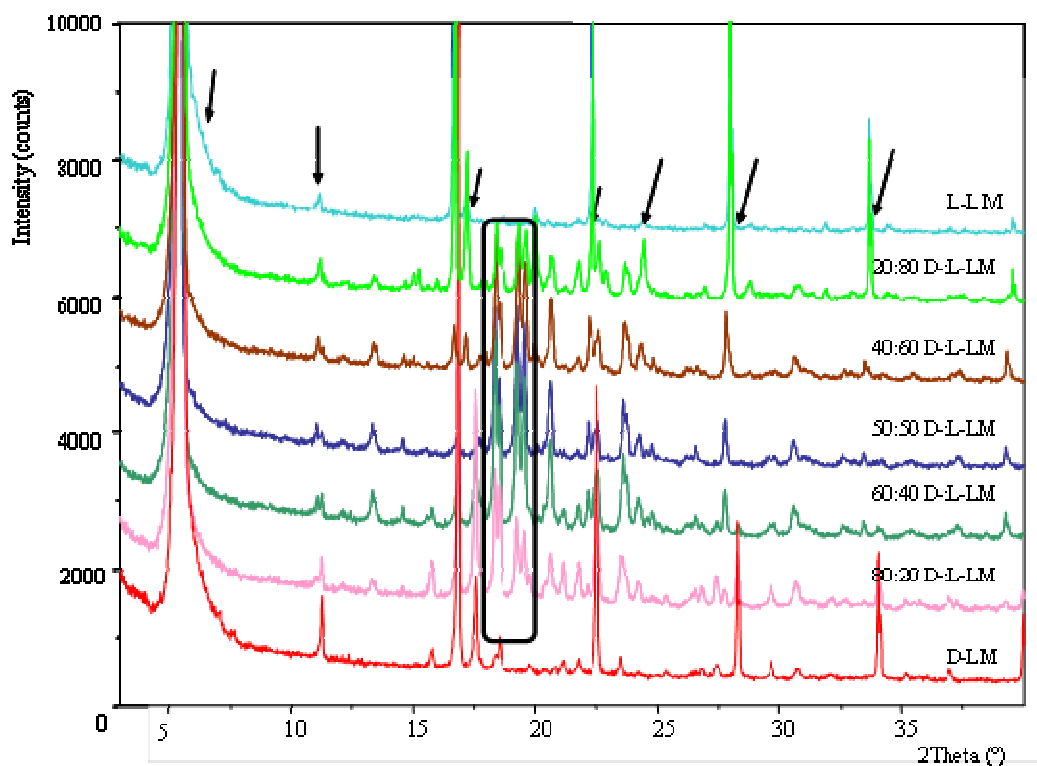


Fig 53: XRPD patterns for pure D-LM and L-LM salts and mixtures of both (arrows indicate the similar peaks present in both salts and the box represent the extra peaks for mixtures)

The potential solid solution behavior of D-LM and L-LM salts was further verified with DSC melting curves. The DSC melting curves for pure and mixtures of both salts are shown in the Fig 54. Both pure D-LM and L-LM salts comprise a single sharp melting peak at almost same melting temperatures of 134.9°C and 135.6°C, respectively. The melting enthalpies of both salts varied significantly (with the values for D-LM: 0.13 J/mol and for L-LM: 0.34 J/mol), which could lead to an asymmetry in the phase diagrams. In the case of mixtures, DSC curves shown in Fig 54 also possess a single sharp peak. No indication of a eutectic melting was observed. Usually this kind of behavior is observed in the binary systems of solid solutions [152]. The DSC melting curves for mixtures, thus further strengthened the assumption that D-LM and L-LM form solid solutions (mixed crystals).

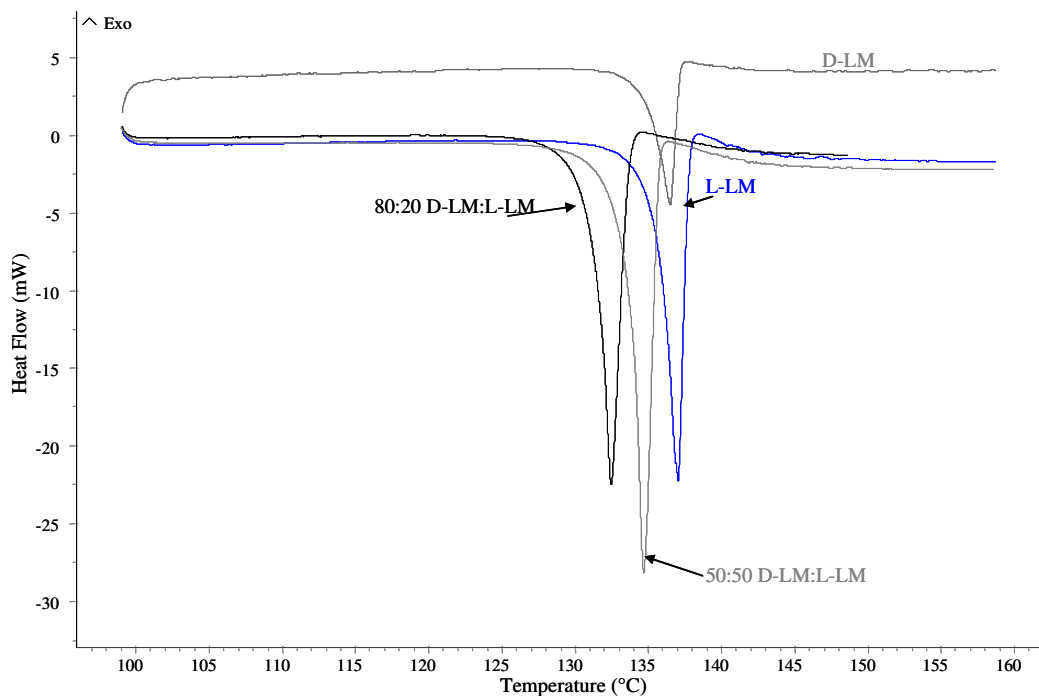


Fig 54: DSC melting curves for pure D-LM and L-LM salts and two mixtures

6.3.3. Ternary solubility phase diagram

The solubility phase diagram for the diastereomeric pair L-LM and D-LM in acetone is shown in Fig 55. In the figure solubility isotherms at temperatures of 5 and 15°C are presented. Both isotherms show similar behavior in the phase diagram. The solubility values for D-LM and L-LM salts are 3.9 wt%, 3.41wt% at 5°C and 4.66 wt%, 4.14wt% at 15°C respectively. Both salts have almost an identical solubility with a slightly higher value for D-LM salt, which is consistent with the slightly lower melting temperature of D-LM. In the case of mixtures, as the composition of one of the salt is increasing from 50:50 mixture of both salts, the solubility of the mixture is gradually decreasing on each side of the phase diagram. The solubility minimum is observed at around the 50:50 mixture of both salts for both the temperatures 5°C and 15°C. This is related to the solubility reducing effect of one salt on the other salt in solution. Moreover, no specific solubility maximum (eutectic composition) was observed in the phase diagram. There are some deviations of the data in the solubility isotherm at 15°C, which are due to the high volatility of acetone during the solubility measurement. Thus the solubility phase diagram for D-LM and L-LM also contains the formation of mixed crystals (solid solutions) within the whole system, equally specified by XRPD patterns and DSC melting curves. Mixed crystal behavior of D-LM and L-LM salts in the binary and ternary systems does not support the crystallization processes and hinders the separation. This usually

also causes very low purity and yields. Hence no corresponding resolution experiments were attempted. From the results obtained for the L-LM and D-LM salts, the conclusion can be driven that L-(+)-mandelic acid as a resolving agent is not suitable for the separation of DL-serine.

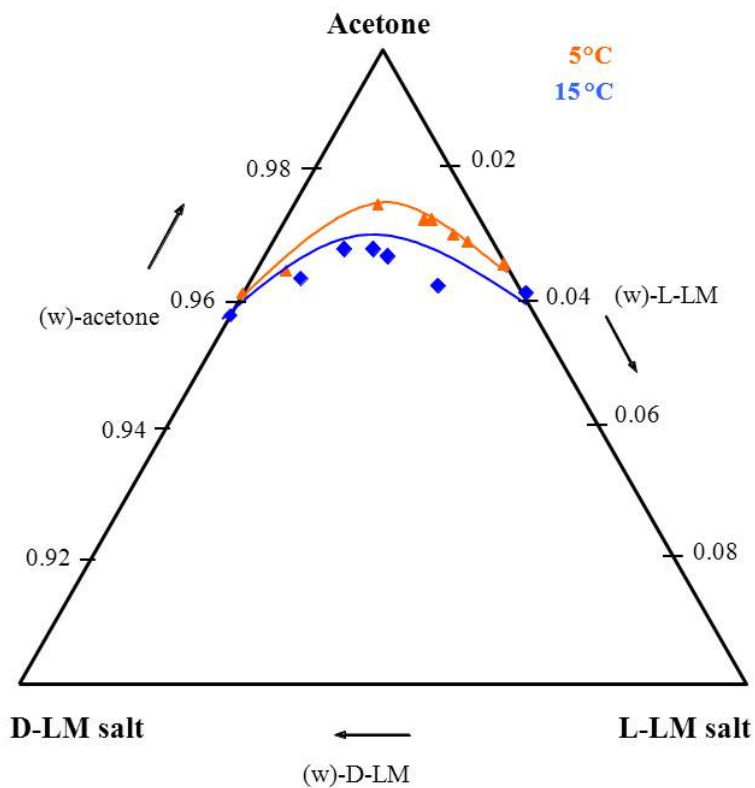


Fig 55: Ternary solubility phase diagram for D-LM and L-LM salts in acetone

6.4. Results for D-LT and L-LT salts (pair 4)

6.4.1. Characterization of D-LT and L-LT salts

The results of ^1H NMR and XRPD phase analysis are shown in Fig 56. Like the other studied salt pairs, also D-LT and L-LT have the same ^1H NMR spectra. The ^1H NMR result is ^1H NMR (400 MHz, d_6 -DMSO) 3.61-3.74 (m, 6H), 3.90 (s, 2H), 5.17 (t, 4H), 7.31-7.38 (m, 10H). In NMR spectra no traces of any impurity was found and also no trace of solvent was found. Thus the salts D-LT and L-LT are chemically pure and also form no solvate. D-LT, L-LT salts have clearly different XRPD patterns. The L(+)/tartaric acid salts L-/D-serine benzyl ester (L-LT, D-LT) are also perfectly crystalline. These patterns are used as reference to compare with all the other solid phases obtained in the binary mixtures preparation and ternary solubility measurements for D-LT, L-LT salts.

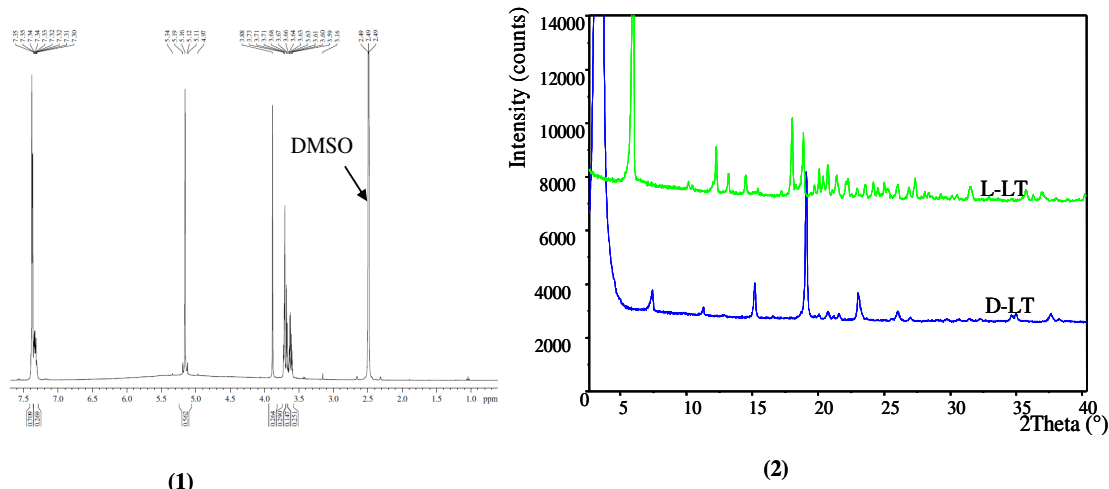


Fig 56: (1) ^1H NMR and (2) XRPD patterns for both D-LT- and L-LT-salts

6.4.2. Binary mixtures behavior analysis of D-LT and L-LT salts

The XRPD patterns of different mixtures of D-LT and L-LT salts were prepared and their solid phase behavior was analyzed with both XRPD and DSC melting behavior. The XRPD results for the mixtures of D-LT, L-LT along with pure L-LT and D-LT salts are given in Fig 57. The XRPD pattern for the 50:50 D-LT: L-LT salt is not the same like any of the pure salts. It has a new pattern. However, mixtures at other compositions of both salts showed XRPD patterns with peaks of both individual salts as well as the peaks of the 50:50 mixture. From these XRPD results a hypothesis can be made that this D-LT, L-LT salts form a double salt near to the 50:50 composition. This hypothesis is further supported by DSC melting curves (shown in Appendix 5). Sharp melting peaks were observed for both pure D-LT and L-LT salts. The melting temperature for the D-LT salt is at 154.7°C , and for the L-LT salt is at

143.3°C. The melting curves for mixtures possess two peaks merged into one another and have different eutectic melting temperatures (initial melting peak) due to the existence of the double salt. In this case also decomposition during melting was observed, which prevented more accurate quantitative analysis.

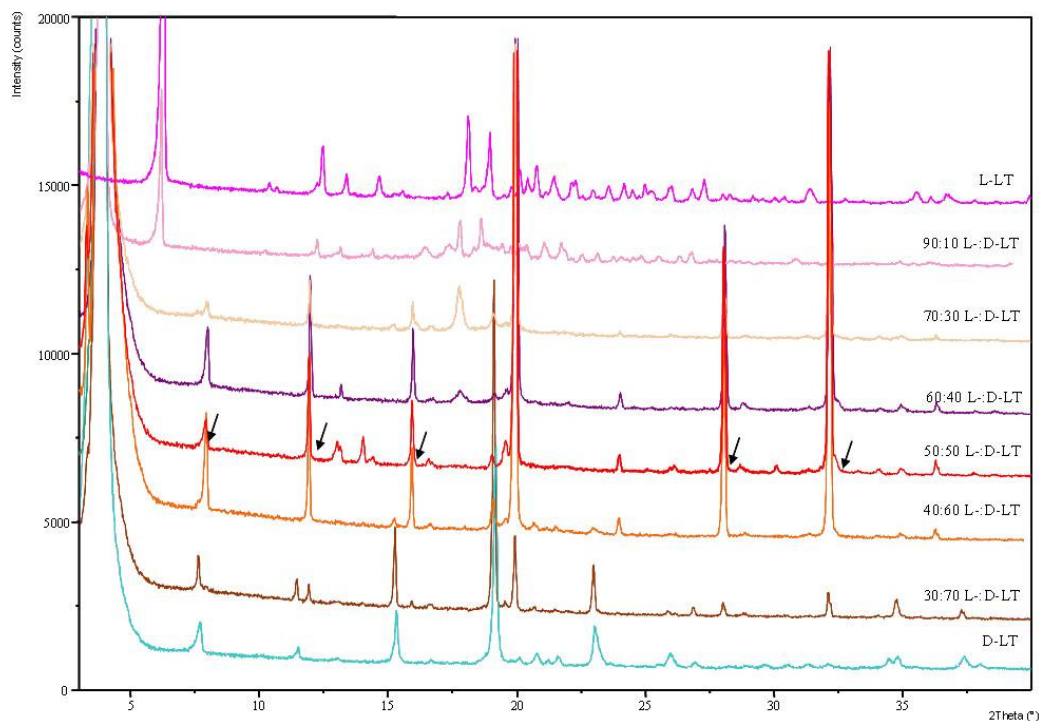


Fig 57: XRPD patterns for both D-LT and L-LT salts and their mixtures

6.4.3. Ternary solubility phase diagram

To confirm the double salt behavior for D-LT, L-LT salts, solubility measurements were performed for both salts and also for different mixtures in water at 25°C. A ternary solubility phase diagram was plotted with the help of results obtained. The upper 20% of total solubility phase diagram is shown in Fig 58. Both pure salts have a solubility difference of just 4 wt% in water at 25°C. Even though it is not a huge difference, it is considerable for separation if the salts would not behave like a double salt. It can also be seen that the salt solubility is increasing from both pure salt solubilities as the fraction of the other salt is increasing. In the isotherm there were observed two local maximum solubilities on the each side of the 50:50 mixture. The composition of maximum solubility points are 79:21 and 5:95 of D-LT:L-LT salts respectively (i.e. 58% diastereomeric excess of D-LT and 90% diastereomeric excess of L-LT salt respectively). Thus the salts D-LT and L-LT behave like double salts in their binary and ternary phase systems. In Fig 58, line segments are used to indicate the different phase

regions originating from the two-salt points. The regions 1, 2 and 3 in the phase diagram represent two phase regions (one solid and one liquid phase), while the regions 4, 5 represent three phase regions (two solid and one liquid phase).

From the solubility phase diagram the conclusion can be drawn that the separation process directly from the 50:50 mixture of the diastereomeric salts is not feasible. To make it feasible a preliminary enrichment by chromatography or by any other separation technique would be necessary [153], which is not practical and in particular not the intention of a diastereomeric salt resolution.

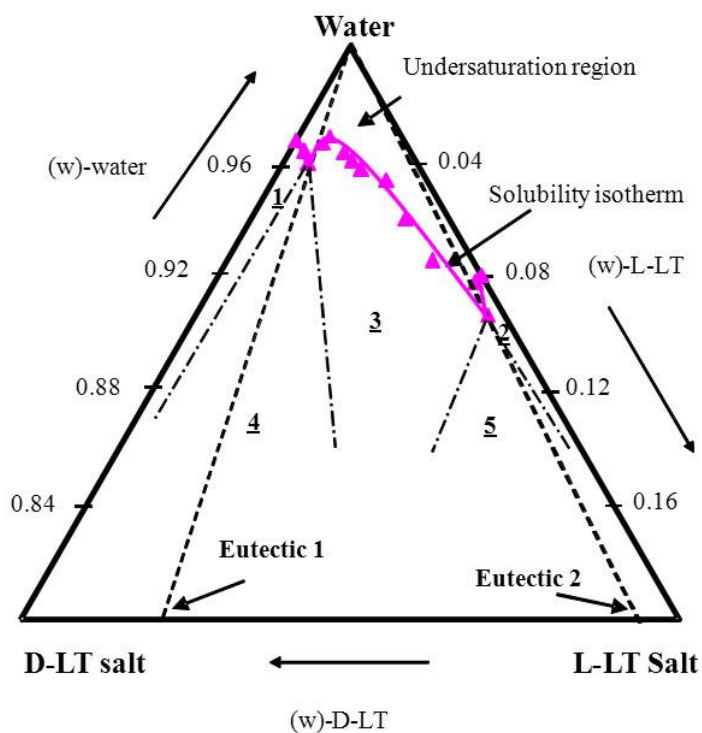


Fig 58: Solubility phase diagram for D-LT and L-LT salts in water for 25°C (just the upper 20% of the phase diagram is shown) incl. illustration of the phase conditions

6.5. Results of L-D-Toluyl, D-D-Toluyl salts (pair 5)

Synthesis results of L-D-Toluyl, D-D-Toluyl salts:

After the synthesis of both L-D-Toluyl and D-D-Toluyl salts, they were allowed to recrystallize in methanol repeatedly until their melting points became constant. The melting curves are given in Appendix 5. The melting temperature for L-D-Toluyl salt is 154.41°C and for D-D-Toluyl salt is 154.95°C (almost same). Both are decomposing during melting. Further, these substances were characterized by ^1H NMR and XRPD. The NMR results for both salts are given in Fig 59 (1) & (2).

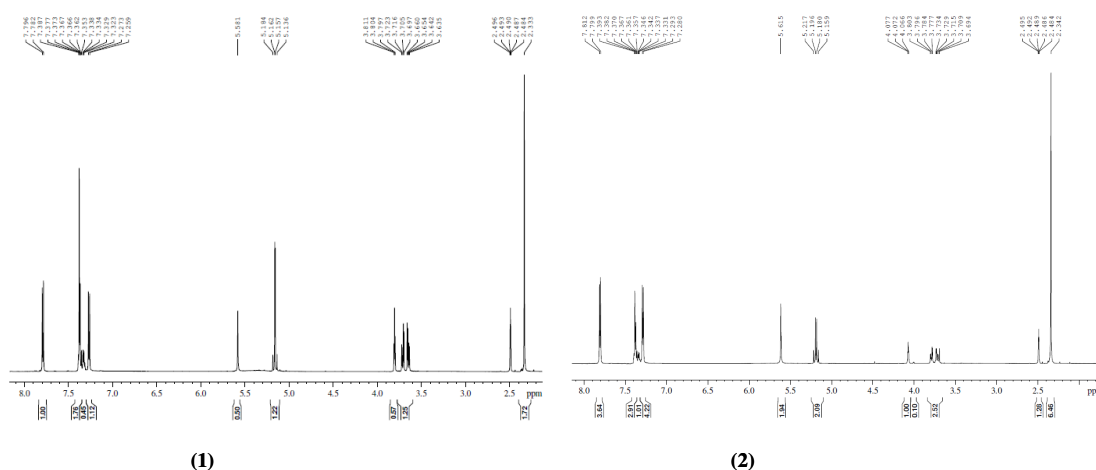


Fig 59: ^1H NMR spectrum for (1) L-D-Toluyl salt (2) D-D-Toluyl salt

Interesting results were found in the case of L-D-Toluyl and D-D-Toluyl salts. Unlike the other diastereomeric salt pairs, L-D-Toluyl and D-D-Toluyl salts possess very considerable difference in their ^1H NMR spectra. The analysis of ^1H NMR spectrum for L-D-Toluyl salt is ^1H NMR (400 MHz, d_6 -DMSO) 2.33 (s, 6H), 3.64-3.72 (m, 4H), 3.8 (t, 2H), 5.16 (q, 4H), 5.81 (s, 2H), 7.26-7.39 (m, 14H), 7.85 (d, 4H). According to the above analysis the substance is chemically pure and has no solvate formation. Analysis also gives the information that the substance contains exactly expected chemical structure (shown in Scheme 7 in Chapter 4.2.1(e)) with two cations of L-serine benzyl ester and one anion of 2,3-ditoluoyl-D-tartaric acid in its molecular structure.

On the other hand, In the case of D-D-Toluyl salt there are some different results in its NMR spectrum. The analysis of ^1H NMR spectra for D-D-Toluyl salt is ^1H NMR (400 MHz, d_6 -DMSO) δ 2.34 (s, 6H), 3.69-3.80 (m, 2H), 4.07 (t, 1H), 5.19 (q, 2H), 5.62 (s, 2H), 7.28-7.39 (m, 9H), 7.81 (d, 4H). From NMR results it is clear that D-D-Toluyl salt is also chemically

pure and no solvent is found, but in its chemical structure it possesses only one cation of D-serine benzyl ester and one anion of 2,3-ditoluoyl-D-tartaric acid. Thus D-D-Toluyl salt did not form the intended chemical structure with two molecules of D-serine benzyl ester. Hence both D-D-Toluyl, L-D-Toluyl salts are not diastereomers to each other. The reason for this behavior is still not found even though there were some examples in literature [154, 155]. The XRPD characterization results of both diastereomeric salts are shown in Fig 60. Absolutely different XRPD patterns were found for both salts. This variation in the patterns is justifiable already due to the difference in the chemical formula of both salts. Both salts are crystalline. These can be used for future analysis as reference.

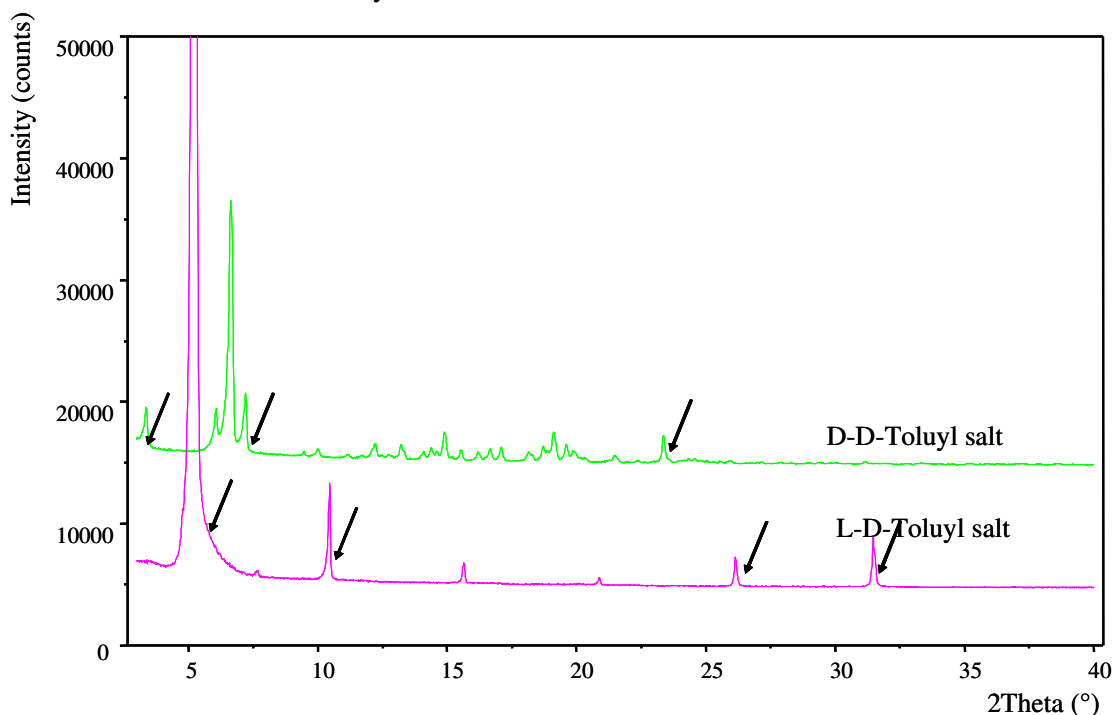


Fig 60: XRPD patterns of pure L-D-Toluyl and D-D-Toluyl salts (main peaks characterized with arrows)

The change in the chemical composition during the formation of diastereomeric salts was also repeated in the case of L-/D-serine methyl ester when they were reacted with 2,3-dibenzoyl-D-tartaric acid in methanol (the results are not shown here).

From the results it can be concluded that proceeding with L-D-Toluyl and D-D-Toluyl salt for resolution would support the separation process if they show simple eutectic behaviour. Due to the presence of one less cation in D-D-Toluyl salt (if it is less soluble salt), the total yield would be reduced to half of the actual yield. On the other hand, if L-D-Toluyl salt is less soluble salt, then amount of resolving agent needed would be reduced.

6.6. Results of LPG-CS, DPG-CS salts (pair 6)

From the Literature it was clear that both DPG-CS, LPG-CS salts form simple eutectic in nature [107]. But certain points like effect of excess resolving agent on the resolution was not verified. As these salts are not available commercially, they were synthesized and characterized. A quick solvent screening was done with different solvents available. Then the solvent with highest solubility (moderate solubility ratio) was selected as a main solvent for resolution and the solvent with least and very low solubility was selected as an anti-solvent. A resolution experiment was designed based on the ternary phase diagram results. The same resolution process was also performed with different concentration of excess resolving agents. All the results are given in the subsections of this chapter.

6.6.1. Characterization of LPG-CS and DPG-CS

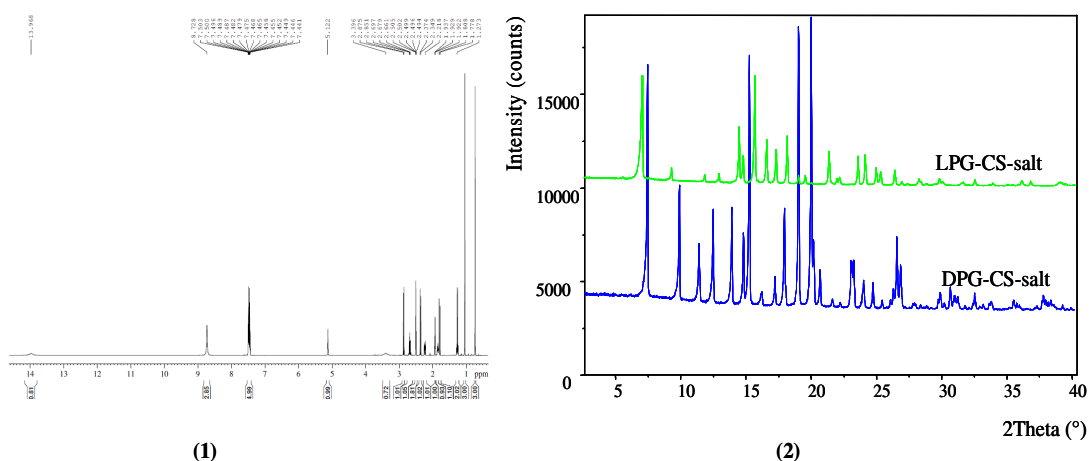


Fig 61: Characterization results of DPG-CS, LPG-CS (1) ¹H NMR spectrum (2) XRPD analysis

Like all the above serine salt pairs, DPG-CS and LPG-CS salts were also characterized with DSC melting point, ¹H NMR and XRPD solid phase analysis. Sharp melting curves were observed with a melting temperature of 191.2°C (onset point) for DPG-CS and 176°C for LPG-CS. The characterization results of both salts measured with ¹H NMR and XRPD are shown in the Fig 61. It is also obvious that both DPG-CS, LPG-CS also have the same ¹H NMR spectra. The ¹H NMR result is ¹H NMR (400 MHz, d₆-DMSO) 0.74(s, 3H), 1.05 (s, 3H), 1.27 (q, 2H), 1.75-1.96 (m, 3H), 2.18-2.92 (m, 4H), 5.12(s, 1H), 7.47(m, 4H), 8.74(s, 3H). The XRPD patterns are different for both salts. Thus the above results support that both salts synthesized are chemically pure with no impurity presence and no solvate

formation. They are also crystalline. The XRPD patterns are used as a reference for substance identification in the future experiments.

6.6.2. Ternary solubility phase diagram

To select a suitable solvent for the resolution experiment a quick screening was done with different solvents. The solubility results of DPG-CS and LPG-CS in suitable solvents are given in Table 8. As expected from the melting point results, the solubility of LPG-CS is higher compared to solubility of DPG-CS in all the selected solvents. Thus, during resolution from 50:50 mixture of both salts, DPG-CS salts crystallizes first. In all the given solvents, the solubility at 5°C is high in methanol and lowest is in acetonitrile. Based on these results methanol was selected as the main solvent for resolution and acetonitrile was selected as anti-solvent.

Table: 8: Solubility of LPG-CS, DPG-CS in different solvents at 5°C

Solvent	Solubility at 5°C (wt%)	
	LPG-CS	DPG-CS
Ethanol	8.41	1.48
Methanol	29.66	9.7
Acetonitrile	0.0675	0.0125

To analyze the ternary phase behavior in the solvent for both DPG-CS and LPG-CS ternary solubility phase diagrams were measured in different solvents like methanol, water, and ethanol. The results are discussed below.

Ternary Solubility phase diagram in methanol:

The solubility data at 5°C in methanol was plotted in a 100% ternary phase diagram and shown in Fig 62. There is a clear asymmetry in the solubility isotherm due to the huge difference in the pure salts solubility. As the composition of other salt is increasing, the solubility of mixtures is increasing at both ends of the isotherm. Only one maximum solubility point (two salt saturation point) is observed at a composition around 15:85 DPG-CS: LPG-CS salts. Thus, reaching to the expectation from the literature, both salts fall under simple eutectic system which is highly supportive for the separation via crystallization. The solubility isotherms at different temperatures were not measured here to investigate the change in eutectic composition in methanol due to considerably high solubility for LPG-CS at

5°C. Eutectic composition is very close to the highly soluble LPG-CS salt and thus, favorably there exists larger two phase area for DPG-CS salt (DPG-CS saturated solution of both salts) than that of LPG-CS as shown in Fig 62. From the phase diagram, the maximum possible yield at 5°C is calculated via lever rule which is [(length of segment bd/ length of segment cd)*100]. To achieve this maximum yield, initial concentration and composition (50:50 mixture of both salts) should be at point b. Two ways can be used to reach point b starting from point a, one of them is by evaporating solvent and the second is by increasing the solution temperature. If the initial solution point is in between points (a) and (b) in the phase diagram, crystallization of DPG-CS would occur with lower yields. Due to the very small two phase region for LPG-CS salt during selective crystallization of DPG-CS, there is a very less possibility for LPG-CS crystallization. If LPG-CS salt needed to be separated then there is a possibility to separate it preferentially from the eutectic composition due to high composition of LPG-CS salt.

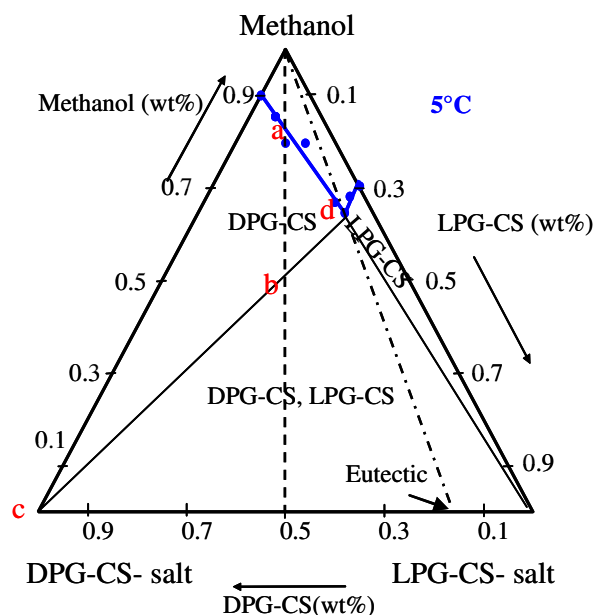


Fig 62: Ternary solubility phase diagram in methanol for DPG-CS, LPG-CS

Solubility phase diagram in water and ethanol:

In Fig 63, the solubility phase diagrams of DPG-CS and LPG-CS in water and ethanol are shown. Just like in methanol, in these both solvents also the solubility of pure DPG-CS is lower than the solubility of LPG-CS. In water and ethanol also there is only one maximum solubility point for mixtures (two-salt-saturation point) at a composition of 15:85 DPG-CS: LPG-CS. Due to the larger difference in the pure salts solubility (of about 11wt%) in water and also presence of eutectic very near to LPG-CS, there is a larger area for DPG-CS two

phase region compared to LPG-CS two phase region (shown in Fig 63(1)). Therefore there is a high possibility to crystallize DPG-CS from 50:50 mixture of both salts without crystallization of counter salt. For the solubility isotherm at 15°C in water, if the initial composition is in between the points (a) and (c) then pure DPG-CS would crystallize. Thus, just like methanol, water is also a suitable solvent for resolution of DPG-CS and LPG-CS via crystallization. Due to the moderate solubilities for both salts, ethanol can also be a suitable solvent but higher temperatures or application of vacuum are needed to increase supersaturation for performing a separation experiment.

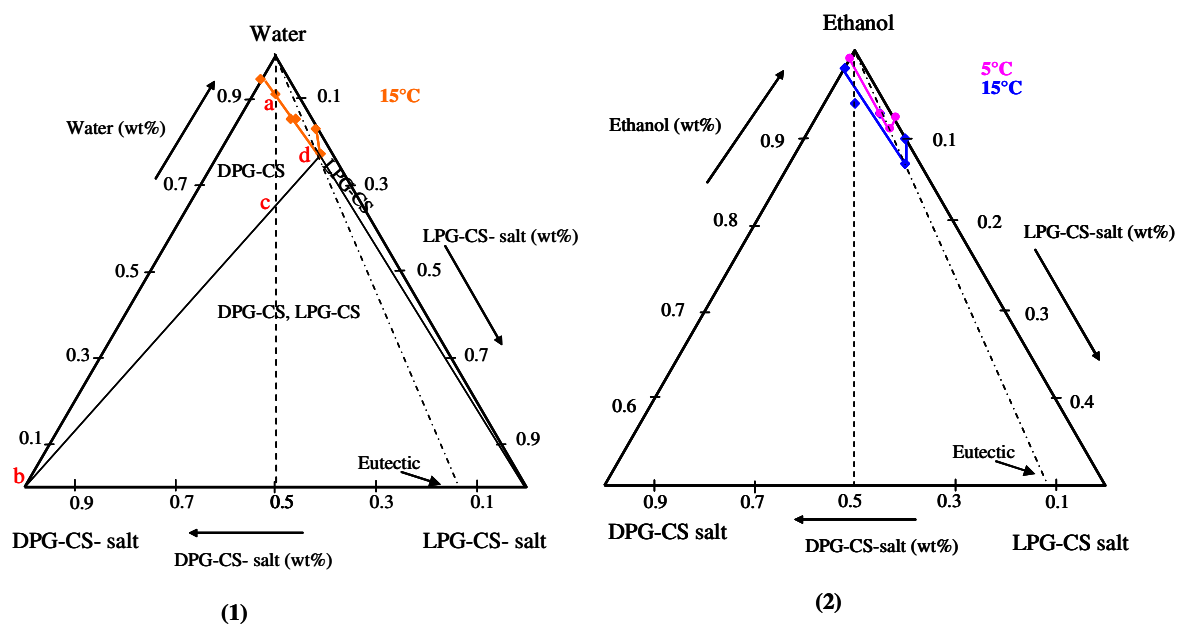


Fig 63: Ternary solubility phase diagram for DPG-CS, LPG-CS in (1) Water (2) Ethanol (upper 50% of phase diagram)

6.6.3. Resolution experiments for (DPG-CS, LPG-CS) salt pair 6

The solubility data presented in chapter 6.6.2 were used to design a separation experiment. Evaporative crystallization or anti-solvent addition coupled with cooling crystallization both can be used for the separation of DPG-CS salt from the 50:50 mixture due to their stability at higher temperature. Here, resolution was attempted based on the cooling and anti-solvent crystallization. The resolution results (with and without excess resolving agent) for salt pair 6 are discussed elaborately in this subchapter.

Cooling and anti-solvent addition resolution design in methanol:

From the solubility results shown in Table 8 in chapter 6.6.2, acetonitrile was selected as anti-solvent and methanol was selected to prepare the initial solution. Cooling step is included in

the separation experiment due to the non-availability of metastable zone width data for both salts in methanol. It was also found to be difficult to define the seeds introducing zone after anti-solvent addition at the given temperature. Hence, the supersaturation was increased moderately by cooling the solution to lower temperature and seeds of less soluble DPG-CS salt were introduced into the solution. The detailed design procedure for resolution is illustrated in Fig 64.

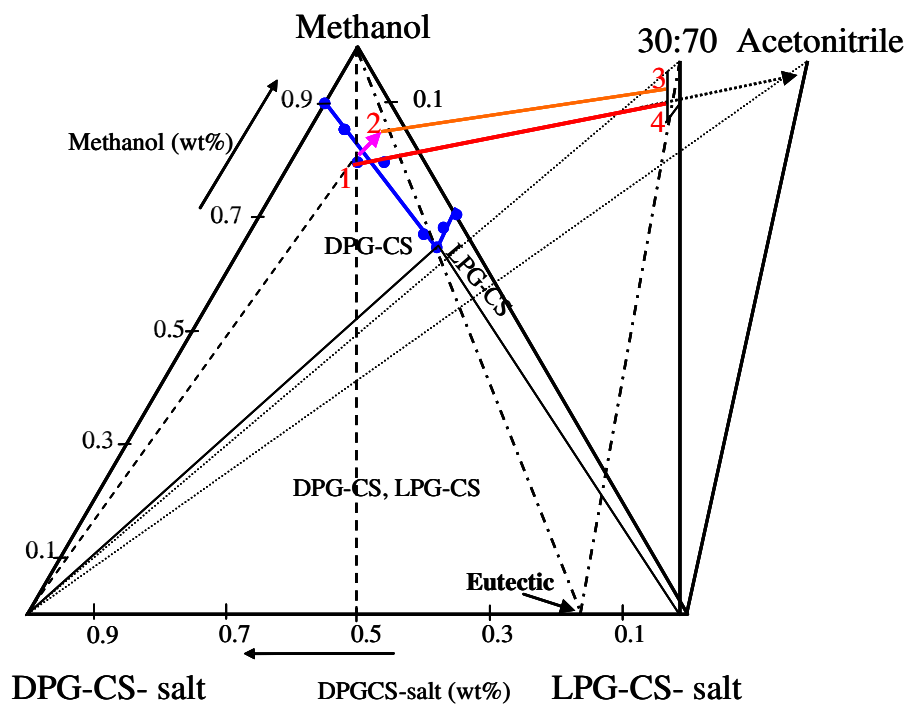


Fig 64: Cooling and anti-solvent crystallization for resolution of DPG-CS, LPG-CS salts

As shown in Fig 64, initially a solution of concentration at point 1 (which is in the two phase region of DPG-CS salt) is considered for separation experiment. Initial composition of both salts would be 50:50 mixture. This point can be reached by increasing the temperature. The next step in the resolution is cooling the solution to 0°C. Seeds of less soluble DPG-CS salt have to be introduced at this temperature to crystallize DPG-CS. With time concentration and composition in the solution moves to point 2 as DPG-CS salt starts crystallizing. The third step is addition of anti-solvent acetonitrile to the methanol solution to increase supersaturation further and enhance the driving force for crystallization of DPG-CS salt. The total quantity of acetonitrile was added in two steps to reach a final solution solvent composition to 30:70 methanol: acetonitrile. Liquid phase composition then moves from point 2 to point 3 in the phase diagram. The overall composition in the crystallizer moves along the line segment

between point 1 and 4. The difference between points 3 and 4 defines the amount of crystallized DPG-CS salt. The final solvent composition was selected rapidly based on the rough solubility data available for pure DPG-CS and LPG-CS salts in different solvent mixtures (methanol, water, ethanol and acetonitrile).

This design procedure was initially executed for an experiment without any excess resolving agent. To find the effect of excess resolving agent on the separation of DPG-CS, different resolution experiments with various concentrations of excess resolving agent 10(+)- camphor-sulphonic acid were executed with the same resolution procedure. The amounts of excess resolving agents in the resolution process were selected randomly.

Resolution results for salt pair 6:

The results of resolution experiments for both DPG-CS and LPG-CS are shown in Table 9 and in Fig 65. According to the XRPD solid phase results shown in Fig 65, the solid phase crystallized in all the three experiments was DPG-CS. No polymorphism or solvate formation was found. There is also no peak belonging to the resolving agent. In Table 9, the HPLC analysis for the solid phase is given. The solid phase crystallized in the experiments with and without excess resolving agent was pure DPG-CS salt with no other impurities in it.

Table 9: Resolution results for DPG-CS and LPG-CS

Experiment	Initial amount of solute and solvent (g)				Anti-Solvent	Purity (HPLC)	Solid phase (XRPD)	Amount of DPG-CS crystallized (g)	Yield calculated DPG-CS salt as basis (%)
	DPG-CS	LPG-CS	R. A	Methanol					
(1) without excess resolving agent	4	4	0	32	Acetonitrile	100% DPG-CS	DPG-CS	1.825	45.6
(2) with excess resolving agent	4	4	0.9	32	Acetonitrile	100% DPG-CS	DPG-CS	1.92	48
(3) with excess resolving agent	4	4	2	32	Acetonitrile	99.15% DPG-CS	DPG-CS	1.425	35.6

As the experimental conditions and the crystallized substances are exactly the same, the effect of excess resolving agent on the resolution can be assessed easily. If the comparison is made between the yields of resolution results of experiment 1 (without any excess resolving agent) and experiment 2 (with excess resolving agent 0.9g) in Table 9, there is a slight increase in the yield of DPG-CS when there is low amount of excess resolving agent in the solution. The

quality of product is same for both experiments. Thus, it can be assumed that low concentrations of excess resolving agent has a slight decreasing effect on the solubility of DPG-CS in methanol, acetonitrile mixture. On the other hand, in the results of experiment 3, the increase in the percentage of excess resolving agent in the initial solution reduced the yield of DPC-CS salt drastically. From these results the postulation can be made, that an increase in concentration of excess resolving agent is increasing the solubility of DPG-CS salt in the methanol-acetonitrile solvent mixture. Therefore, in the phenyl glycine salt system, the excess resolving agent as an impurity in the solution did not enhance the yield of crystallizing the less soluble DPG-CS salt and higher quantities of excess resolving agent even have detrimental effect on the yields.

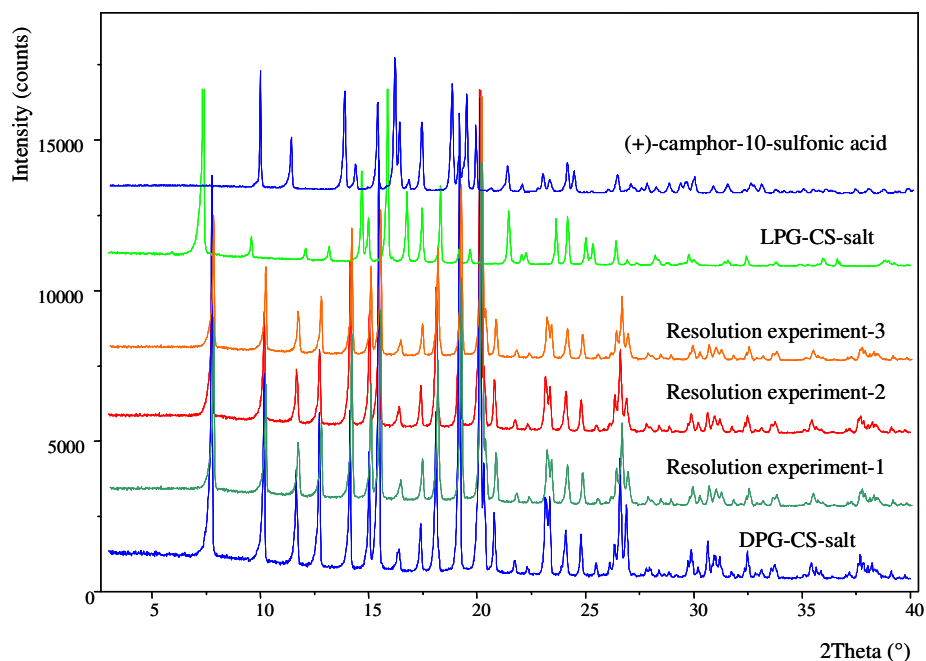


Fig 65: XRPD solid phase analysis for resolution of DPG-CS, LPG-CS salts

6.7. Summary

In this chapter all the results which are obtained from the experiments are discussed. Initially the results of different diastereomeric salt pairs of serine are introduced later the diastereomeric salt pair of phenyl glycine was discussed. In all the above results the salt characterization with different analytical techniques, pure salt properties and behavior of salt pairs in binary system and ternary solubility system are given comprehensively. The results of metastable zone width for primary nucleation for salt pair 1 and 2 were discussed in detail. The systematically approached resolution design based on crystallization and results were provided. Advantages of presence of excess resolving agent were explained.

7. Conclusions and outlook

Chapter 7

Conclusions and outlook

7.1. Conclusions

The separation of chiral racemic acids or bases is carried out in industry frequently via Classical Resolution. In Classical Resolution, the first reaction step is the formation of diastereomeric salts using typically in equimolar stoichiometry. The reactant and a suitable resolving agent, followed by separating in a second step the resulting diastereomeric salts via a suitable separation technique. Regarding this second step especially cost effective crystallization processes are attractive.

In the present work both parts of the Classical Resolution were investigated systematically. Initially, the whole process was studied using the typically applied equimolar stoichiometry of chiral compounds and resolving agents. Then the effect of using the resolving agent in excess in the solution was investigated. To study the whole complex process including all steps is complicated. For this reason several sub-steps were separately considered. A first task was the synthesis of chemically pure diastereomeric salts with suitable resolving agent candidates. The feasibility, design and execution of separation of the formed diastereomeric salts via crystallization were considered then using asystematic approach. This approach consists of determining the behavior of both salts in binary and ternary systems (thermodynamic effect) and the determination of metastable zone width data (kinetic effect). It was applied for two amino acids (as model compounds) using six resolving agents. The effect of several resolving agents belonging to the same family was evaluated to check the potential of the so-called *Dutch Resolution*.

The following conclusions can be drawn from the results presented in this thesis.

The synthesis of DL-serine and DL-phenyl glycine diastereomeric salt pairs ((1) L-D, D-D; (2) D-L, L-L; (3) D-LM, L-LM; (4) D-LT, L-LT; (5) L-D-ToluyI, D-D-ToluyI; and (6) DPG-CS, LPG-CS) with different selected acidic resolving agents (2,3-dibenzoyl-D-tartaric acid, 2,3-dibenzoyl-L-tartaric acid, L-(+)-mandelic acid, L-(+) tartaric acid, 2,3-ditoluyI-D-tartaric acid, 10-(+)-camphor sulphonic acid) was successful, as proven by characterization results from different analytical techniques used like ^1H NMR, DSC and XRPD. With these six salt pairs, extensive experiments were carried out. At first thermodynamic data and kinetic data were determined and conclusions are drawn regarding the resolution options.

Salt pairs 1 and 2 (L-D, D-D; D-L, L-L):

The serine diastereomeric salt pairs L-D, D-D (resolving agent 2,3-dibenzoyl-D-tartaric acid) and D-L, L-L (resolving agent 2,3-dibenzoyl-L-tartaric acid) behave like simple eutectic

systems both in binary (XRPD, DSC, Melting point phase diagrams) and in the ternary solubility phase diagrams (in presence of a solvent). Thus, for both salt pairs chiral separation via a simple crystallization-based resolution process is feasible. There was a considerable change in the eutectic composition with temperature (supportive for separation) for both salt pairs. This change was solvent dependent. In both salt pairs, the less soluble L-D or D-L salts have very small metastable zone width compared to highly soluble D-D or L-L salts. Hence for a given saturated solution at particular temperature, at 50:50 composition of both salt pairs, less soluble L-D or D-L salt would crystallize first upon cooling (primary nucleation). For both of the salt pairs evaporative crystallization and vacuum crystallization was not suitable due to the uncertainty of chemical stability at higher temperature. Moreover the separation experiments based on cooling crystallization coupled with anti-solvent addition were successful and yielded the desired less soluble pure L-D or D-L salts from the respective salt pairs (from L-D, D-D salt pair L-D salt thus L-serine and from D-L, L-L salt pair D-L salt thus D-serine). The enhanced preferential crystallization for the high soluble counter salt from the eutectic composition gave positive results with low yields. There is a high potential for further increasing yields. An excess of resolving agent above the stoichiometric feed reaction ($\lambda_r > 1$) can act as either an impurity or as a tailor-made additive in the solution. In the case of the L-D, D-D salt pair, there is a considerable effect on the solubility of both salts in methanol, which finally increased the yield of less soluble L-D salt during separation experiment. The enhancement in the yield for D-L was also observed in the presence of excess resolving agent in the case of D-L, L-L salt pair. Thus, it was clearly demonstrated in this work that stoichiometry changes have a considerable effect on the final yields.

Salt Pair 3 (D-LM, L-LM):

The prediction of mixed crystal behavior for D-LM and L-LM salts (resolving agent L-(+)-mandelic acid) was initialized from the XRPD patterns of both salts, as the similarity of their XRPD patterns is very high. This fact was clarified with thermodynamic data like DSC curves for mixtures and solubility phase diagram in acetone. The complex solid solution behavior of salt pair L-LM and D-LM is in this case not supportive for a straight forward crystallization based separation process.

Salt Pair 4 (D-LT, L-LT):

Even though there is a high molecular similarity in the structure of resolving agents 2,3,-dibenzoyl-L/D-tartaric acid and L-(+)-tartaric acid, the diastereomeric salts of D-/L-serine benzyl ester with L(+)-tartaric acid (D-LT, L-LT) behave like double salts (in both binary and ternary systems). This behavior is not suitable for a separation process starting from a 1:1

mixture. The mostly used resolving agent L-(+)-tartaric acid does not fit for separation of DL-serine benzyl ester as such separation requires an enrichment step.

Salt Pair 5 (L-D-Toluyl, D-D-Toluyl):

Special results were observed during the synthesis of L-D-Toluyl, D-D-Toluyl salts (resolving agent 2,3-ditoluyl-D-tartaric acid) with difference in their chemical structure. If D-D-Toluyl salt is less soluble compared to L-D-Toluyl salt, during resolution the yield would be rather low. To improve the yield a doubled amount of resolving agent must be used. On the other hand if the L-D-Toluyl salt has lower solubility, 25% of resolving agent can be saved.

Salt Pair 6 (DPG-CS, LPG-CS):

DPG-CS and LPG-CS salt pair (L-/D-phenyl glycine with resolving agent 10-(+)-camphor sulphonic acid) shows simple eutectic nature in the ternary system and also in the binary system (reported by Ryuzo et al.). There was no change in the eutectic composition with respect to temperature as well as solvent. During the resolution, the application of an excess of resolving agent generated different effects depending on the concentration present in the solution. Relative low excess amounts of the resolving agent gave a slight increase in the yield of the less soluble DPG-CS, while higher amounts of excess reduced the yield drastically.

From the specific results obtained for the 6 pairs studied, the following more general conclusions can be drawn. The results ascertain the fact that always a number of resolving agents have to be tested for successful separation of a chiral compound-forming substance into its pure enantiomers. Purity and identity of each diastereomeric salt formed with each resolving agent should be analyzed by various techniques (as e.g. ^1H NMR, DSC and XRPD). Solid phase analysis helps to identify possible polymorphism and solvate formation, which will have a strong effect on the execution and the resultant yield of crystallization processes.

It was confirmed, that in order to design an optimized crystallization separation process basic thermodynamic and kinetic data are very essential. An accurate measurement of the basic thermodynamic data, like binary melting and ternary solubility phase diagrams, is mandatory to classify the behavior of salt pairs (simple eutectic, double salts or mixed crystals). Out of these three main types the simple eutectic is highly favorable for a crystallization based separation process. If a salt pair belongs to the simple eutectic type (e.g. salt pairs 1 and 2), the composition of the 'two-salt saturation point' is very significant. In general eutectic

composition is found near to the salt with high solubility. High yields can be achieved for the less soluble salt, if the eutectic composition is very close to the highly soluble salt. If the eutectic composition is near to the 50:50 mixture of both salts, then yields will reduce drastically. For these systems preferential crystallization based separation processes can be designed from the ternary solubility phase diagrams.

The second set of basic data necessary to design a good crystallization based separation process are metastable zone widths for primary nucleation. If these data for both salts are known in a solvent selected, the crystallization process can be controlled more precisely. Maximum yields would be achieved during resolution if the final liquid phase compositions reach the eutectic composition of both salts.

Before starting a concrete resolution process it is in general necessary to evaluate the effect of excess resolving agent on basic thermodynamic data and accordingly the amount of resolving agent which should be introduced into the solution. Innovative aspect of the presented work was the careful elevation of the relative amount of resolving agent during the initial reaction process. The excess resolving agent has an impact on the basic thermodynamic and kinetic properties of both diastereomeric salts. It was found that these effects change for each diastereomeric salt of the pair. If the salt system has variable effect on its solubility data (e.g. for one salt solubility increases and for other salt solubility decreases) from excess resolving agent then it will show a positive effect on the final yield. A maximum yield (eutectic composition in the liquid phase) can be reached with less driving force (e.g. L-D, D-D or D-L, L-L salt systems). An excess of resolving agent reduces the final yield (e.g. DPG-CS, LPG-CS salt system) if there is the same effect of the R.A on solubility of both salts.

Finally, the interesting concept of using various resolving agents together (Dutch Resolution), was considered based on the insight acquired during this work. The present study verifies the potential of this concept for the amino acid DL-serine. Here during the main part of the work, the family of resolving agents 2,3-dibenzoyl-D-tartaric acid, 2,3-dibenzoyl-L-tartaric acid, L-(+)-tartaric acid and 2,3-ditoluyl-D-tartaric acid were used separately. Out of these salt pairs, the first two resolving agents showed simple eutectic behavior, salt pair with L-(+)-tartaric acid showed double salt behavior and finally salt pair with 2,3-ditoluyl-D-tartaric acid formed salts which are no diastereomers. Strong differences were observed for these resolving agents during the investigations. Hence, combination of them as a family and using them for Dutch Resolution might probably provide reduced purities and yields. Based on the results obtained

in this work for e.g. DL-serine with the tartaric acid family, requires detailed preliminary investigations to understand the effect of applying families of resolving agents for a successful Dutch Resolution.

As the last part of Classical Resolution, the ease in the recovery of the pure enantiomers and the resolving agent from the separated diastereomeric salts has a considerable impact on the process. This part is relatively easy to achieve and was not studied in detail in this thesis.

With the results presented, this thesis has attempted to contribute to further improve the understanding of Classical Resolution and to promote further more efficient application.

7.2. Outlook

Some future possible work is recommended for further improvement of Classical Resolution in this chapter.

Point 1: The selection of resolving agent is still under trial and error basis. To reduce some efforts in this direction, molecular modeling can be a better option. In this area research work can be done in the direction of introducing the molecular structure of both enantiomer, resolving agent and optimizing the salt structure for both corresponding diastereomeric salt. Building different possible unit cells for each diastereomeric salt and developing corresponding XRPD pattern through commercial Material Studio software is possible. Out of those results, according to the similarity of XRPD patterns, the behavior of both diastereomeric salts in the binary mixtures can be predicted. This requires strong computational ability and software package.

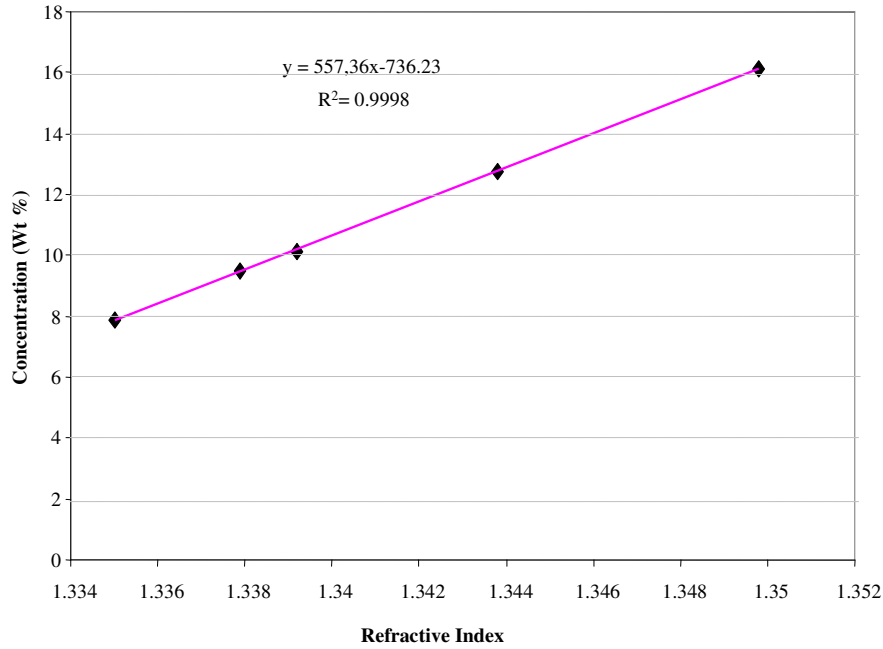
Point 2: Solubility prediction for decomposable diastereomeric salts is also one of the challenges faced during the work. The future work in this direction would save most of the strenuous experimental data measurement. This can also be achieved by calculating melting enthalpies of substances by molecular modeling if the Unit cell parameters are predicted correctly from the practically measured XRPD patterns.

Point 3: From the present work, it is proven that resolution for both diastereomeric salts is possible (less soluble salt via selective crystallization and more soluble salt via preferential crystallization) if they show simple eutectic behavior. Preferential crystallization for highly soluble salt is not yet clear for the salt pairs which have eutectic composition near to the highly soluble salt. It is required to do more intensive research in this direction to improve the

total yields for both salts. Recycling of mother liquor is more lucrative if the final composition of mother liquor is 1:1 mixture of both salts.

Point 4: In addition, to achieve both salts in pure form, integration of preparative chromatography or membrane separation with crystallization would facilitate the resolution. These integrated processes are also useful for producing pure diastereomeric salts from the other two types of behaviors (mixed crystals and double salts). Feasibility of separation and cost of production needed to be considered for scale up processes.

Appendices



Appendix 1: Calibration of concentration vs. refractive index for D-D salt in methanol at 40°C

Appendix 2: Evaluating feed compositions (Chiral racemate and resolving agent)

Below is given a calculation of excess of resolving agent for the example of L-D, D-D salts produced from L-/D-serine benzyl ester and 2,3-dibenzoyl-D-tartaric acid (See also Eq-1 and Fig 33) :

General synthesis reaction of L-D/D-D salts (salt pair -1) (chapter 4.1.1)



Stoichiometric coefficients of reactants: $v_{SBE} = -2$; $v_{DBT} = -1$

According to the reaction two moles of DL-SBE react with 1 mole of DBT to form 0.5 mole of L-D and 0.5 mol of D-D salt.

Stoichiometric molar feed ratio of reactants λ_r :

$$\lambda_r = \left(\frac{n_{DBT}^{Feed}}{n_{SBE}^{Feed}} \right) * \frac{|v_{SBE}|}{|v_{DBT}|} \quad \text{-- Apx eq-1}$$

For above reaction $\lambda_r = 1$ is fulfilled if $n_{SBE}^{Feed} = 2 * n_{DBT}^{Feed}$.

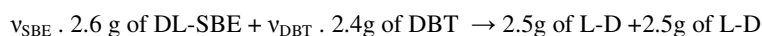
If $\lambda_r > 1$ an excess of resolving agent DBT is used in the solution

If $\lambda_r < 1$ an excess of racemate SBE is used in the solution

The actual feed amounts used for the resolution carried out and described in Chapter 6.1.5 is:



With the molecular weights of the compounds $MW_{\text{DL-SBE}} = 195.18 \text{ g/mol}$; $MW_{\text{DBT}} = 358.30 \text{ g/mol}$; $MW_{\text{L-D/D-D}} = 748.6 \text{ g/mol}$ the following masses are applied.

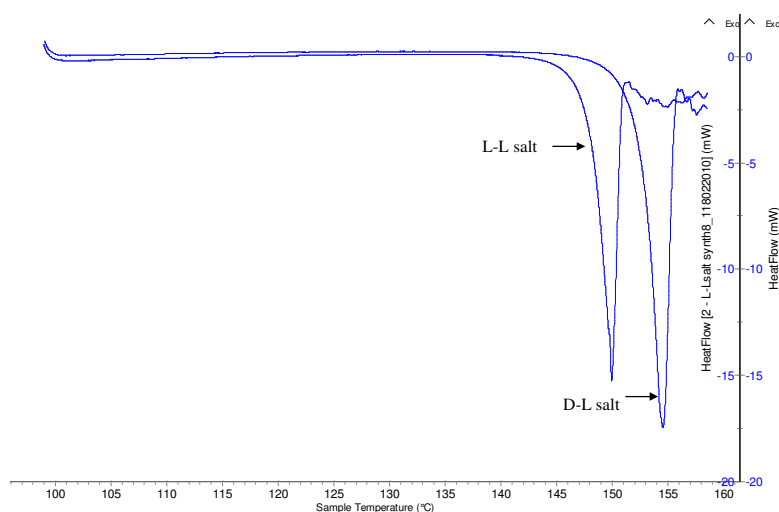


For above case $\lambda_r = 1$.

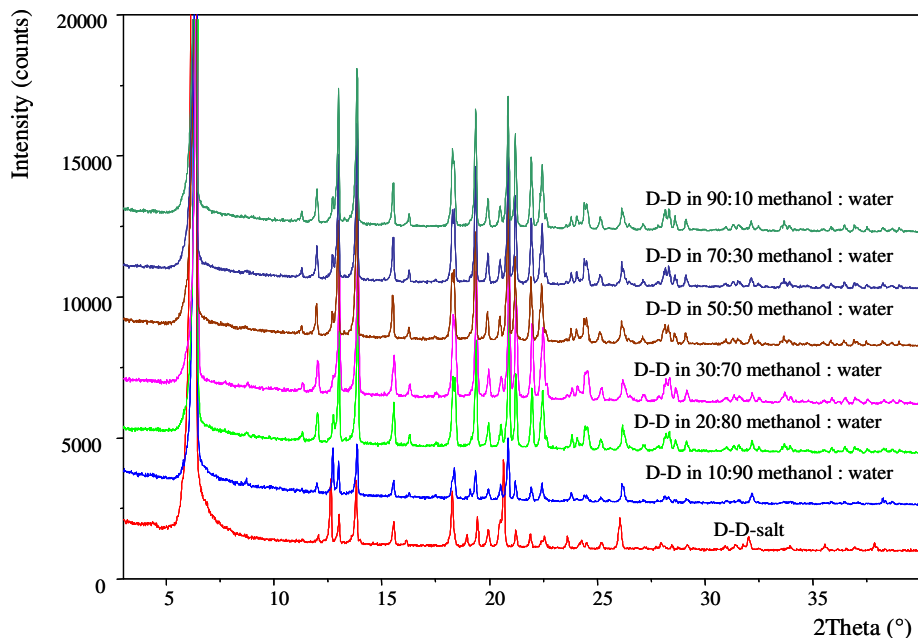
According to the clear effect from an excess of DBT on the solubility of pure L-D, D-D salts (results given in the chapter 6.1.3), a λ_r value of 1.58 appeared to be attractive to carry out another experiment.

Applying $\lambda_r = 1.58$ in the equation by inserting the same values for $n_{\text{SBE}}^{\text{Feed}} = 0.01332$, $v_{\text{SBE}} = -2$; $v_{\text{DBT}} = -1$ in Apx eq-1; results for the amount of R.A $n_{\text{DBT}}^{\text{Feed}} = 0.01059$ moles.

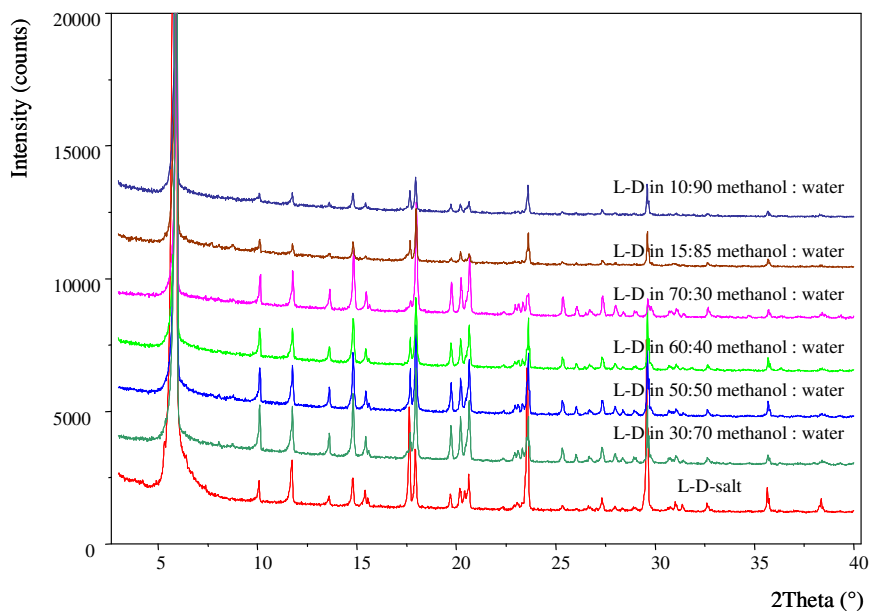
Converting this excess of DBT from moles to grams results 1.4g of DBT which were used in the resolution experiment.



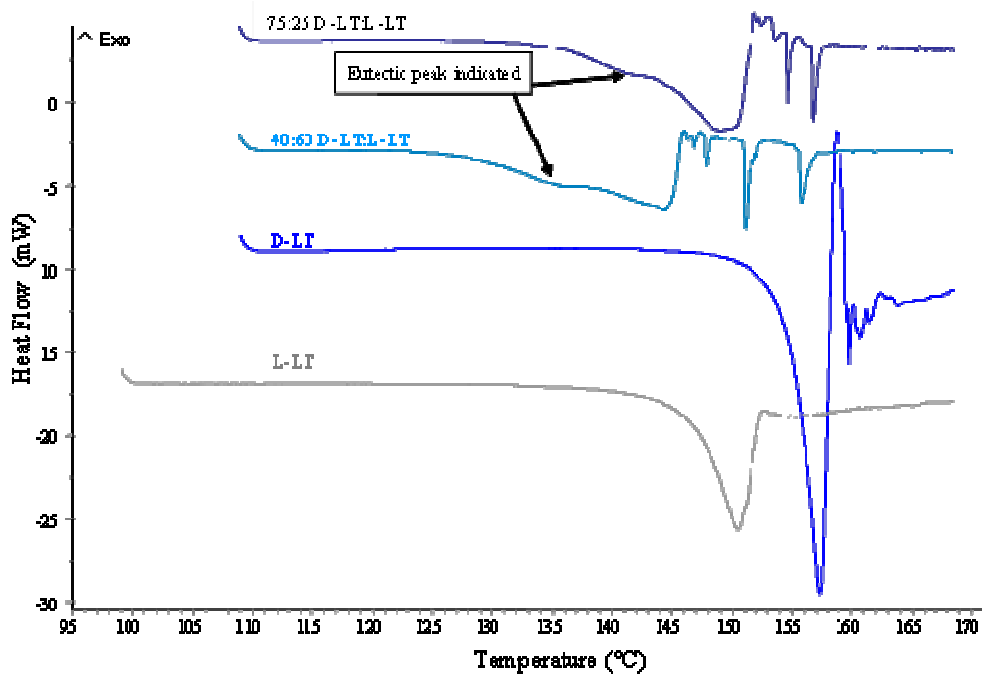
Appendix 3: Melting curves for L-L, D-L salt



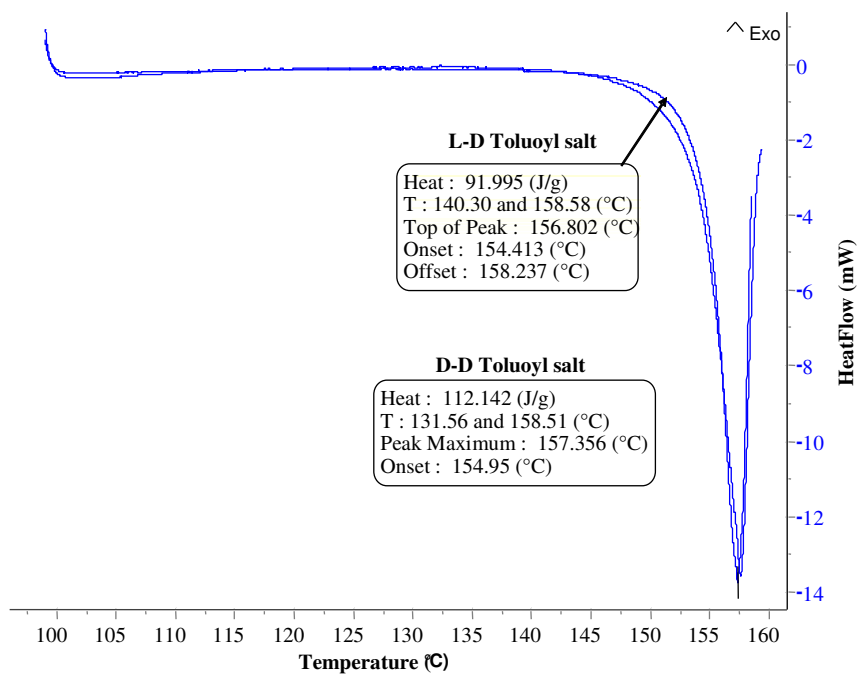
Appendix 4.1: XRPD patterns of D-D salt in methanol-water mixture of different compositions at 25°C



Appendix 4.2: XRPD patterns of L-D salt in different compositions of methanol-water mixture of at 25°C



Appendix 5: DSC curves for pure D-LT, L-LT and different mixtures of both salts



Appendix 6: Measured DSC curves for L-D-Toluyl and D-D-Toluyl salts synthesized

Bibliographie

1. Bhintade, Y., *Determination and Description of Solid Liquid Equilibria in Chiral Systems*, in *Institute of Process engineering* 2008, MPI-Magdeburg: Magdeburg.
2. Kozma, D., ed. *CRC Handbook of optical resolutions via diastereomeric salt formation*. 2002, CRC Press: Boca Raton, Florida.
3. Eliel, E.L., S. Wilen, and M. Doyle, *Basic Organic Stereochemistry.*, 2001, Wiley-Interscience: New York.
4. Cahn, R., Ingold, S. C., Prelog, V., *Spezifikation der molekularen Chiralität*. *Angewandte Chemie*, 1966. **78**: p. 413-447.
5. Moss, G.P., *Basic terminology of stereochemistry (Recommendations 1996)*. *Pure Appl. Chem.*, 1996. **68**(12): p. 2205-2216.
6. Bonner, W.A., *Parity violation and the evolution of biomolecular homochirality*. *Chirality*, 2000. **12**: p. 114-126.
7. Ariens, E.J., *Stereochemistry, a Basis for Sophisticated Nonsense in Pharmacokinetics and Clinical Pharmacology*. *European Journal of Clinical Pharmacology*, 1984. **26**: p. 663-668.
8. Rouhi, A.M., *Chirality at work*. *Chemical and Engineering News*, 2003. **81**: p. 56-61.
9. Rouhi, A.M., *Thalidomide*. *Chemical & Engineering News*. American Chemical Society., 2006: p. 09-21.
10. Maier, N.M., P. Franco, and W. Lindner, *Separation of enantiomers: needs, challenges, Perspectives*. *J. Chrom. A.*, 2001. **906**: p. 3-33.
11. Caner, H., H. Groner, and L.A. Levy, I, *Trends in the development of chiral drugs*. *Drug Discov. Today* 2004. **9**: p. 105-110.
12. Kaspereit, M., *Separation of Enantiomers by a Process Combination of Chromatography and Crystallisation*, in *Fakultät für Verfahrens- und Systemtechnik* 2006, Otto-von-Guericke Universität Magdeburg: Shaker Verlag Aachen: Magdeburg. p. 1-140.
13. Jacques, J., A. Collet, and S.H. Wilen, *Enantiomers, racemates and resolutions* 1994: Malabar, FL: Krieger Publishing Company
14. Lorenz, H., Perlberg, A., Sapoundjiev, D., Elsner, M. P., Seidel-Morgenstern, A., *Crystallization of enantiomers*. *Chemical Engineering and Processing*, 2006. **45**(10): p. 863-873.
15. Weissbuch, I., Addadi, L., Leiserowitz, L., *Molecular Recognition at Crystal Interfaces*. *Science*, 1991. **253**(5020): p. 637-645.
16. IUPAC, *Compendium of Chemical Terminology, (the "Gold Book")*. 2 ed, A.D.M.a.A. Wilkinson 2006.
17. Knabe, J., *On the Enantioselectivity of Drugs*. *Arzneimittel-Forschung/Drug Research*, 1989. **39-2**(11): p. 1379-1384.
18. Mullin, J.W., *Crystallization*, 2000, Butterworth-Heinemann: Oxford.
19. Perlberg, A., *Untersuchungen zum Einfluss des Gegenenantomers bei der enantioselektiven Kristallisation aus Lösungen*, in *Ph.D Thesis* 2007, Otto-von-Guericke Universität Magdeburg: Magdeburg.
20. Tulashie, S., *The potential of chiral solvents on enantioselective crystallization*, in *Ph.D Thesis, Fakultät für Verfahrens- und Systemtechnik*. 2010, Otto-von-Guericke Universität Magdeburg: Magdeburg.
21. Roozeboom, H., W, B., *Zeitschrift fuer Physikalische Chemie*. *Stoichiometrie und Verwandtschaftslehre*, 1899. **28**: p. 494-517.
22. Czapla, F., *Modeling of polythermal preferential crystallization*, in *Ph.D thesis, Fakultät für Verfahrens- und Systemtechnik* 2010, Otto-von-Guericke Universität Magdeburg: Magdeburg.
23. Lorenz, H., D. Sapoundjiev, and A. Seidel-Morgenstern, *Enantiomeric Mandelic Acid System-Melting Point Phase Diagram and Solubility in Water*. *J. Chem. Eng. Data*, 2002. **47**: p. 1280-1284.
24. Predel, B., *Heterogene Gleichgewichte: Grundlagen und Anwendungen*, 1982, Steinkopff: Darmstadt.
25. Roozeboom, H.W.B., *Löslichkeit und Schmelzpunkt als Kriterien für racemische Verbindungen, pseudoracemische Misch-Krystalle und inaktive Konglomerate*. *Z. Phys. Chem.*, 1899. **28**: p. 494-517.

26. Collins, A.N., G.N. Sheldrake, and J. Crosby, *Chirality in Industry: The Commercial Manufacture and Applications of Optically Active Compounds* 1992, Chichester: John Wiley & Sons.
27. J.Prakt. Chem, 1866. **99**: p. 6.
28. Strecker, A., *Justus Liebigs. Ann. Chem.*, 1850. **75**: p. 27.
29. Baer, E., *Biochem. Prep.*, 1952. **2**: p. 31.
30. Emons, C.H.H., Kuster, B.F.M., Vekemans, J.A.J.M., and Sheldon, R.A., *Tetrahedron: Asymmetry*, 1991. **2**: p. 359.
31. M. D. Fryzuk, B.B., *Asymmetric synthesis. Production of optically active amino acids by catalytic hydrogenation*. *J. Am. Chem. Soc.*, 1977. **99**: p. 6262–6267.
32. Jacobsen, P., Yamamoto, ed. *Comprehensive Asymmetric Catalysis* 1999, Springer.
33. Ojima, ed. *Catalytic Asymmetric Synthesis*. 2000, Wiley-VCH, Weinheim.
34. Blaser, S., ed. *Asymmetric Catalysis on Industrial Scale*. 2004, Wiley-VCH, Weinheim.
35. Crosby, J., *Synthesis of optically active compounds: a large scale perspective*. *Tetrahedron*, 1991. **47**: p. 4789-4846.
36. Harrington, P.J. and E. Lodewijk, *Twenty Years of Naproxen Technology*. *Organic Process Research & Development* 1997. **1**: p. 72-76.
37. Koeller, K.M., Wong, C., , *Enzymes for chemical synthesis*. *Nature*, 2001. **409**: p. 232-240.
38. Subramanian, G., ed. *Chiral Separation Techniques*. 2001, WILEY-VCH Verlag GmbH: Weinheim.
39. Francotte, E.R., *Enantioselective chromatography as a powerful alternative for the preparation of drug enantiomers*. *Journal of chromatography*, 2001. **906**: p. 379-397.
40. Rekoske, J.E., *Chiral separations*. *AIChE J.*, 2001. **47**: p. 2-5.
41. Collet, A., *Separation and purification of enantiomers by crystallisation methods*. *Enantiomer*, 1999. **4**(3-4): p. 157-172.
42. Rodrigo, A.A., Lorenz, H., Seidel-Morgenstern, A., *Online monitoring of preferential crystallization of enantiomers*. *Chirality*, 2004. **16**: p. 499-508.
43. Lorenz, H., Polenske, D., Seidel-Morgenstern, A., *Application of preferential crystallization to resolve racemic compounds in a hybrid process*. *Chirality* 2006. **18**: p. 828–840.
44. Tulashie, S., Lorenz, H., Hilfert, L., Edelmann, F. T., Seidel-Morgenstern, A., *Potential of chiral solvents for enantioselective crystallization. 1. Evaluation of thermodynamic effects*. *Crystal Growth & Design*, 2008. **8** p. 3408–3414.
45. Tulashie, S., Lorenz, H., Seidel-Morgenstern, A. *Potential of chiral solvents for enantioselective crystallization. 2. Evaluation of kinetic effects*. *Crystal Growth & Design*, 2009. **9**: p. 2387–2392.
46. Gedicke, K., Kaspereit, M., Beckmann, W., Budde, U., Lorenz, H., Seidel-Morgenstern, A.: , *Conceptual design & feasibility study of combining continuous chromatography and crystallization for stereoisomer separations*. *Chem. Eng. Res. Des.*, 2007. **85**: p. 928–936.
47. Svang-Ariyaskul, A., *Chiral separation using hybrid of preferential crystallization moderated by a membrane barrier* 2010, GEORGIA INSTITUTE OF TECHNOLOGY. p. 1- 220.
48. Collins, A.N., G.N. Sheldrake, and J. Crosby, *Chirality in Industry II: Developments in the Manufacture and Applications of Optical Active Compounds* 1997, Chichester: John Wiley & Sons.
49. Roth, H.J., Kleeman, A., Beisswenger, T., *Pharmaceutical Chemistry*, 1988, Ellis Horwood Ltd: Chichester.
50. Wuilen, S.H., A , Jacques, J. , *Tetrahedron*, 1977. **33**.
51. Wuilen, S.H., *Topics Stereochem*, 1971. **6**: p. 107.
52. DePuy, C.H., Breitbeil, F.W., DeBruin, K.R., *Brucine Salts*. *J. Am. Chem. Soc.*, 1966. **88**.
53. Jacques, J., Fouquey, C., Viterbo, R., *For an example of acid decomposition of a salt, followed by crystallization of the organic acid substrate, see the resolution of binaphthylphosphoric acid*. *Tetrahedron Lett.*, 1971: p. 4617.
54. Greenstein, J.P., Winitz, M, ed. *Chemistry of Amino Acids*. Vol. 1. 1961, Wiley: New York. 715.
55. Jaeger, D.A., Broadhurst, M.D., Cram, D.J, *J. Am. Chem. Soc.*, 1979. **101**: p. 717.
56. Adams, R., ed. *Organic reactions*. Vol. 2. 1944, Wiley: New York.

57. Sarett, L.H., Arth, G.E., Lukes, R.M., Beyler, R.E., Poos, G.I., Johns, W.F., Constantin, J.M., *J. Am. Chem. Soc.*, 1952. **74**: p. 4974.
58. Werner, A., *Ber.*, 1911(44).
59. Newmann, M.S., Lutz, W.B., *J. Am. Chem. Soc.*, 1956. **78**.
60. Woodward, R.B., Katz, T.J., *tetrahedron*, 1959. **5**.
61. Carpino, L.A., *Chem. Comm*, 1966.
62. H. Nohira, K.M., T. Murata, Y. Yazaki, M. Kanazawa, Y. and Aoki and M. Nohira, *Heterocycles*, 2000. **3**: p. 1359.
63. Marckwald, W., *Ber.*, 1896., **29**: p. 42.
64. Marckwald, W., *Ber.*, 1896. **29**: p. 43.
65. Read, J., Reid, W.G., *J. Soc. Chem. Ind.*, 1928. **47**: p. 8T.
66. Pope, W.J., Peachy, S.J., *J. Chem. Soc.*, 1899. **75**: p. 1066.
67. Pope, W.J.G., *C.S. J. Chem. Soc.*, 1912. **101**: p. 939.
68. Pope, W.J.W., J.B., *Proc. Roy. Soc.*, 1931. **A134**: p. 357.
69. Pearson, D.E., Rosenberg, A.A., *J. Med. Chem.*, 1975. **18**: p. 523.
70. Armstrong, M.D., *J. Am. Chem. Soc.*, 1951. **73**: p. 4456.
71. Hoeve, W., Wynberg, H., *J. Org. Chem.*, 1985. **50**: p. 4508.
72. Karamertzanis, P.G., Anandamohan, P.R., Fernandes, P., Cains, P.W., Vickers, M., Tocher, D.A., Florence, A.J., Price, S.L., *J. Phys. Chem. B*, 2007. **111**: p. 5326-5336.
73. Heinrich, S., P., Wermuth, C. G., ed. *Handbook of Pharmaceutical salts :properties, Selection and Use*. 2002, Wiley-vch: Weinheim.
74. Eger, D., ed. *Handbook of chiral chemicals*. 2005, CRC press LLC: London.
75. Leclercq, M., Jacques, J., *Bull. Chem. Soc. Fr.*, 1975: p. 2052.
76. Kellogg, M.R., Kaptein, B., Vries, T.R., *Dutch resolution of racemates and the roles of solid solution formation and nucleation inhibition*. *Top Curr Chem*, 2007. **269**: p. 159-197.
77. Gervais, C., Grimbergen, R.F., Markovits, I., Ariaans, G.J., Kaptein, B., Bruggink, A., Broxterman, Q.B., *Prediction of solid solution formation in a family of diastereomeric salts. A molecular modeling study*. *J. Am. Chem. Soc.*, 2004. **126**: p. 655-662.
78. McBlain, W.A., Wolfe, F.H., *Tetrahedron Lett.*, 1975: p. 6351.
79. Fogassy, E., Faigl, F. Darvas, F., *ACS*, A., Toke, L., *Tetrahedron. Lett.*, 1980. **21**: p. 2841.
80. Kozma, D., Pokol, G., *ACS*, M., *Calculation of the efficiency of optical resolutions on the basis of the binary phase diagram for the diastereomeric salts*. *J. Chem. Soc. Perkin Trans. 2*, 1992: p. 435.
81. Schroeder, I., *Z. Phys. Chem.*, 1893. **11**: p. 449.
82. Collet, A., M.-J. Brienne, and J. Jacques, *Optical Resolution by Direct Crystallization of Enantiomer Mixtures. Chem. Rev.*, 1980. **80**: p. 215-230.
83. Marchand, P., Lefebvre, L., Querniard, F., Cardinael, P., Perez, G., Couniouxc, J.J., Coquerel, G., *Tetrahedron: Asymmetry* 2004. **15**: p. 2455–2465.
84. Colles, W.M., G., *C.S.*, *J. Chem. Soc.*, 1928: p. 100.
85. Korovessi, E., Linninger, A.A., ed. *Batch Processes*. 2006, CRC Taylor & Francis group: New York.
86. Jones, A.G., ed. *Crystallization process systems*. 2002, Butterworth Heinmann: London.
87. Davey, R.J., Allen, K., Blagden, N., Cross, W. I., Lieberman, H. F., Quayle, M. J., Righini S., Seton, L., Tiddy, G. J. T., *Crystal engineering - nucleation, the key step*. *Cryst Eng Comm*, 2002: p. 257-264.
88. Dalmolen, J., Tiemersma-Wegman, T.D., Nieuwenhuijzen, J.W., van der Sluis, M., van Echten, E., Vries, T.R., Kaptein, B., Broxterman, Q.B., Kellogg, R. M., *The Dutch Resolution Variant of the Classical Resolution of Racemates by Formation of Diastereomeric Salts: Family Behaviour in Nucleation Inhibition*. *Chem. Eur. J.*, 2005. **11**: p. 5619 – 5624.
89. Sangwal, K., ed. *Additives and Crystallization processes*. 2007, John Wiley & Sons, Ltd.: West Sussex.
90. Weissbuch, R., Popovitzbiro, M., Lahav, L., Leiserowitz., *Understanding and Control of Nucleation, Growth, Habit, Dissolution and Structure of 2-Dimensional and 3-Dimensional Crystals Using Tailor-Made Auxiliaries*. *Acta Crystallographica Section B-Structural Science*, 1995. **51**: p. 115-148.

91. Nieuwenhuijzen, J.W., Grimbergen, R.F.P., Koopman, C., Kellogg, R.M., Vries, T.R., Pouwer, K., van Echten, E., Kaptein, B., Hulshof, L.A., Broxterman Q.B., *The Role of Nucleation Inhibition in Optical Resolutions with Families of Resolving Agents*. *Angewandte Chemie* Volume 2002. **114**(22): p. 4457-4462.
92. Ten Hoeve, W.W., H. , *J. Org. Chem.*, 1985. **50**: p. 4508.
93. Wynberg, H.t.H., W., *Chem. Abstr*, 1989. **105**: p. 134150u.
94. Vries, T., et al., *The Family Approach to the Resolution of Racemates*. *J. Angewandte Chemie-International Edition*, 1998. **37**: p. 2349-2354.
95. Broxterman, Q.B.v.E., E., Hulshof, L. A., Kaptein, B., Kellogg, R. M., Minnaard, A. J., Vries, T. R., Wynberg, H., *Chem. Today* 1998. **129**: p. 4278.
96. Kwok, K.S., Chan, H. C., Chan, C. K., Ng, K.M. , *Ind.Eng. Chem. Res.*, 2005. **44**: p. 3788.
97. Chikara, H., Ryuzo, Y., Masanori, T., Shigeki, Yamada., Ichiro, C., *Racemization of Optically Active Amino Acid Salts and an Approach to Asymmetric Transformation of DL-Amino Acids*. *Bull. Chim. Soc. Jap.*, 1983. **56**(12): p. 3744-3747.
98. *Nomenclature and symbolism for amino acids and peptides (IUPAC-IUB Recommendations 1983)*. *Pure Appl. Chem.*, 1984. **56**(5): p. 595-624.
99. *Data for Biochemical Research*, R.M.C. Dawson., Editor 1959, Clarendon Press: Oxford.
100. *CRC Handbook of Chemistry and Physics*, R.C. Weast, Editor 1981, CRC Press: Boca Raton, FL. p. C-512.
101. Bergmeyer, H.U., ed. *Methods of Enzymatic Analysis*. Vol. 3rd edition 1983, Vch Pub: Weinheim.
102. Kleemann, A.E. J., Kutscher, B., Reichert, D., ed. *Pharmaceutical substances: synthesis, patents and applications of the most relevant APIs*; 2009, Thieme, : Stuttgart.
103. Danysz, W., Parsons, A. C., *Glycine and N-methyl-D-aspartate receptors: Physiological significance and possible therapeutic applications*. *Pharmacol. Rev.*, 1998. **50**: p. 597-664.
104. Alessandra, B., Marina, C., Pier, G. R., *Production of D-Phenylglycine from Racemic (D,L)-Phenylglycine Via Isoelectrically-Trapped Penicillin G Acylase*. *BIOTECHNOLOGY AND BIOENGINEERING* 1998. **60**(4): p. 454-461.
105. Kim, D.M., Kim, H. S., *Enzymatic synthesis of D-phydroxyphenylglycine from DL-p-hydroxyphenylhydantoin in the presence of organic solvents*. *Enzyme Microb. Technol.*, 1993. **15**.
106. Moriarty, C.L., Tritch, G.L., *L-Asparatyl-L-Phenylglycine Esters of Lower Alkanols*, 1976: United states
107. Ryuzo, Y., Hajime, H., Kimio, O., Ikuko, T., Shin-ichi, Y., *Crystal structure-solubility relationships in optical resolution by diastereomeric salt formation of DL-phenylglycine with (1S)-(+)-camphor-10-sulphonic acid*. *J.AM.Chem.Soc., Perkin Trans 2*, 2000: p. 2121-2128.
108. Teske, J., Weller, J.P., Albrecht, U.V, Fieguth, A., *Fatal intoxication due to brucine*. *J Anal Toxicol. , 2011. 35*(4): p. 248-53.
109. Nicholas, J.W., Adrian, J. P., Richard, J. R., Michael J. C. R., *Toxicity of quinoline alkaloids to cultured Cinchona ledgeriana cells* *Biomedical and Life Sciences Plant Cell Reports*. **6**(2): p. 118-121.
110. Genne, P., Duchamp, O., Solary, E., Pinard, D., Belon, J.P., Dimanche-Boitrel, M.T., Chauffert, B., *Comparative effects of quinine and cinchonine in reversing multidrug resistance on human leukemic cell line K562/ADM*. *Leukemia* 1994).
111. Seon, Y.P., Bang, S.L., Sung, K.N., *L-tartaric acid-mediated isolation of optically pure L-pencillamine from racemic pencillamine*. *J. Ind. Eng. Chem.*, 2002. **8**(6): p. 515-518.
112. Shiraiwa, K., Shinjo., K., Maekawa, A., Gien., 1996. **88**: p. 40.
113. Ingersoll, A., W., Adams, R., *J.Am.Chem.Soc*, 1922. **44**: p. 2930.
114. *Synthesis and applications of isotopically labeled compounds* E. Buncl, Kabalka, W.G., , Editor 1991, Elsevier science pub.
115. Bialonska, A., Ciunik, Z., *Acta Cryst. , 2006. B62*, 1061-1070.
116. R M Kellogg et al., *Synthesis and Applications of Isotopically Labelled Compounds*, 2003. **0**(10): p. 1626-1638.
117. Losse, G., Augustin, M., *Racematspaltung des DL-Serins*. *Chem.Ber.*, 1958. **91**: p. 157-159.
118. Sistla, V.S., von Langermann, J., Lorenz, H., Seidel-Morgenstern, A., *Application of Classical resolution for Separation of DL-Serine*. *Chem. Eng. Tech.*, 2010. **33**: p. 780-786.

119. Lorenz, H., Sapoundjiev, D., Seidel-Morgenstern, A., *Enantiomeric Mandelic Acid Systems Melting Point Phase Diagram and Solubility in Water*. J.Chem. Eng. Data, 2002. **47**: p. 1280-1284.
120. Lorenz, H., Seidel-Morgenstern, A., *Binary and ternary phase diagrams of two enantiomers in solvent systems*. Thermochim. Acta Biochimica Et Biophysica Sinica, 2002. **382**: p. 129-142.
121. Hefter, G.T. and R.P.T. Tomkins, eds. *The experimental determination of solubilities*. 2003, J.Wiley & Sons.Ltd: New York.
122. Dongwei, W., Limei, C., Jingjing, X., Fusheng, L., *Measurement and correlation of solid-liquid equilibria of Irganox 1010 with n-hexane*. Fluid phase equilibria, 2009. **287** p. 39-42.
123. Sherman, G., Shenoy, S., Weiss, R.A., Erkey, C., *A Static Method Coupled with Gravimetric Analysis for the Determination of Solubilities of Solids in Supercritical Carbon Dioxide*. Ind. Eng. Chem. Res., 2000. **39**: p. 846-848.
124. Zhang, Y., Li, Z., *Effects of Cooling Rate, Saturation Temperature, and Solvent on the Metastable Zone Width of Triethanolamine Hydrochloride*. Ind. Eng. Chem. Res., 2011. **50** (10): p. 6375-6381.
125. J. Nyvlt, J., Rychly, R., Gottfried, J., Wurzelova, J., *Metastable zone-width of some aqueous solutions*. J. Cryst. Growth, 1970. **6**: p. 151.
126. Nyvlt, J., *The Kinetics of Industrial Crystallisation*, 1985, Amsterdam, Elsevier,.
127. Technologies, A., *Crystal16™ User Manual 1.1*, Amsterdam, Netherland, 2008.
128. Lorenz, H., Polenske, D., Seidel-Morgenstern, A., *Application of preferential crystallization to resolve racemic compounds in a hybrid process*. Chirality, 2006. **18**: p. 828-840.
129. Kui, S.K., Hok, C. C., Chak, K. C., Ka M. Ng., *Experimental Determination of Solid-Liquid Equilibrium Phase Diagrams for Crystallization-Based Process Synthesis*. Ind. Eng. Chem. Res., 2005. **44**: p. 3788-3798.
130. Wunderlich, B., *Thermal Analysis*., 1990, Academic Press: New York. p. 137-140.
131. O'Neill, M.J., *The Analysis of a Temperature-Controlled Scanning Calorimeter*. Anal. Chem., 1964. **36** (7): p. 1238-1245.
132. Pungor, E., *A Practical Guide to Instrumental Analysis*, 1995, Boca Raton: Florida. p. 181-191.
133. Silverstein, R.M., Bassler, G.C., Morrill, T.C., *Spectrometric Identification of Organic Compounds*, 1991, Wiley.
134. Rouessac, F. and A. Rouessac, *Chemical Analysis: Modern Instrumentation Methods and Techniques*. 4th ed 2000: John Wiley & Sons: Chichester.
135. Macomber, R.S., *A Complete Introduction to Modern NMR Spectroscopy*, R.S. Macomber, Editor 1998, John Wiley & Sons, Inc: Weinheim.
136. Cullity, B.D., *Chapter 14 of Elements of X-ray diffraction*, 1977, Addison-Wesley.
137. Basavaiah, D. and P.R. Krishna, *Synthesis of Chiral Alpha-Aryl-Alpha-Hydroxyacetic Acids - Substituent Effects in Pig-Liver Acetone Powder (Plap) Induced Enantioselective Hydrolysis*. Tetrahedron, 1995. **51**(8): p. 2403-2416.
138. Jenkins, R. and R.L. Snyder, *Introduction to X-ray Powder Diffractometry* 1996, New York: John Wiley & Sons.
139. Britain, H.G., *Physical Characterisation of Pharmaceutical Solids* 1995: Marcell Dekker, Inc.
140. Tulashie, S.K., Lorenz, H., Hilfert, L., Edelman, F. T., Seidel-Morgenstern, A., *Potential of chiral solvents for enantioselective crystallization. 1. Evaluation of thermodynamic effects*. Crystal Growth & Design, 2008. **8**(9): p. 3408-3414.
141. Lindsay, S., Kealey, D., *High Performance liquid chromatography*, 1987, John Wiley and Sons: New York, NY.
142. Yingjie, L., Chunhui, Song., Lingyi, Zhang., Weibing, Zhang., Honggang, Fu., *Fabrication and evaluation of chiral monolithic column modified by β -cyclodextrin derivatives*. Talanta 2010. **80** (3): p. 1378-1384.
143. Mettler-Toledo and GmbH, *Operating Instructions: RE40, Refractometer, Version 4.0* 2001: Schwerzenbach, Switzerland.
144. Ulrich, J., *Is Melt Crystallization a Green Technology?* Crystal Growth & Design, 2004. **4**(5): p. 879-880.

145. Nass, K.K., *Rational Solvent Selection for Cooling Crystallizations*. Ind. Eng. Chem. Res., 1994. **33**(6): p. 1580–1584.
146. Kwok, K.S., Chan, C.H., Chan, C.K., Ng, K.M., Ind. Eng. Chem. Res., 2005. **44**.
147. Crisp, J.L., Dann, S.E., Blatchford, C.G., *Antisolvent crystallization of pharmaceutical excipients from aqueous solutions and the use of preferred orientation in phase identification by powder X-ray diffraction*. Eur J Pharm Sci., 2011 **42**(5): p. 568-577.
148. Liu, X.Y., *A new kinetic model for three-dimensional heterogeneous nucleation*. Journal of chemical physics, 1999. **111**(4).
149. Yoshiea, N., Asakab, A., Yazawab, K., Kurodab, Y., Inoueb, Y., *In situ FTIR microscope study on crystallization of crystalline/crystalline polymer blends of bacterial copolyesters*. Polymer 2003. **44**: p. 7405–7412.
150. Tjakko, G.Z., Rob, M.G., Geert-Jan, W., Gerda, M. R., Jan .de.G., *Antisolvent Crystallization as an Alternative to Evaporative Crystallization for the Production of Sodium Chloride*. Ind. Eng. Chem. Res, 2000. **39**(5): p. 1330–1337.
151. Diedrichs, A., *Evaluation and extension of thermodynamic models for the solubility prediction of active pharmaceutical ingredients*, in *Fakultät V - Mathematik und Naturwissenschaften* 2010, University of Oldenburg: Oldenburg.
152. Jarabek, B.R., Grier, D.G., Simonson, D.L., Seidler, D.J., Boudjouk, P., McCarthy, G.J., *XRD and TEM Characterization of Compound Semiconductor Solid Solutions: Sn(S,Se) and (Pb,Cd)S*. JCPDS-International Centre for Diffraction Data 1997.
153. Polenske, D., Lorenz, H., Seidel-Morgenstern, A., *Separation of propranolol hydrochloride enantiomers by preferential crystallization: thermodynamic basis and experimental verification*. Crystal Growth & Design, 2007. **7**: p. 1628–1634.
154. Hiroshi, K., Masao, M., Kenichi, S., *A pair of diastereomeric 1:2 salts of (R)- and (S)-2-methylpiperazine with (2S,3S)-tartaric acid*. Acta Cryst. , 2010. **C66**: p. o20–o24.
155. Hiroshi, K., Masao, M., Kenichi, S., *A pair of diastereomeric 1:1 salts of (S)- and (R)-2-methylpiperazine with (2S,3S)-tartaric acid*. Acta Cryst. , 2009. **C65**: p. o357–o360.

Curriculum Vitae

Curriculum Vitae

Name: M.Sc. VenkataSubbarayudu. Sistla
Date of birth: 10.07.1983
Nationality: Indian
Marital status: Married
Address: N2:15, MPI, Sandtor Str-1, 39106, Germany.
Email: sistla@mpi-magdeburg.mpg.de
sistlasubbu@googlemail.com

Career Interests

Separation Technology, Downstream process development, Integrated process design, Process Simulation, Biological process design, Energy engineering, Pilot plant experimentation and Scale up to Industrial level.

Academics

Ph.D. (May 2008- July 2012)

Thesis title • Formation and crystallization based separation of diastereomeric salts

Institution • Max Planck Institute for dynamics of Complex technical systems, Magdeburg, Germany.

University • Otto von Guericke University, Magdeburg, Germany

Post-Graduation (April 2006- March 2008)

Degree • Master of Science in Chemical and Process Engineering

University • Otto von Guericke University, Magdeburg, Germany

Final Grade • 2.2 (best-1, fail-5)

Bachelor Degree (Nov 2000- May 2004)

Degree • Bachelor of Technology in Chemical Engineering

University • Acharya Nagarjuna University, Guntur, A.P, India

Final Grade • First class with distinction (73%)

Work Experience

Research

10/09/2007 – 31/03/2008 • Potential of a Chiral Solvent in enantioselective Crystallization as a part of Master thesis, Max Planck Institute for Dynamics of Complex Technical Systems (MPI), Magdeburg, Germany.

10/2006 - 09/2007 • Worked as a research assistant (HiWi) on the topic 'Crystallization from Chiral Solvents' in MPI, Magdeburg, Germany.

08/2003 - 04/2004 • Worked in M/S JOCIL Ltd, Guntur, A.P, India, (a soap manufacturing industry where glycerin and gasses like H₂ and O₂ are side products) worked as a part of Bachelor Thesis.

27/05/03-24/06/03 • Industrial training was attended on the 'Manufacturing Process of DASDA (a die intermediate) and Case study on Incineration', in M/S Vasanth Chemicals Pvt.Ltd, Hyderabad, A.P, India.

Professional Experience

06/2005 - 02/2006 • Worked as a Production Associate trainee in M/S Global Calcium Pvt.Ltd, Hosur, T.N, India(a bulk drug industry for various calcium related products). During this tenure- shift supervising for drug production, documentation work for ISO-9001 and GMP standards maintenance was experienced.

02/2005-06/2005 • Worked as a marketing associate for Acid India (a small scale chemical distribution company for M/S Solaris ChemtechPvt.Ltd and Solaris Biotech Pvt. Ltd), Bangalore, Karnataka, India.

Publications/Conferences

Publications

Sistla, V. S.; von Langermann, J.; Lorenz, H.; Seidel-Morgenstern, A. : Application of Classical resolution for Separation of DL-Serine. *Chem. Eng. Tech.*, **2010**, 33, 780-786.

Sistla, V. S.; von Langermann, J.; Lorenz, H.; Seidel-Morgenstern, A.: Analysis and Comparison of Commonly Used Acidic Resolving Agents in Diastereomeric Salt Resolution – Examples for DL-Serine, *Cryst. Growth Des.*,**2011**, 11 (9), 3761–3768

Conference proceedings

Sistla, V. S., H. Lorenz and A. Seidel-Morgenstern: Influence of an excess resolving agent on diastereomeric salt resolution. 18th International Workshop on Industrial Crystallization BIWIC, 07-09th Sept 2011, TU Delft, Netherlands (2011) 321-326.

Sistla, V. S., J. von Langermann, H. Lorenz and A. Seidel-Morgenstern: Application of different acidic resolving agents for diastereomeric salt separation of serine. 17th International Workshop on Industrial Crystallization BIWIC, Halle (Saale), Germany (2010) 42-48.

Sistla, V. S., J. von Langermann, H. Lorenz and A. Seidel-Morgenstern: Phase Diagrams of Diastereomeric Salts and Their Application. 16th International Workshop on Industrial Crystallization BIWIC, Lappeenranta, Finland (2009) 142-148.

Conferences and workshops actively participated

Sistla, V. S., H. Lorenz and A. Seidel-Morgenstern: Introduction to classical resolution- a prominent industrial enantioselective separation technique (Poster). 2nd Indo-German workshop on 'Advances in Reaction and Separation Processes', 20-22 Feb 2012, Bad-Herrenalb, Germany.

Sistla, V. S., J. von Langermann, H. Lorenz and A. Seidel-Morgenstern: Systematic approach for chiral separation via diastereomeric salt formation (Presentation). AICHE-annual meeting, 16-21.10.2011, Minneapolis, U.S.A.

Sistla, V. S., H. Lorenz and A. Seidel-Morgenstern: Influence of an excess resolving agent on diastereomeric salt resolution (Poster). 18th International Workshop on Industrial Crystallization BIWIC, 07-09th Sept 2011, TU Delft, Netherlands.

Sistla, V. S., J. von Langermann, H. Lorenz and A. Seidel-Morgenstern: Application of different acidic resolving agents for diastereomeric salt separation of serine (Presentation & Poster). BIWIC 2010 - 17th International Workshop on Industrial Crystallization, 08.-10.09.2010, Halle (Saale), Germany

Sistla, V. S., J. von Langermann, H. Lorenz and A. Seidel-Morgenstern: Phase Diagrams of Diastereomeric Salts and Their Application (Poster). BIWIC 2009 - 16th International Workshop on Industrial Crystallization, 09-11.09.2009, Lappeenranta, Finland

Sistla, V. S., J. von Langermann, H. Lorenz and A. Seidel-Morgenstern: Diastereomeric resolution -systematic approach via phase diagrams (Poster). IntEnant – 2nd Technical Meeting and Training, 10-12.06.2009, ETH Zürich, Switzerland

Sistla, V.S., von Langermann, J., Lorenz, H., Seidel-Morgenstern, A.: Diastereomeric resolution of DL-Serine -systematic approach via phase diagrams, Presentation at the GVC-Fachausschuss, Dortmund, Germany, 12/13-03-2009.

Computer Skills

Programming languages • Matlab, C, C++.

Documentation • LaTeX, Microsoft Office

Simulation tools • FLUENT, Gambit, ASPEN, Material Studio

Language Skills

Fluent • Telugu, Hindi, English

Basic • Tamil, Kannada, German

Extra Curriculum activities

10/2009- 03/2012 • Yoga trainer in Otto von Guericke University Sports Center, Magdeburg, Germany.

References

1. Prof. Dr.-Ing. Andreas Seidel-Morgenstern

Address: Max Planck Institute for dynamics of complex technical Systems,

Sandtorstraße 1, D-39106 Magdeburg, Germany

E-mail and Phone: seidel-morgenstern@mpi-magdeburg.mpg.de, 0049-391-6110401

2. Apl.Prof. Heike Lorenz

Address: Max Planck Institute for dynamics of complex technical Systems,

Sandtorstraße 1, D-39106 Magdeburg, Germany

E-mail and phone: Lorenz@mpi-magdeburg.mpg.de, 0049-391-611029